

Document downloaded from:

<http://hdl.handle.net/10251/181523>

This paper must be cited as:

Villca, AR.; Soriano Martinez, L.; Font, A.; Tashima, MM.; Monzó Balbuena, JM.; Borrachero Rosado, MV.; Paya Bernabeu, JJ. (2021). Lime/pozzolan/geopolymer systems: Performance in pastes and mortars. *Construction and Building Materials*. 276:1-15.
<https://doi.org/10.1016/j.conbuildmat.2020.122208>



The final publication is available at

<https://doi.org/10.1016/j.conbuildmat.2020.122208>

Copyright Elsevier

Additional Information

1 **Lime/pozzolan/geopolymer systems: performance in pastes and mortars.**

2 Ariel R. Villca ⁽¹⁾, Lourdes Soriano ⁽¹⁾, Alba Font ⁽¹⁾, Mauro M. Tashima ⁽²⁾, José Monzó
3 ⁽¹⁾, María Victoria Borrachero ⁽¹⁾, Jordi Payá ⁽¹⁾.

4 ⁽¹⁾ ICITECH – GIQUIMA Group – Grupo de Investigación en Química de los
5 Materiales de Construcción, Instituto de Ciencia y Tecnología del Hormigón,
6 Universitat Politècnica de València, Valencia, Spain.

7 ⁽²⁾ Universidade Estadual Paulista (UNESP), Faculdade de Engenharia de Ilha
8 Solteira. MAC – Grupo de Pesquisa em Materiais Alternativos de Construção, Ilha
9 Solteira-SP, Brazil.

10
11 **Abstract**

12 Use of lime as construction material is limited mainly by low initial strength. These
13 properties can be improved by adding pozzolanic materials, but the evolution of the
14 reaction usually needs older ages than 7 days. Alkali-activated materials, or geopolymers,
15 are good-performance materials that can be produced with residual waste. The
16 combination of traditional and new materials can lead to new uses of lime mortars. This
17 paper studies a lime/pozzolan and geopolymer mixture. The chosen pozzolan is fluid
18 catalytic cracking catalyst residue (FCC), a material employed as a precursor in alkali-
19 activated material. FCC is activated by two activators: a mixture of NaOH and waterglass;
20 a mixture of NaOH and rice husk ash (RHA). The new materials were studied in
21 microstructure and mechanical behaviour terms. The results demonstrated that
22 lime/pozzolan/geopolymer obtained superior compressive strengths after 1 curing day to
23 that obtained for the corresponding lime/pozzolan mortar after 90 days. An improvement
24 in compressive strength of around 145% was achieved for the mortar with 40%
25 geopolymer compared to the mortar with only lime/pozzolan at 28 curing days.

26
27 **Keywords:** lime, pozzolan, geopolymer, waste material, fluid catalytic cracking catalyst
28 residue

1
2
3
4
5
6
7
8
9
10
11
12
13
14
15
16
17
18
19
20
21
22
23
24
25
26
27
28
29
30
31
32
33
34
35
36
37
38
39
40
41
42
43
44
45
46
47
48
49
50
51
52
53
54
55
56
57
58
59
60
61
62
63
64
65

29 1 Introduction

30 Lime mortar is an ancient construction material that has been used in different
31 places and periods of history [1,2]. The Romans are certainly responsible for the main
32 technological contribution to lime mortars: addition of volcanic ash or calcined clay
33 significantly improved mechanical properties, and allowed it to set and harden under
34 water. The durability of lime mortars is demonstrated by today's good conditions from
35 the architectural heritage of Roman times [3].

36 After the discovery of Portland cement, the use of lime mortar drastically reduced
37 due to the new binder's excellent mechanical and durability properties: fast setting,
38 excellent strength development, etc. Nevertheless, current Portland cement (PC) mortars
39 do not meet some sustainability criteria designated by the international community
40 (sustainability development goals) [4]. PC production generates large amounts of CO₂
41 emissions to the atmosphere, and is responsible for about 5-8% of CO₂ emissions
42 worldwide [5]. Thus a good option is to use alternative binders (lime/pozzolan,
43 geopolymer systems, magnesium oxide cements, etc.) that are often associated with a
44 lower environmental impact [6].

45 Studies about lime/pozzolan binders report good mechanical strength and
46 durability aspects, depending on the type of used pozzolan [1,7–10]. However, in most
47 cases, the mechanical strength for early curing times (< 28 days) is reduced due to the
48 slow setting and hardening process of lime/pozzolan systems.

49 Palomo et al. studied the similarity between the ancient lime/pozzolan mortars of
50 historic Roman marine concrete and hybrid-Portland alkaline cement [11]. More
51 specifically, these researchers found similar products of reaction by comparing ancient
52 concrete in marine structures and hybrid alkaline materials (a combination of Portland
53 cement and alkali-activated fly ash). The particularity of seawater concretes in Roman
54 times was studied in depth in the last few years by paying attention to the formation of
55 the so-called "Al-tobermorite" [12,13]. The stability of Al-tobermorite can be a starting
56 point in an attempt to synthesise similar products.

57 Alkali-activated materials (AAM) are relatively new construction materials, and
58 geopolymer is often used as an additional terminology. Research into these systems is
59 growing and they are expected to be used in many applications in the construction
60 domain. These materials are basically a mixture of an aluminosilicate source and an

1
2
3
4
5
6
7
8
9
10
11
12
13
14
15
16
17
18
19
20
21
22
23
24
25
26
27
28
29
30
31
32
33
34
35
36
37
38
39
40
41
42
43
44
45
46
47
48
49
50
51
52
53
54
55
56
57
58
59
60
61
62
63
64
65
66
67
68
69
70
71
72
73
74
75
76
77
78
79
80
81
82
83
84
85
86
87
88
89
90
91

alkaline-activating solution [14]. The most typically used precursors are metakaolin (MK), fly ash (FA), ground granulated blast furnace (BFS), etc. Alkaline solutions are normally a mixture of sodium hydroxide and sodium silicate (or potassium as a cation), although other activators can be used: sodium carbonate, sodium sulphate, etc.[15,16].

The new geopolymer technology goal is to use residual materials to prepare alkaline solutions. The carbon footprint related to alkali hydroxides is smaller than that for alkali silicates. Many research groups are investigating the use of alternative silica sources to obtain a commercial silicate or waterglass alternative. These silica sources are mainly rice husk ash (RHA), diatomaceous earth residue, glass waste, sugar cane straw ash and silica fume, among others [17–22].

In some studies on geopolymeric systems, the addition of calcium compounds enhances the activation reaction to result in improved compressive strength [23,24]. Moreover, the use of materials that include calcium in their composition can improve the reactivity of waste, **but an excess of calcium** has negative effects on compressive strength [25].

The combination of these two binder types (lime/pozzolan and geopolymer) would reduce environmental issues caused by CO₂ emissions, increase waste valorisation and improve the mechanical properties at curing ages lasting less than 28 days.

Allali et al. studied the influence of calcium content on geopolymeric matrices for their use in restoration mortars [26]. They substituted metakaolin (MK) for calcium hydroxide in mortars with potassium and sodium salts as an alkaline solution. When they employed calcium hydroxide in both sodium or potassium solution, Ca(OH)₂ totally or partially dissolved. They observed fast setting and compressive strength was lower than for the mortar with only MK (42 MPa for the mortar without hydrated lime and 10 MPa for the mortars with 41% replacement of MK with hydrated lime at 7 curing days).

Recently, glass powder in different systems has been used. In mixtures with PC, it reacted as pozzolanic material. In geopolymeric systems, it was blended with slag, fly ash and lime [27]. With the glass powder and lime mixtures, which were activated by a 4M NaOH solution, a compressive strength of 31MPa was achieved in systems cured at 60°C for 28 days. The formation of a similar calcium silicate hydrate to tobermorite was suggested for the SEM/EDS study.

92 Several authors have studied the alkaline activation of MK with calcium
93 hydroxide [28,29]. They followed different analytical techniques to characterise the
94 products formed in this mixture, and concluded that reaction products differed depending
95 on the OH⁻ concentration in the aqueous medium. When the activator concentration was
96 high (> 10M of NaOH), the formed alkaline aluminosilicate gel was the principal product,
97 while hydrated calcium silicate was the secondary product. However, when the activator
98 concentration was low (< 5M of NaOH), dissolved aluminates were insufficient to
99 produce aluminosilicate gel and pozzolanic products predominated.

100 Boonjaeng et al. studied the system of lime and calcined clay materials with
101 different alkaline solutions of sodium hydroxide (NaOH). When comparing several
102 molarities (0.1M -10M), they concluded that the reaction of the mixture was dominated
103 by the NaOH concentration [30]. At low concentrations (<1M), the pozzolanic reaction
104 was dominant, while the zeolite-formation reaction predominated at medium NaOH
105 molarities (1M<NaOH<5M). Finally, at a high NaOH molarity (>5M), the principal
106 reaction was the geopolymerization process.

107 Fluid catalytic cracking catalyst residue (FCC) has been employed as a precursor
108 in geopolymeric mixtures in some reported studies. Tashima et al. made samples with
109 different SiO₂/Na₂O molar ratios [31]. These authors obtained mortars with a compressive
110 strength of 68 MPa after 3 curing days at 65°C. Trochez et al. obtained similar
111 compressive strength in pastes after curing at ambient temperature for 7 days [32].

112 The use of RHA has been studied by different research groups as an alternative
113 activator (source of silica). Mejía et al. employed two types of RHA and sodium silicate
114 (as a control mix) to activate mixtures with FA and BFS as precursors[17]. The samples
115 with sodium silicate displayed better mechanical strength than the mortars with RHA, but
116 the results of these mixtures gave a compressive strength close to 42 MPa. Bouzón et al.
117 employed RHA in systems with FCC as a precursor [18]. These authors obtained mortars
118 with very similar compressive strengths to the mortar with sodium silicate (40 MPa).
119 Another research work has reported poor results when RHA was compared to commercial
120 reagents. Luukkonen et al. compared the use of RHA and microsilica with that of sodium
121 silicate [33]. The compressive strength of mortars with an alternative activator was lower
122 than the commercial one, but proved sufficient for certain uses, and performed well with
123 freeze-thawing cycles. Villaquirán-Cacedo and Mejía de Gutiérrez [34] studied MK-
124 based geopolymers using mixtures of RHA or silica fume with KOH as activators. They

125 achieved a 47% reduction in the warming potential emissions for this system compared
126 to the corresponding commercial potassium silicate-activated system.

127 The present research studies the development of binary mixtures where the
128 lime/pozzolan binder was partially replaced with a geopolymeric mortar.

129 Lime mortars were made with a residual pozzolan, namely FCC. The
130 geopolymeric material was a mixture of FCC activated in two different ways: i) a solution
131 of sodium silicate (waterglass) and sodium hydroxide; ii) a suspension prepared as a
132 mixture of sodium hydroxide and RHA.

133 2 Materials and Methods

134 A commercial hydrated lime supplied by Cales Pascual (Paterna, Spain) was used.
135 This material is designed as CL90-S according to Spanish standard UNE-EN 459-1 [35].
136 The FCC residue was supplied by BP Oil España, S.A.U (Grao de Castellón, Spain). RHA
137 was supplied by Dacsa S.A (Tabernes Blanques, Spain).

138 FCC was employed as both the mineral admixture in the lime/pozzolan system
139 and a precursor in the geopolymer formulation.

140 The geopolymer was activated by two activators:

- 141 • A conventional alkaline solution prepared with a mix of waterglass (Na_2SiO_3 ,
142 commercial sodium silicate) (Merck, 28% SiO_2 ; 8% Na_2O and 64% H_2O) and
143 sodium hydroxide (Panreac-SA, 98% purity).
- 144 • An environmental-friendly alkaline solution where RHA was employed as an
145 alternative source of “sodium silicate”. RHA was mixed with water and sodium
146 hydroxide in a thermal bottle [22].

147 The chemical composition of FCC and RHA was analysed by X-Ray fluorescence
148 (XRF) equipment (Magic Pro Spectrometer-Philips). The results are summarised in Table
149 1.

150 **Table 1.** Chemical composition of the used materials: fluid catalytic cracking catalyst
151 residue (FCC) and rice husk ash (RHA)

| | SiO ₂ | Al ₂ O ₃ | Fe ₂ O ₃ | CaO | MgO | SO ₃ | K ₂ O | Na ₂ O | P ₂ O ₅ | Others | *LOI |
|-----|------------------|--------------------------------|--------------------------------|------|------|-----------------|------------------|-------------------|-------------------------------|--------|------|
| FCC | 47.76 | 49.26 | 0.60 | 0.11 | 0.17 | 0.02 | 0.02 | 0.31 | 0.03 | 1.20 | 0.54 |
| RHA | 85.58 | 0.25 | 0.21 | 1.83 | 0.50 | 0.26 | 3.39 | - | 0.67 | 0.32 | 6.99 |

152 *LOI: loss on ignition

153 The mean particle diameter of the supplied FCC was 21 μm . RHA was milled in
154 an industrial mill and its mean particle diameter was 20 μm . All the granulometric
155 measurements were taken in a Malvern Mastersizer 2000 in aqueous medium.

156 The amorphous content of RHA was 31.5%, calculated by an extractive method
157 using HCl and KOH [36].

158 Lime/pozzolan mortars and pastes were prepared at the following ratios:
159 lime/FCC = 1/1; water/binder = 0.8; sand/binder = 3. The lime/pozzolan ratio was chosen
160 based on the research group's previous research [37]. The employed sand was siliceous
161 in nature with a fineness modulus of 4.3. Mortars were moulded in cubic 40*40*40 mm^3
162 casts and stored at 25°C and RH 73% for 24 h. Specimens were wrapped in film until
163 tested. Pastes were moulded in sealed polyethylene phials and stored at 25°C.

164 For the geopolymeric binder, the formulation of the alkaline activator solution was
165 selected according to a previous work [18]. The solution had a $\text{SiO}_2/\text{Na}_2\text{O}$ molar ratio of
166 1.17, a sodium molality of 7.5 and a water/binder ratio of 0.6.

167 The replacements of lime/pozzolan binder mass with geopolymeric binder were
168 0% (control sample), 10%, 20%, 30% and 40%.

169 Table 2 summarises the quantity (expressed as grams) of the materials employed
170 in mortars. The control mortar was the mixture with only lime and pozzolan (CON). The
171 geopolymeric mortar (GEOP) was the mixture of FCC with the activator of NaOH and
172 Na_2SiO_3 . The lime/pozzolan/GEOP mixtures were named CCx or CAx, where: i) CC is
173 the geopolymer activated by the conventional solution (waterglass and sodium hydroxide)
174 and CA is the geopolymer when RHA was employed as a silica source in alkaline
175 activator (RHA + water + sodium hydroxide); ii) x is the lime/pozzolan replacement
176 percentage with FCC geopolymer. For example, mortar CA10 contained 10%
177 geopolymer (FCC and an alkaline activator composed of a mixture of RHA, NaOH and
178 water).

179 The abbreviation FCC^{P} represents the quantity of FCC in the lime/pozzolan
180 binder, while the abbreviation FCC^{G} denotes the quantity of FCC in the geopolymeric
181 binder. $\text{H}_2\text{O}^{\text{P}}$ was the water content in the lime/pozzolan system. The water used to
182 prepare the geopolymeric binder is indicated in the activator as $\text{H}_2\text{O}^{\text{G}}$.

183 **Table 2.** Composition of lime/pozzolan mortar, lime/pozzolan/GEOP mortars and GEOP
 184 mortar (weight in grams).

| | Lime/pozzolan binder | | GEOP binder | | | | | | Sand |
|-------------|-------------------------|------------------|-------------------------------|------------------|-------------------------------|------|----------------------------------|------|--------|
| | Lime | FCC ^P | H ₂ O ^P | FCC ^G | Activator | | | | |
| | | | | | H ₂ O ^G | NaOH | Na ₂ SiO ₃ | RHA | |
| CON | 262.5 | 262.5 | 420.0 | - | - | - | - | - | 1575.0 |
| CC10 | 236.3 | 236.3 | 378.0 | 52.5 | 12.6 | 6.4 | 29.5 | - | 1575.0 |
| CA10 | 236.3 | 236.3 | 378.0 | 52.5 | 31.5 | 9.4 | | 9.2 | 1575.0 |
| CC20 | 210.0 | 210.0 | 336.0 | 105.0 | 25.2 | 12.8 | 59.1 | - | 1575.0 |
| CA20 | 210.0 | 210.0 | 336.0 | 105.0 | 63.0 | 18.9 | - | 18.4 | 1575.0 |
| CC30 | 183.8 | 183.8 | 294.0 | 157.5 | 37.8 | .2 | 88.6 | - | 1575.0 |
| CA30 | 183.8 | 183.8 | 294.0 | 157.5 | 94. | 28.4 | - | 27.6 | 1575.0 |
| CC40 | 157.5 | 157.5 | 252.0 | 210.0 | 50.4 | 25.6 | 118.3 | - | 1575.0 |
| CA40 | 157.5 | 157.5 | 252.0 | 210.0 | 126.0 | 37.8 | - | 36.7 | 1575.0 |
| GEOP | - | - | - | 525.0 | 126.0 | 64.0 | 295.3 | - | 1575.0 |

185

186 Pastes lime/pozzolan, lime/pozzolan/GEOP and GEOP had the same proportions
 187 of materials as the corresponding mortars, but without sand. An additional paste
 188 containing 80% GEOP and 20% hydrated lime was fabricated and called GEOP-CH.

189 Compressive strength was measured in an INSTRON 3282 machine for the ages
 190 of 1, 2, 3, 7, 28 and 90 days, and was the average of four individual tests.

191 The microstructural analysis of pastes was carried out by a thermogravimetric
 192 analysis (TG/DTG), powder X-Ray diffraction (XRD), Fourier transform infrared
 193 spectroscopy (FTIR) and field emission scanning electron microscopy (FESEM).

194 The TG analysis was done using a TGA 850 Mettler-Toledo thermobalance. The
 195 TG experiments were performed from 50°C to 600°C at a heating rate of 10°C.min⁻¹.
 196 Aluminium-sealed crucibles (70 µL volume) were used with a pinholed lid and a nitrogen
 197 atmosphere (flow gas rate of 75 mL.min⁻¹). The XRD analyses were carried out in a
 198 Bruker AXS D8 Advance device from 10° to 70° 2θ (2s accumulation time in a 0.02 angle
 199 step). The FTIR analyses were run in a Bruker Tensor 27 and analysed within the 400-
 200 4000 cm⁻¹ range. The FESEM micrographs were taken in a Zeiss ULTRA 55. Pastes were
 201 carbon-coated and images were taken at 2kV. For the EDS analysis (X-ray energy
 202 dispersive spectroscopy), data were taken at 15kV.

203 3 Results and Discussion

204 3.1 Compressive strength development

205 In the first stage, the study of incorporating the geopolymer fabricated with
206 commercial reagents (sodium silicate as a silica source) was analysed. The substitution
207 percentages went from 10% to 40%, and the selected curing ages were 1, 2, 3, 7, 28 and
208 90 days. The results are represented in Figure 1. For all the curing ages, the mortars with
209 geopolymer obtained higher compressive strengths than that for the mortar with only FCC
210 and lime (the control mortar: CON). After 1 curing day, mortar CC40 (14.9 MPa) had the
211 same compressive strength as CON (14.3 MPa) after 90 curing days.

212 It is highlighted the compressive strength gain at early ages with the incorporation
213 of the geopolymer into the lime/pozzolan systems. With the 10% substitution (sample
214 CC10), compressive strength was 45% greater than the strength for CON after 1 curing
215 day and was 152% greater after 7 curing days.

216 Figure 1 illustrates how the CON mortars had a low compressive strength (< 2
217 MPa) until 7 days. Compressive strength evolution was 190% from 7 days to 28 days,
218 with 37% evolution from 28 days to 90 curing days. Mixture CC40 yielded fast evolution
219 between 1 and 7 days (65%), when its evolution was asymptotic until 90 days with
220 compressive strength at around 25 MPa.

221 The evolution of mortar CC10 was remarkable. The sample began with only 2.08
222 MPa at 1 curing day, but reached 21.09 MPa at 90 curing days (913% evolution). This
223 compressive strength was only slightly lower than that found for the mortar with the
224 highest geopolymer content (CC40). The effect of a small amount of geopolymer on the
225 lime/pozzolan system was marked. The incorporation of geopolymer enhanced the
226 formation of the new reaction products, which improved the strength of the mortars. The
227 new aluminosilicate gel type C(N)ASH was probably formed in the
228 lime/pozzolan/geopolymer systems. García-Lodeiro et al.[38] reported the formation of
229 this product type in hybrid alkaline cements using FA and Portland cement. Sodium ions
230 replaced calcium ions as charge balancers.

231

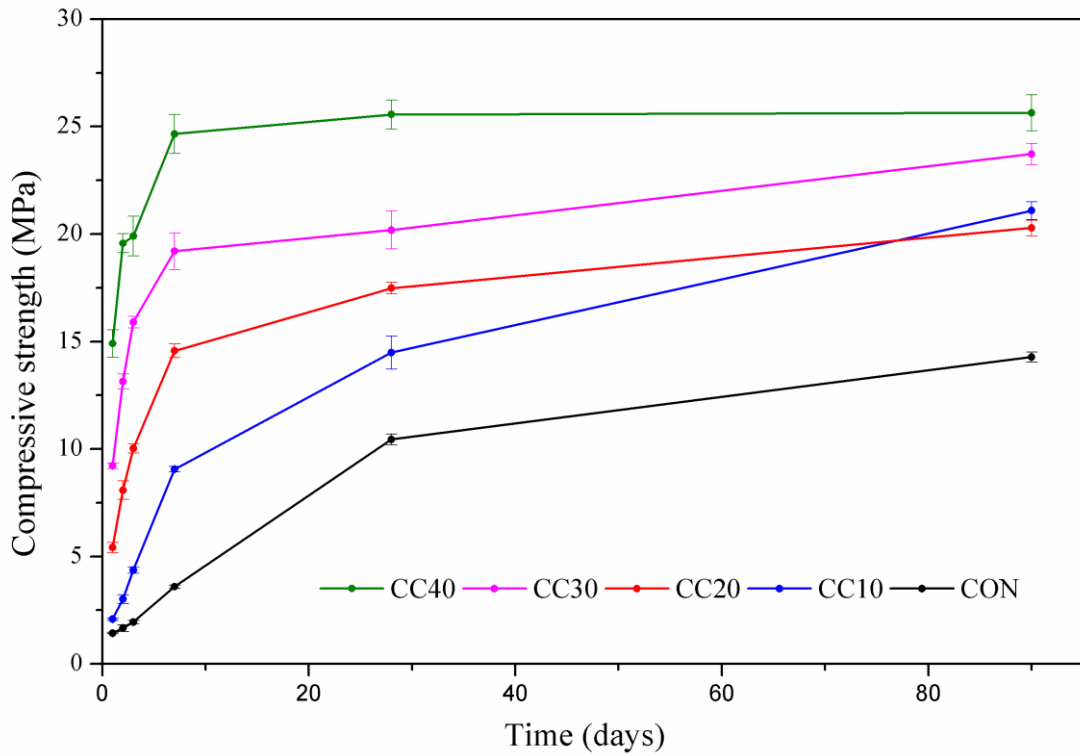


Fig 1. Evolution of the compressive strength of mortars CON and CC at 1, 2, 3, 7, 28 and 90 curing days.

232

233 For this above-discussed first stage, the obtained results contrasted those obtained
 234 by other researchers. Boonjaeng et al, used MK and lime systems, and indicated that
 235 geopolymeric gel was not as strong as CASH and CSH gel [30]. In the present work, the
 236 alkaline activator dose was used only for FCC as a precursor, and the other part of mortar
 237 (lime-pozzolan) was mixed only with water. Conversely in the research by Boonjaeng et
 238 al, the lime/MK mixture was considered the binder and was activated with NaOH [30].

239 The geopolymeric mortar without lime (pure geopolymer, GEOP) was analysed
 240 for the same curing ages. The compressive strength of this sample was generally very
 241 high, especially at early curing ages, between 1 and 7 curing days. After the first curing
 242 day the GEOP mortars yielded 13.38 MPa and the compressive strength increases until
 243 53.90 MPa at 7 curing days. No CCx system had a compressive strength greater than 25
 244 MPa. The nature of the gel in these mortars was the NASH type [39].

1
2
3
4
5
6
7
8
9
10
11
12
13
14
15
16
17
18
19
20
21
22
23
24
25
26
27
28
29
30
31
32
33
34
35
36
37
38
39
40
41
42
43
44
45
46
47
48
49
50
51
52
53
54
55
56
57
58
59
60
61
62
63
64
65

245 A comparison of the strength values at early (1-7 days) and long-term (28-90 days)
 246 ages can be made to analyse strength development in the different mortars CC.
 247 Theoretical strength (R_{th}) can be calculated by taking into account the contribution of the
 248 lime/pozzolan and geopolymer fractions as follows (Equation 1):

$$R_{th}=R_{lp}*X_{lp}+R_g*X_g \quad (1)$$

249
 250 Where R_{lp} and R_g are the strength of the mortar lime-pozzolan (CON) and the
 251 mortar pure geopolymer (GEOP), respectively; X_{lp} and X_g are the mass fractions of both
 252 mortars in the CC mixtures (0.9-0.6 for X_{lp} ; 0.1-0.4 for X_g).

253 Table 3 compares the theoretical values (R_{th}) to the experimental values (R_{ex}), and
 254 the difference in strength (D) is summarised for the mortars cured within the curing time
 255 range of 1-90 days. The D values for CC20, CC30 and CC40 were positive at early curing
 256 ages (1-3 days), which suggests that the role of calcium from lime is crucial for
 257 developing a strong cementing gel. In this case, gels CASH or C(N)ASH formed. For
 258 longer curing times, the opposite trend was seen, and the D values were negative after 28
 259 and 90 curing days. This behaviour suggests that the contribution of the NASH gel to
 260 strength became less relevant when the binary system was fabricated. It was noteworthy
 261 that for 1-3 curing days, the presence of calcium in the mixture enhanced the gel's
 262 strength properties, which confirmed the positive effect by mixing both types of
 263 cementing systems.

264 **Table 3.** Difference (D, in MPa) in mortar strengths, calculated as experimental strength
 265 (R_{ex}) minus theoretical strength (R_{th}).

| System | Curing days | | | | | |
|--------|-------------|-------|-------|------|-------|-------|
| | 1 | 2 | 3 | 7 | 28 | 90 |
| CC10 | -0.55 | -1.10 | -0.83 | 0.44 | -0.34 | 2.54 |
| CC20 | 1.59 | 1.52 | 1.59 | 0.91 | -1.71 | -2.55 |
| CC30 | 4.19 | 4.12 | 4.21 | 0.52 | -3.39 | -3.40 |
| CC40 | 8.69 | 8.11 | 4.97 | 0.94 | -2.39 | -5.76 |

266

267 In the second stage, the use of an alternative alkaline activator was explored.
 268 Resorting to RHA as a silica source was investigated as a sodium silicate substitute. The
 269 RHA and NaOH mixture in a thermal bottle was used as an activator at the same
 270 proportions as the commercial reagents. A strength variation percentage (VR) was
 271 calculated for the alternative mixtures (CA) using Equation 2:

$$VR = 100 * (R_{CAx} - R_{CCx} / R_{CCx}) \quad (2)$$

272
 273 Where R_{CAx} is the compressive strength for a given percentage of geopolimer (x)
 274 in a mortar with RHA (CA); R_{CCx} is the compressive strength for the same percentage (x)
 275 in a mortar with sodium silicate (CC).

276 Figure 2 represents the VR evolution for all the replacement percentages and
 277 curing ages. The samples with values over the red line yielded a compressive strength
 278 that was more than 2-fold higher than the values yielded by mortars CC.

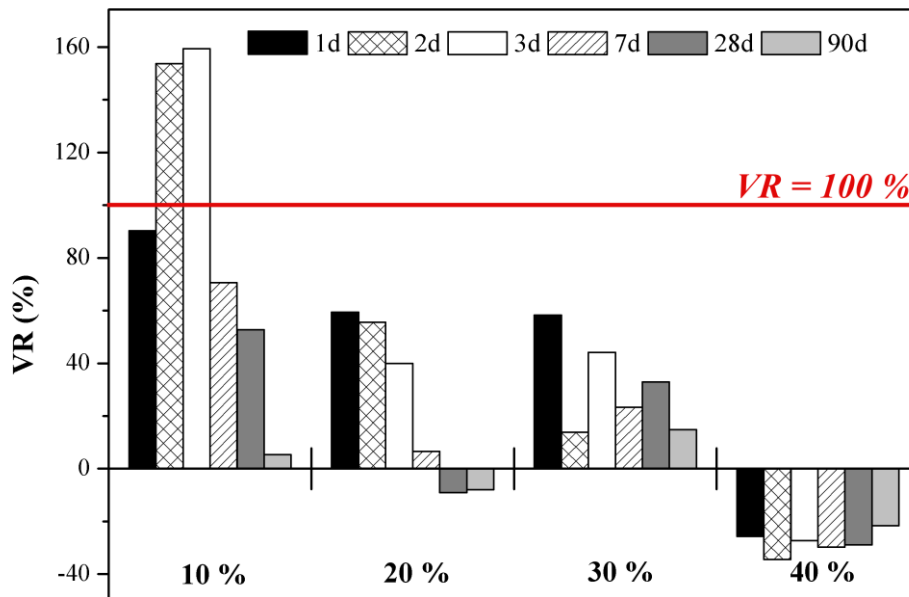


Figure 2. Strength variation (VR) percentages for the mortars with alternative silicate (CA samples).

279

1
2
3
4
5
6
7
8
9
10
11
12
13
14
15
16
17
18
19
20
21
22
23
24
25
26
27
28
29
30
31
32
33
34
35
36
37
38
39
40
41
42
43
44
45
46
47
48
49
50
51
52
53
54
55
56
57
58
59
60
61
62
63
64
65

280 Higher VR values were obtained for the 10% substitution percentage. For 2 and 3
281 curing days, these values were higher than 100% (153.7% and 159.3%, respectively) and
282 the minimum value was obtained at 90 curing days (5.34%). The systems with 20% and
283 30% geopolymers were less effective. With 20% (CA20 samples), mortars had low
284 negative VR values (-9.1% and -7.92%, respectively), even at 28 and 90 days. The
285 samples with the 40% substitution yielded negative VR values for all the curing ages.
286 These negative values can be attributed to the poor workability of the RHA-containing
287 mortars, whereas the mixtures with the commercial reagent were easily compacted.

288 The good behaviour of RHA as silica source may be the result of a more enhanced
289 connectivity in microstructure of the samples activated with this material as said
290 Villaquirán- Caicedo in the paper published in 2019 [40]. The results were very
291 interesting from a practical viewpoint because mixtures can be obtained with good
292 compressive strength without using commercial sodium silicate, which is a synthetic
293 chemical reagent with a large carbon footprint, as previously reported [41]. The
294 replacement of commercial sodium silicate with RHA led to very good mortar
295 performance in terms of early-age compressive strength, which makes the small
296 geopolymer dose in the lime/pozzolan system more appealing.

297 3.2 Thermogravimetric studies

298 The lime-pozzolan (CON), lime-pozzolan/geopolymer (CC and CA samples) and
299 geopolymer (GEOP) pastes had the same proportions as the mortars, but without sand.
300 To simplify the study, it represented only the pastes with the 10% and 40% substitution
301 percentages, CON and GEOP. The selected curing ages were 3, 28 and 90 days. Figure 3
302 depicts the DTG curves.

303 Three principal zones of mass loss were observed in the CON paste, but a
304 continuous mass loss fell within the 100-600°C range. Zone 1 (100-180°C) was attributed
305 to the dehydration of CSH; zone 2 (180-300°C) was related to the dehydration of CASH
306 and CAH; zone 3 was assigned to the dehydroxylation of $\text{Ca}(\text{OH})_2$ [42]. The GEOP paste
307 had only one peak centred at about 150°C, attributed to the dehydration of the NASH gel
308 [43]. In the pastes with lime-pozzolan/geopolymer, peaks differed in accordance with the
309 substitution percentage. Pastes CC10 and CA10 with the 10% substitution looked a lot
310 like the CON paste, while pastes CC40 and CA40 with the 40% substitution had a similar
311 profile to the geopolymeric paste (GEOP).

312 The main peak in pastes CON, CC10 and CA10 at 3 and 7 curing days was centred
 313 in zone 2, and was attributed to the dehydration of CASH and CAH. At 90 days, a well-
 314 defined peak was seen for CSH dehydration on the DTG curves. The presence of hydrated
 315 lime was observed until 28 days for the control pastes, and in paste CC10 at 3 curing days.
 316 Hence, the reaction of hydrated lime to FCC was much faster when the geopolymer was
 317 present.

318 The principal peak in GEOP, CC40 and CA40 at all the curing ages was centred
 319 at about 150°C. This peak was attributed to the NASH gel for GEOP and a mixture of
 320 NASH and C(N)ASH gels for CC40 and CA40. The peak in paste GEOP was much wider
 321 than that in pastes CC40 and CA40. The NASH gel probably had a higher temperature
 322 decomposition range than the C(N)ASH gel.

323 The mass losses within the different temperature ranges were analysed to
 324 understand the evolution of the geopolymeric and pozzolanic reactions. The chosen mass
 325 loss zones were: 50°C to 180 °C (ML₁); 80°C to 300°C (ML₂); total mass loss went from
 326 35°C to 600°C (ML_T). Table 4 summarises the results.

327 **Table 4.** Mass loss (TG analysis) of pastes for 3, 28 and 90 curing days.

| | ML₁ (50-180°C) | ML₂ (180-300°C) | ML_T (35-600°C) |
|-----------------|--|---|--|
| CON 3d | 2.14 | 4.21 | 15.88 |
| CON 28d | 4.44 | 8.61 | 20.61 |
| CON 90d | 5.69 | 8.36 | 18.67 |
| CC10 3d | 3.49 | 4.87 | 15.43 |
| CC10 28d | 4.70 | 7.07 | 16.75 |
| CC10 90d | 5.43 | 8.09 | 18.05 |
| CA10 3d | 3.68 | 5.97 | 12.00 |
| CA10 28d | 4.28 | 10.17 | 18.59 |
| CA10 90d | 4.88 | 6.63 | 15.12 |
| CC40 3d | 6.12 | 3.79 | 14.67 |
| CC40 28d | 6.57 | 4.86 | 16.04 |
| CC40 90d | 6.92 | 4.13 | 15.27 |
| CA40 3d | 5.24 | 3.83 | 13.04 |
| CA40 28d | 5.32 | 3.78 | 13.51 |
| CA40 90d | 6.48 | 4.10 | 14.66 |
| GEOP 3d | 7.96 | 3.94 | 14.07 |
| GEOP 28d | 9.23 | 4.25 | 15.49 |
| GEOP 90d | 9.38 | 3.69 | 15.19 |

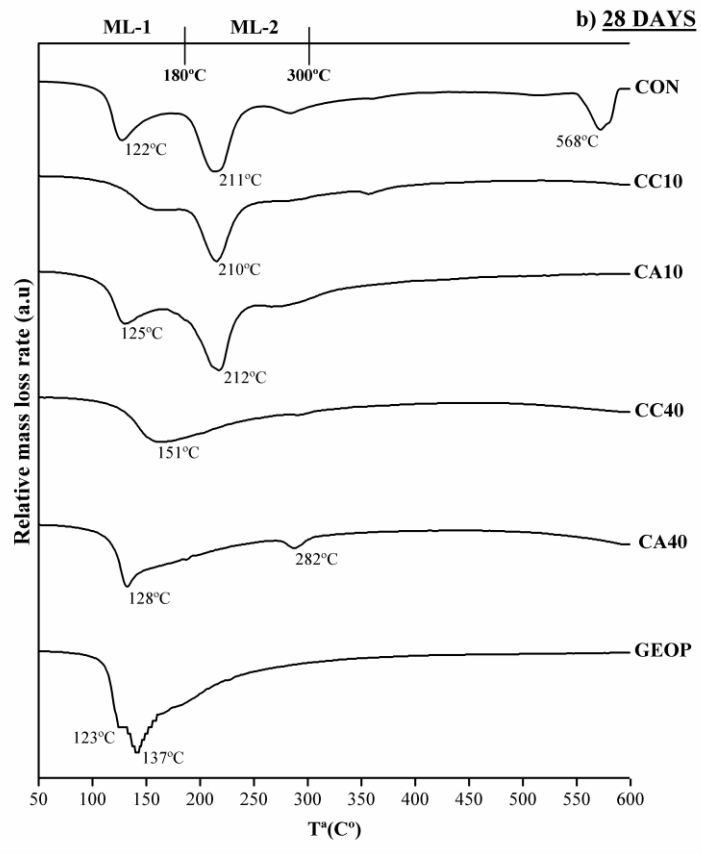
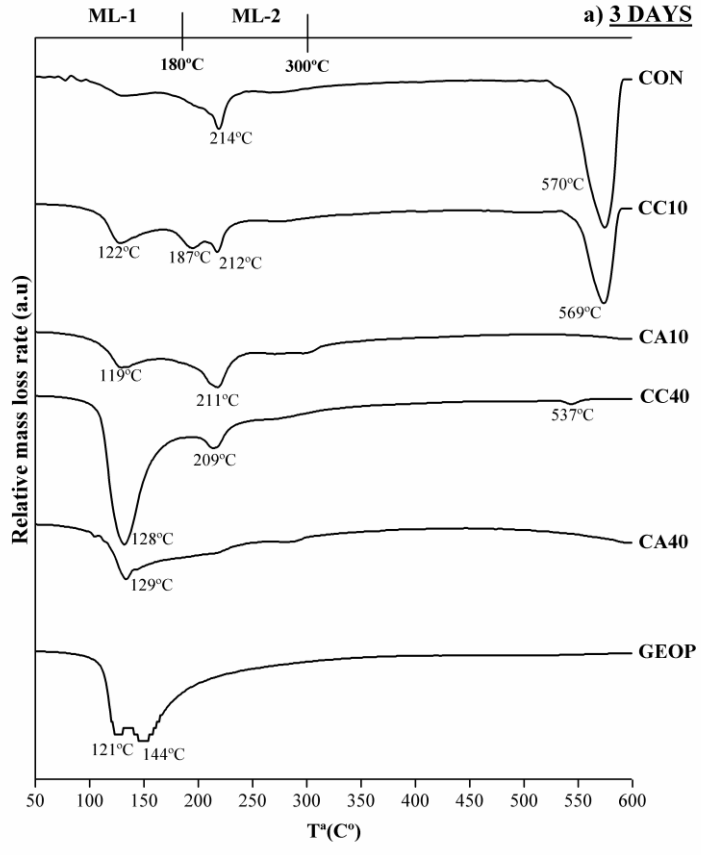
328 For the pastes in which the geopolymer reaction was the principal reaction and the
 329 gel C(N)ASH or NASH were the main products, the mass loss within the ML₁ range was
 330 greater than within the ML₂ range. The mass loss within interval ML₂ was, in this case,

1 331 attributed to the same product as the decomposition peak was wide. The geopolymer
2 332 reaction was the predominant reaction in pastes GEOP, CC40 and CA40 as the activator
3 333 concentration was higher than that in the samples with only the 10% substitution. This
4 334 conclusion falls in line with previously reported papers [28, 29, 44], which studied
5 335 lime/MK mixtures at different sodium hydroxide concentrations. When the activator
6 336 concentration was low, the principal reaction product was CSH; when the concentration
7 337 was high, the main product was the C(N)ASH gel and CSH formed as a secondary
8 338 reaction product.

9 339 In the paper published in 2013 by García-Lodeiro et al.[38] the authors explained
10 340 the conversion of NASH gel into C(N)ASH gel. The presence of a solution enriched with
11 341 Al(OH)_4^- and Si(OH)_4 species, in addition to the presence of sodium ions, induced this
12 342 type of NASH gel. Depending on the calcium concentration in the medium, total
13 343 conversion into CASH gel can take place.

14
15
16
17
18
19
20
21
22
23
24
25
26
27
28
29
30
31
32
33
34
35
36
37
38
39
40
41
42
43
44
45
46
47
48
49
50
51
52
53
54
55
56
57
58
59
60
61
62
63
64
65

1
2
3
4
5
6
7
8
9
10
11
12
13
14
15
16
17
18
19
20
21
22
23
24
25
26
27
28
29
30
31
32
33
34
35
36
37
38
39
40
41
42
43
44
45
46
47
48
49
50
51
52
53
54
55
56
57
58
59
60
61
62
63
64
65



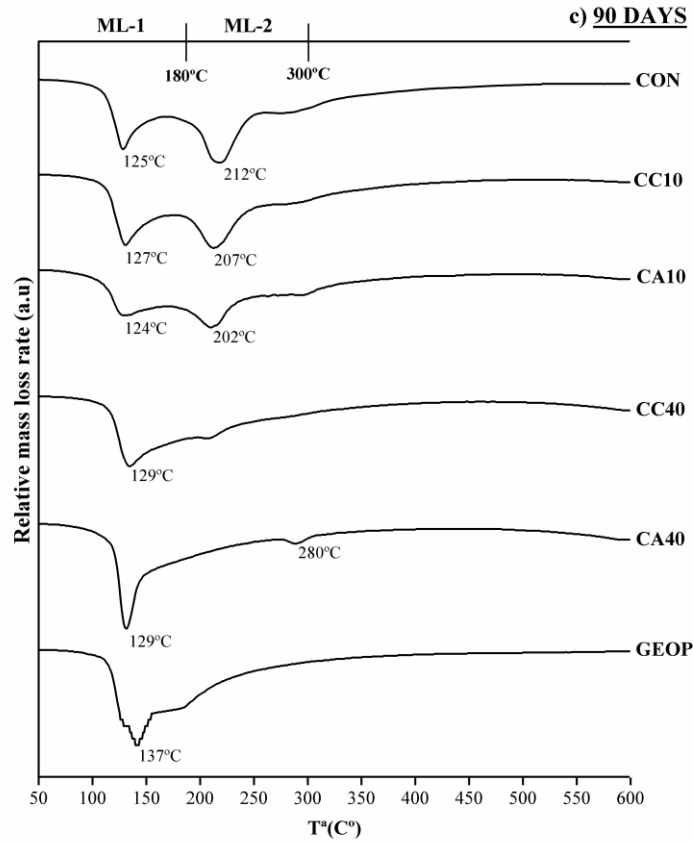


Figure 3. DTG curves for the pastes cured at: a) 3; b) 28; and c) 90 curing days.

To analyse the role of calcium in a geopolymeric paste, a paste (GEOP-CH) was fabricated by mixing 80% GEOP paste (FCC with NaOH and Na₂SiO₃ as an alkaline activator) and 20% hydrated lime. The first problem was that this paste (GEOP-CH) needed water, which was added because it was impossible to prepare paste at the 0.6 water/FCC ratio (lack of workability), and the new water/FCC ratio was increased to 1.1. The paste was analysed after 7 curing days. Figure 4 represents the DTG curves for pastes GEOP and GEOP-CH. GEOP-CH did not present a peak for the dehydroxylation of hydrated lime within the 500-600°C range. The calcium from the hydrated lime was incorporated into the aluminosilicate gel. Its decomposition peak fell within the same decomposition temperature range observed for the paste without hydrated lime.

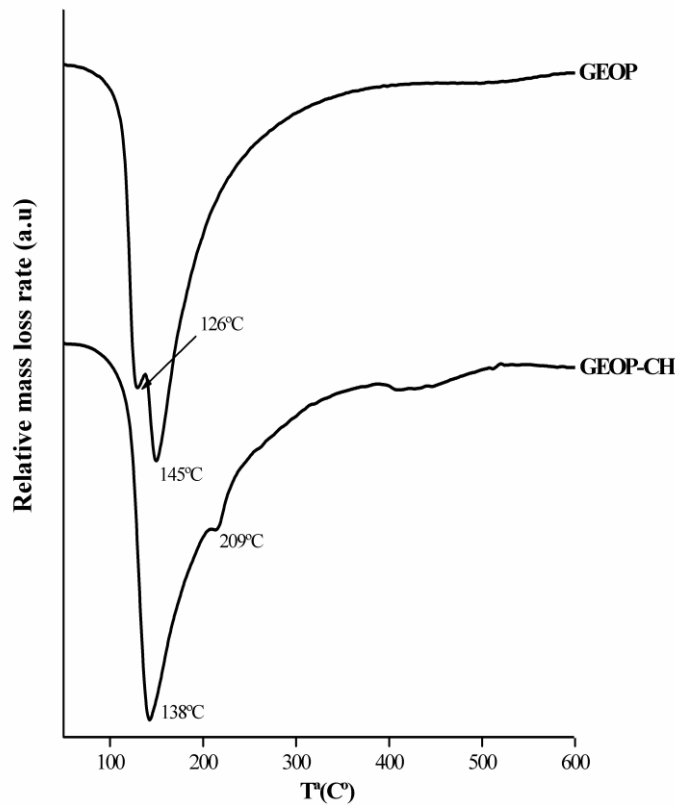


Figure 4. DTG curves for pastes GEOP and GEOP-CH after 7 curing days.

3.3 FTIR studies

Figure 5 illustrates the evolution of the reaction process for pastes CON, CC10, CA10, CC40, CA40 and GEOP at 3, 28 and 90 curing days by the FTIR technique.

The evolution of lime/pozzolan paste is represented in Figure 5.a, and the principal peaks were: i) presence of carbonates and carboaluminates (bands at 1,700, 1,435 and 875 cm^{-1}). The asymmetric stretching vibrations of the C-O group were represented at a wave number of around 1,435 cm^{-1} and the band at 875 cm^{-1} corresponded to the bending mode of the carbonate ion [40, 45]; ii) the bands of CSH caused by the bending of SiO_4 tetrahedral units fell within an approximate range of 400-500 cm^{-1} and the asymmetric Si-O stretching vibration of the CSH within the 1,100-960 cm^{-1} interval [42,46]; iii) the presence of the signals attributed to vibrations Si-O-Si, Si-O-Al and Al-O at 528 and 709 cm^{-1} as a result of the presence of CASH and CAH [42,47,48]. The presence of carbonates could be due to a number of factors: presence of calcite in the hydrated lime; formation of carboaluminate by a reaction of carbonate and the alumina of FCC; carbonation of reaction products. The band of the asymmetric Si-O stretching vibration

1
2
3
4
5
6
7
8
9
10
11
12
13
14
15
16
17
18
19
20
21
22
23
24
25
26
27
28
29
30
31
32
33
34
35
36
37
38
39
40
41
42
43
44
45
46
47
48
49
50
51
52
53
54
55
56
57
58
59
60
61
62
63
64
65

370 of CSH for the samples cured for 3 days was located at a higher wave number than for
371 the pastes cured for 28 and 90 days.

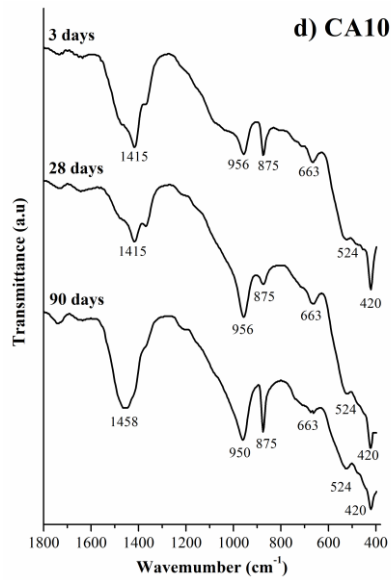
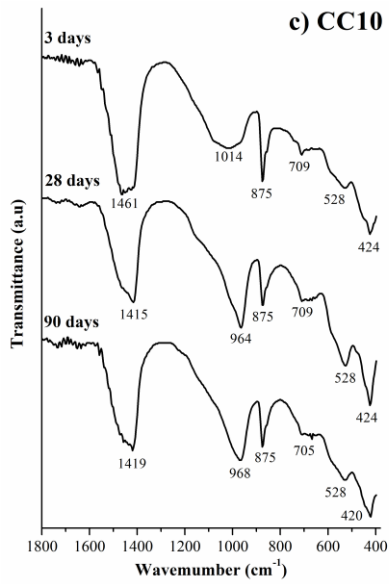
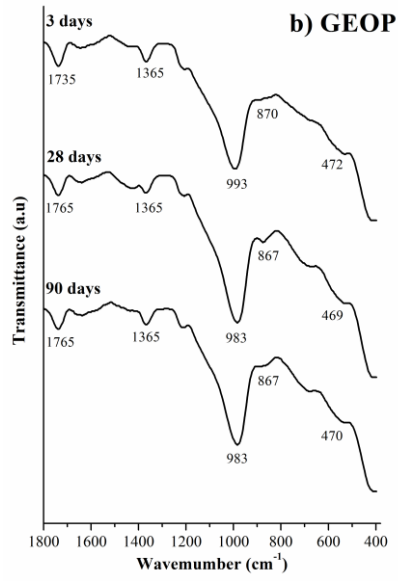
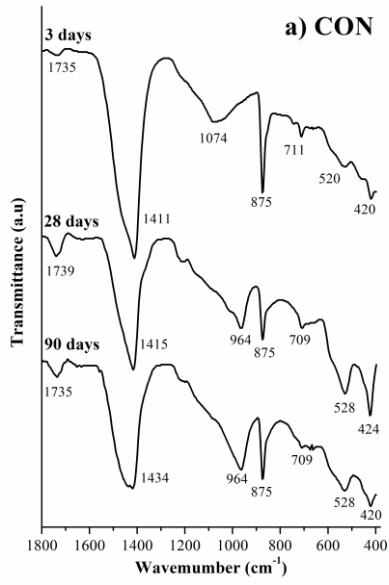
372 The geopolymeric paste is represented in Figure 5.b. The observed principal peak
373 was due to the presence of the NASH gel, with a band at $983\text{-}993\text{ cm}^{-1}$ for the
374 geopolymeric binder. A high-intensity broad band of between $1,200\text{-}900\text{ cm}^{-1}$ was
375 identified, which corresponded to the asymmetrical stretching of Si-O-T (T = Si or Al
376 bonds [40]). In particular, the SiQ^2 unit showed infrared absorption at around 950 cm^{-1} .
377 The bands at $1,735$ and $1,365\text{ cm}^{-1}$ were attributed to the presence of carbonate [47,48].
378 The bands with lesser intensity, around 867 cm^{-1} , were identified as Si-O stretching and
379 OH bending (Si-OH). The peak was attributed to bending bands (Si-O-Si and O-Si-O)
380 with those at around 470 cm^{-1} [49].

381 The pastes containing 10% geopolymer showed similar peaks to the lime-
382 pozzolan paste. These peaks were located at around $1,460\text{-}1,420$, $1,014\text{-}950$, 875 and 435-
383 420 cm^{-1} . Allali et al.[26] established that when the MK geopolymer included calcium in
384 the system, the Si-O-Si band was displaced from 985 cm^{-1} to an Si-O-Ca band at 930 cm^{-1} .
385 In the present research, this displacement was especially observed for the CA sample
386 at 90 curing days. The corresponding band was found at 950 cm^{-1} , and significantly
387 differed from that for the CC sample (968 cm^{-1}). This meant that the presence of a
388 different source of silica in the geopolymer changed the final geopolymeric gel structure.

389 For the CC40 paste, the signal attributed to the gel (NASH) was found at 968 cm^{-1}
390 (after 90 curing days). For the CA40 paste, the corresponding signal was displaced at a
391 lower wave number (950 cm^{-1}). Once again, the different source of silica modified the
392 gel's nature.

393 García Lodeiro et al. established that adding Ca to the NASH gel would change
394 the orientation of the structure, but this change was not easily observed by FTIR [50].

1
2
3
4
5
6
7
8
9
10
11
12
13
14
15
16
17
18
19
20
21
22
23
24
25
26
27
28
29
30
31
32
33
34
35
36
37
38
39
40
41
42
43
44
45
46
47
48
49
50
51
52
53
54
55
56
57
58
59
60
61
62
63
64
65



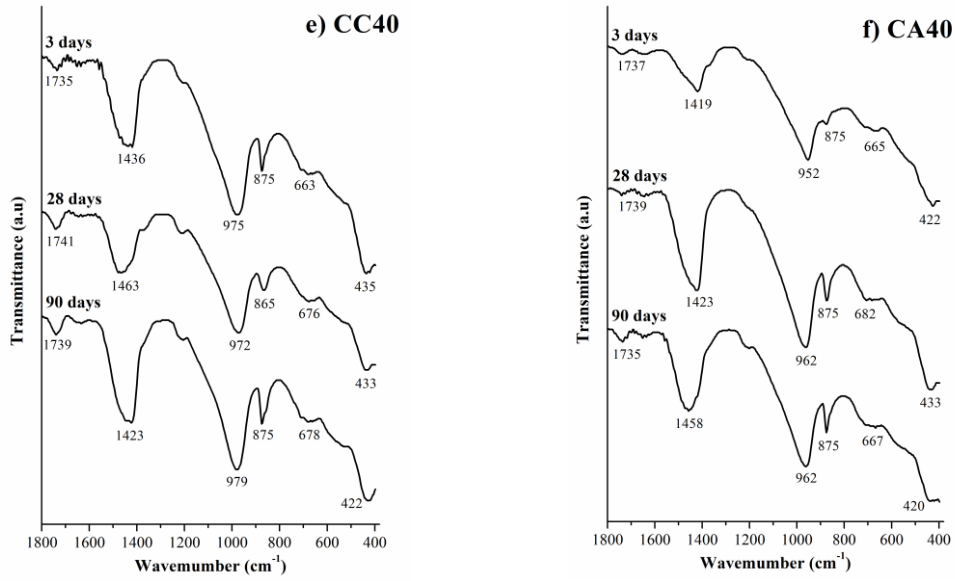


Figure 5. FTIR curves for the pastes cured at 3, 28 and 90 days

395

396 Paste GEOP-CH was also studied by FTIR. Figure 6 represents pastes GEOP-CH
 397 and GEOP at 7 curing days. A displacement of the band (995 cm^{-1} vs. 948 cm^{-1}) related
 398 to the NASH gel took place in the paste with lime (GEOP-CH). This spectrum confirmed
 399 the incorporation of Ca into the aluminosilicate gel's structure.

400

401

1
2
3
4
5
6
7
8
9
10
11
12
13
14
15
16
17
18
19
20
21
22
23
24
25
26
27
28
29
30
31
32
33
34
35
36
37
38
39
40
41
42
43
44
45
46
47
48
49
50
51
52
53
54
55
56
57
58
59
60
61
62
63
64
65

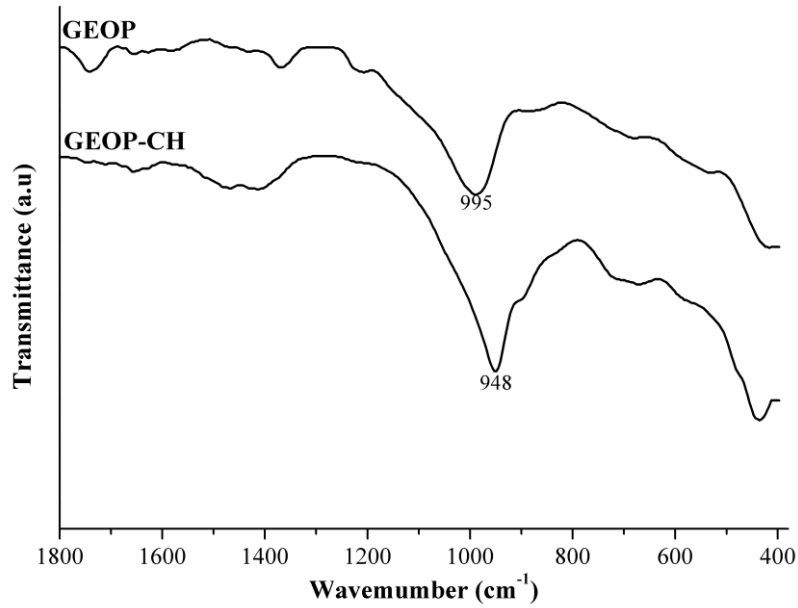


Figure 6. FTIR curves for GEOP and pastes GEOP-CH after 7 curing days.

402

403 3.4 XRD studies

404 The X-ray diffraction patterns are depicted in Figures 7-10. Pastes CON, CC10,
 405 CC40, CA10 and CA40 were studied by comparing 3, 28 and 90 curing days, and pastes
 406 GEOP and GEOP-CH were also compared. In general, a baseline deviation within the
 407 $2\Theta=20^\circ - 40^\circ$ range in all the studied pastes suggested the presence of an amorphous
 408 phase. With the progress made in curing time, the baseline deviation was more evident
 409 given the progress made in the geopolymerization reaction. Table 5 summarises the
 410 employed key, name of phases, chemical formula and PDF Card for the mineral phases
 411 found in the pastes.

412

413

414

415

416

417

418

419 **Table 5.** PDF Card of the phases and chemical formula of phases present in pastes.

| Key | Phase | Chemical formula | PDF Card |
|-----|----------------|--|----------|
| P | Portlandite | Ca(OH) ₂ | #040733 |
| S | Strätlingite | Ca ₂ Al ₂ SiO ₇ .8H ₂ O | #290285 |
| Q | Quartz | SiO ₂ | #331161 |
| A | Albite | NaAlSi ₃ O ₈ | #191184 |
| M | Mullite | Al ₆ Si ₂ O ₁₃ | #150776 |
| C | Calcite | CaCO ₃ | #050586 |
| L | Carboaluminate | Ca ₄ Al ₂ O ₆ CO ₃ .11H ₂ O | #410210 |
| B | Carboaluminate | Ca ₈ Al ₄ O ₁₄ CO ₂ .24H ₂ O | #360129 |
| Z | Zeolite A | Na ₂ Al ₂ Si _{3.3} O _{10.6} .7H ₂ O | #120228 |
| T | Trona | Na ₃ H(CO ₃) ₂ .2H ₂ O | #291447 |
| W | Wollastonite | CaSiO ₃ | #100489 |
| V | Vaterite | CaCO ₃ | #240030 |
| X | Zeolite X type | Na ₂ Al ₂ Si _{2.4} O _{8.8} .6.7H ₂ O | #120246 |
| Za | Zeolite ZK5 | 2.85Na ₂ O.1.89Al ₂ O ₃ .7.92SiO ₂ .12.2H ₂ O | #370360 |
| Cr | Cristobalite | SiO ₂ | #391425 |
| F | Faujasite | Na ₂ Al ₂ Si ₄ O ₁₂ .8H ₂ O | #391380 |

420

421 Figure 7 shows the XRD patterns of paste CON (lime-pozzolan) after 3, 28 and
 422 90 curing days. The peaks of the non-reacted portlandite (P) were observed after 3 curing
 423 days. Characteristic peaks of albite (A) and traces of faujasite were also found. It was
 424 noteworthy that calcite was not present in the CON paste at an early age and carbonate
 425 was combined with aluminium as carboaluminates (characteristic L and B peaks). Other
 426 authors have made these observations in lime-pozzolan samples [51,52]. After 28 curing
 427 days, less intense portlandite peaks were detected as the FCC reaction progressed, and no
 428 faujasite peaks appeared in the XRD pattern. Traces of quartz (Q), A and mullite (M)
 429 were also observed. Characteristic strätlingite (S) peaks were noted in the CON paste at
 430 this age, which confirmed the peak observed on the DTG curves within the 210-280°C
 431 temperature range. This compound is typical in lime-pozzolan materials with a high
 432 aluminium content [52,53], as for FCC (Al₂O₃ = 49.26 %; see Table 1). After 90 curing
 433 days, the diffractogram of paste CON was similar to that for 28 curing days. To a large
 434 extent, the P peaks had mitigated and the main S peak appeared more intensely, which

435 suggests high pozzolanic reactivity with curing time. A broad peak was seen within the
 436 28.5°-29.5° 2 θ range, which suggests the presence of the CSH/CASH gel, especially after
 437 90 curing days.

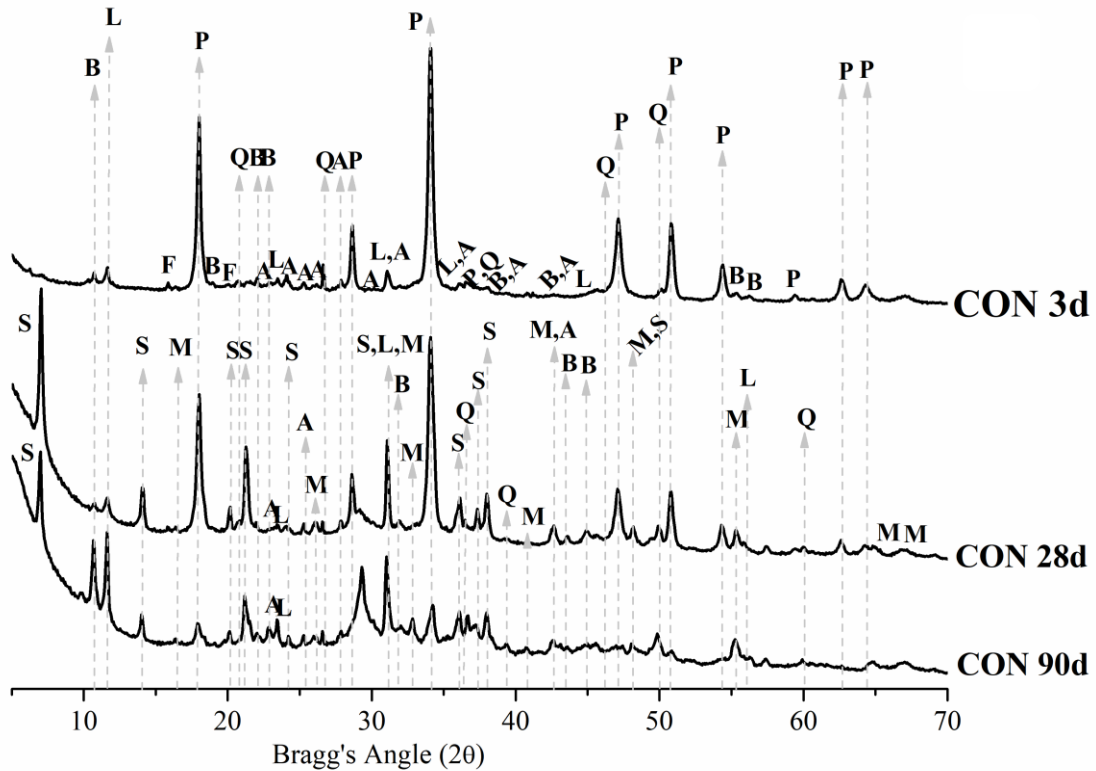


Figure 7. XRD patterns of the CON paste after 3, 28 and 90 days

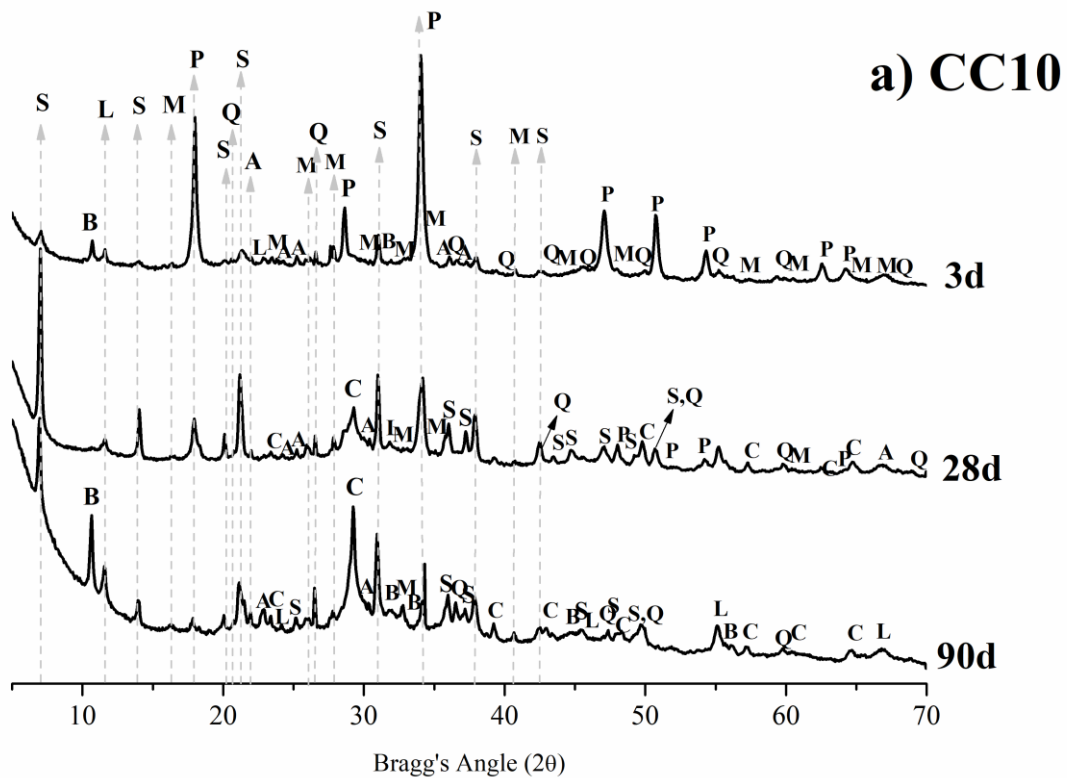
438
 439 Figures 8-9 show the XRD patterns of the lime-pozzolan/geopolymer activated
 440 with the alkali solution prepared by using commercial sodium silicate and RHA,
 441 respectively. The pastes with 10% geopolymer (CC10 or CA10) and with 40%
 442 geopolymer (CC40 or CA40) were tested and analysed after 3, 28 and 90 curing days.

443 In paste CC10 (Figure 8a), the main characteristics peaks were P and S at 28 at 90
 444 curing day. Strätlingite (S) was attributed to the pozzolanic reaction. As with the CON
 445 paste, the intensity of the peaks corresponding to P and S diminished and increased,
 446 respectively, with curing time. Minority peaks (Q and A) were present at the three
 447 analysed curing times. Carboaluminate peaks (L and B) were found, whose intensity
 448 increased with time. Calcite (C) peaks were also found after 28 and 90 curing days. In
 449 this case, the broad peak related to CSH/CASH, together with the main C peak whose

450 intensity was significant after 28 days, which was earlier than for CON and suggests a
 451 faster reaction rate for this gel type to form.

452 When the 40% geopolymer was employed (CC40), the portlandite peaks were low
 453 in intensity (especially for 90 curing days) and the peak of the CSH/CASH gel was strong
 454 in this XRD pattern. A new crystalline phase Z (Zeolite A) was also detected, mainly at
 455 90 curing days. The formation of Zeolite A and Zeolite X has been reported in other
 456 papers in which geopolymers were prepared with the activation of MK/RHA [54]. As the
 457 CC10 paste pattern shows, traces of Q and A and B/L carboaluminate peaks were present
 458 throughout the three analysed ages for paste CC40. No S was detected in this paste, which
 459 suggests that its formation by the pozzolanic reaction was not favourable, and gels NASH
 460 or C(N)ASH should be preferably produced, as corroborated by the large broad peak
 461 shown (28.5°-29.5° 2 θ ,) after 3 curing days.

462



463

1
2
3
4
5
6
7
8
9
10
11
12
13
14
15
16
17
18
19
20
21
22
23
24
25
26
27
28
29
30
31
32
33
34
35
36
37
38
39
40
41
42
43
44
45
46
47
48
49
50
51
52
53
54
55
56
57
58
59
60
61
62
63
64
65

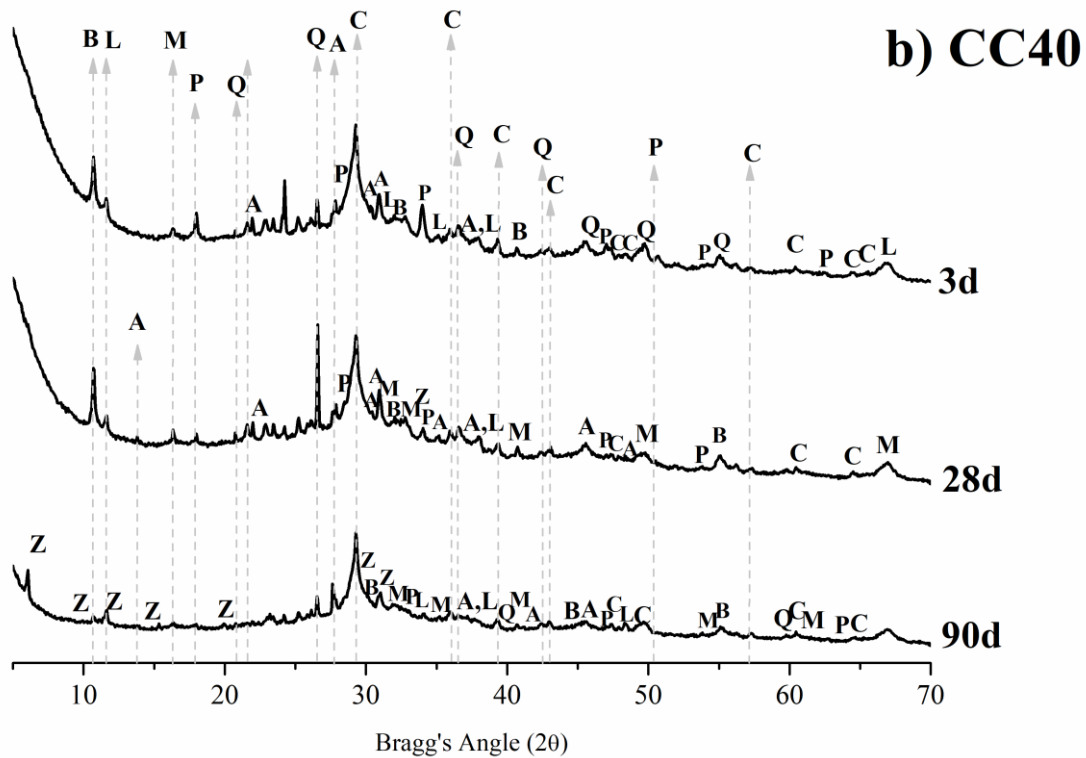
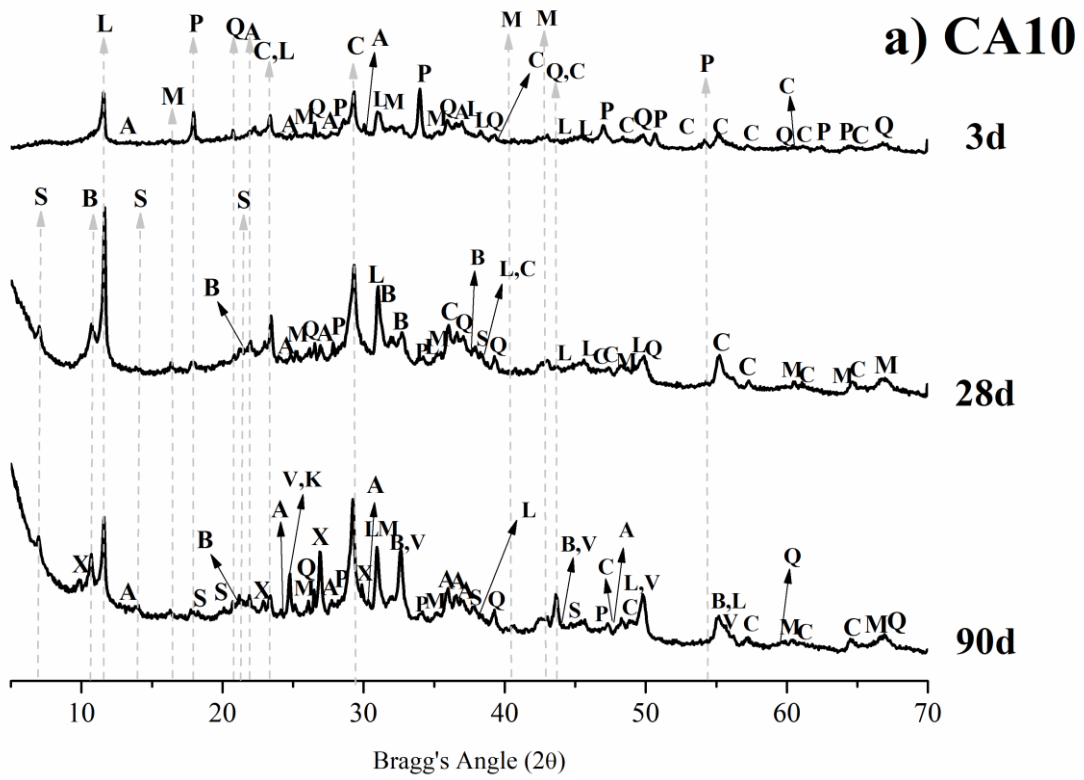
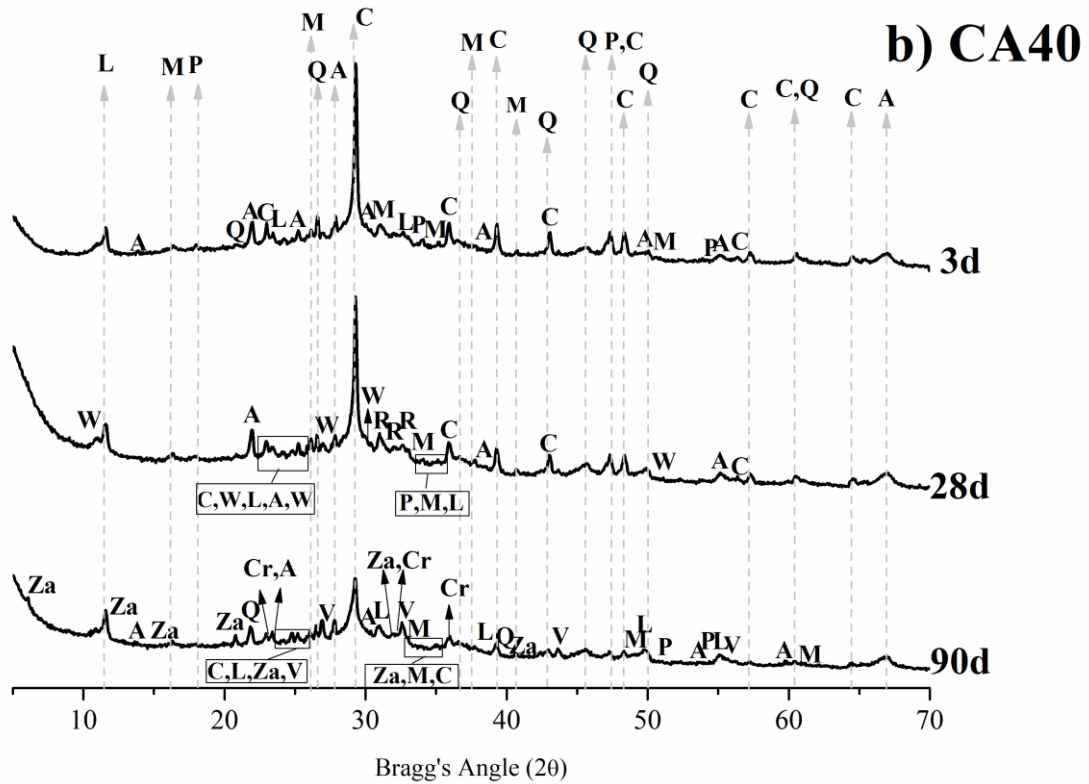


Figure 8. XRD patterns of the lime-pozzolan/geopolymer pastes activated with the alkali solution prepared using commercial sodium silicate (CC) after 3, 28 and 90 days: a) paste CC10; b) paste CC40.

When RHA was employed as the silica source in the alkali activator for the lime-pozzolan/geopolymer systems, changes were evidenced in the XRD patterns. Figures 9a and 9b show the patterns for paste CA10 and paste CA40, respectively. We can see that the signals corresponding to P for the 10% geopolymer paste were not intense after 28 curing days, unlike CC10, which suggests that the presence of RHA favoured the pozzolanic reaction rate. The signals for S were also slightly intense after 28 and 90 days, which indicates that S formation was not favoured. Probably due to the presence of amorphous SiO_2 in RHA, the pozzolanic reaction was activated and more CSH was formed. The main signal for this gel was considerably intense in the XRD pattern in CA10. The broad peak related to the presence of gel was intense after 3 curing days. Some traces of zeolite X (X) were identified after 90 curing days. For paste CA40, the intensity of the P signals in the XRD pattern were very low at the early curing age and a baseline deviation appeared within the 28-32° 2θ range in relation to the formed gels (NASH, C(N)ASH, CSH). Some zeolitic structures (Z) appeared after 90 curing days.



483

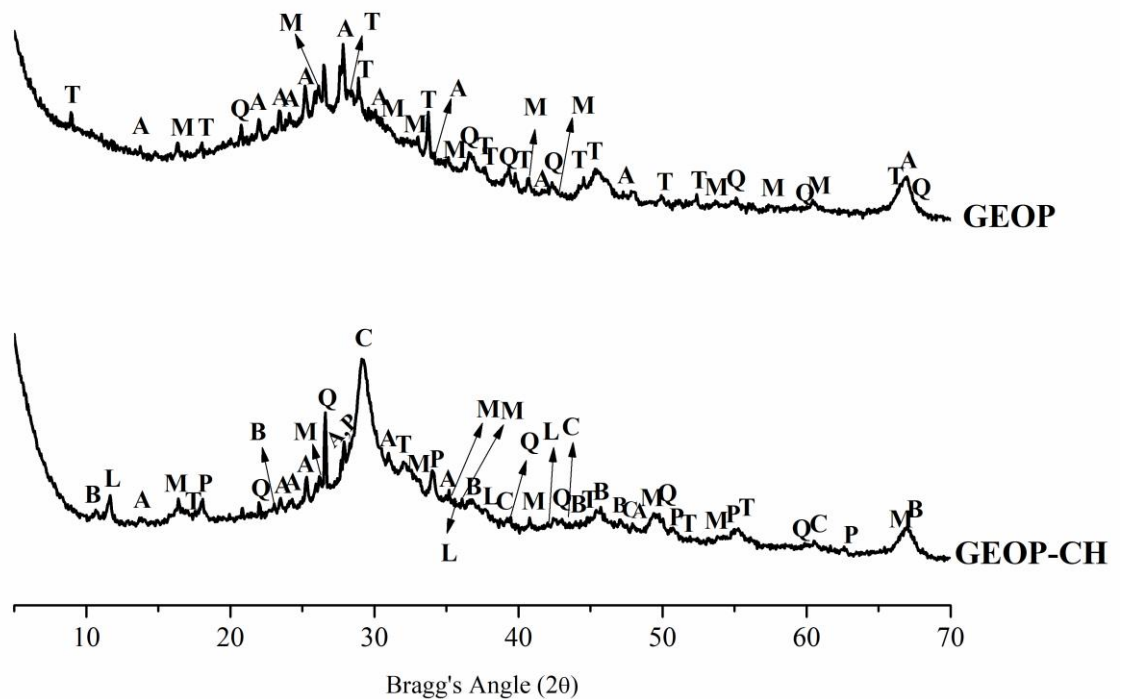


484

485 **Figure 9.** XRD patterns of the lime-pozzolan/geopolymer pastes activated with the
 486 alkali solution prepared by using RHA (CA pastes) after 3, 28 and 90 days: a) paste
 487 CA10; b) paste CA40.

488

489 The XRD patterns (Figure 10) of GEOP and GEOP-CH at 28 days displayed
 490 major changes. A baseline deviation was observed in GEOP and GEOP-CH, with a
 491 relative high intensity of peaks Q, M and A due to the crystalline phases from FCC. The
 492 F peaks disappeared in these two pastes, which indicated that the zeolitic fraction of FCC
 493 was highly reactive. Excess sodium ions favoured the formation of trona (T) in paste
 494 GEOP. In this case, the nature of the gel, mainly NASH, was shown as a baseline
 495 deviation within the 20-32° range. Due to calcium addition, carboaluminate peaks (L and
 496 B) were identified in the GEOP-CH pattern. In this case, the baseline deviation was strong
 497 and the broadness within the 25-32° range indicates CASH/C(N)ASH formation. This
 498 means that if a large amount of calcium is present, CASH/C(N)ASH gels form. They are
 499 easily observed in the XRD patterns for CC10, CC40, CA10 and CA40. It was more
 500 difficult to identify the presence of NASH because this gel showed less intensity and a
 501 more broadly shaped diffraction signal.

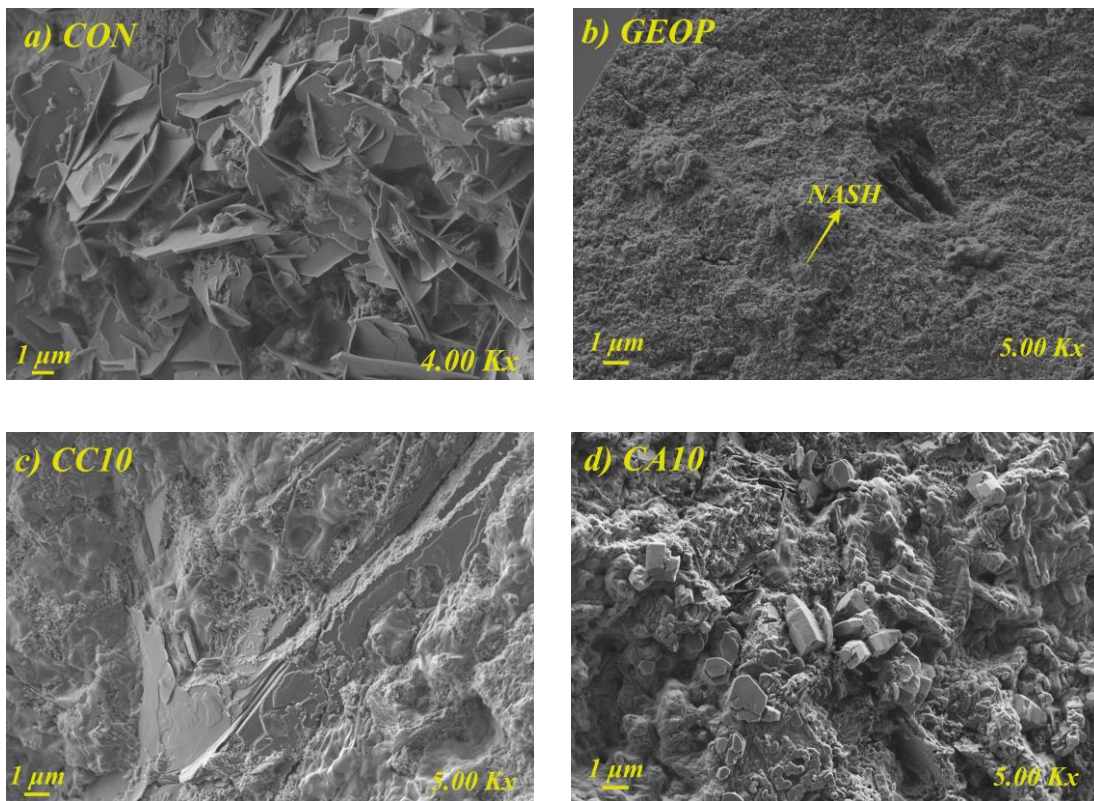


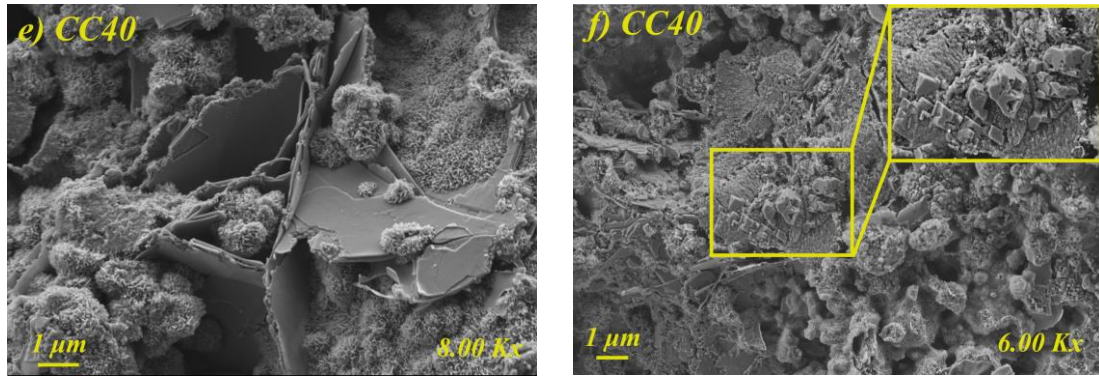
502
 503 **Figure 10.** XRD patterns for pastes GEOP and GEOP-CH after 28 curing days.

506 3.5 FESEM studies

507 The FESEM images for all the pastes cured for 28 days are depicted in Figure 11.
508 In the lime-pozzolan paste (CON), the typical reaction product from the pozzolanic
509 process was observed (Figure 11.a) (strätlingite) [53] Figure 11.b represents the GEOP
510 paste, where the paste's microstructure was denser and the principal formed product was
511 the NASH gel [55, 56].

512 In pastes CC10 and CA10 (Figures 11.c and 11.d), products were observed with a
513 different appearance to those for pastes CON and GEOP. In these pastes, pozzolanic and
514 geopolymeric products probably coexisted. Finally, in pastes CC40 and CA40 (Figures
515 11.e and 11.f), the principal reaction product was C(N)ASH gel, although some NASH
516 gel was probably present. Duramae et al reported C(N)ASH formation as a result of partial
517 NASH substitution in the system [57]. In the CA40 paste, the formation of little cubic-
518 shape particles took place, which may be attributed to the presence of zeolite A [58].





519 **Figure 11.** FESEM micrographs for pastes after 28 curing days: a) CON; b)
 520 GEOP; c) CC10; d) CA10; e) CC40; f) CA40.

521 **4 CONCLUSIONS**

522 The mechanical behaviour and microstructure of lime-pozzolan/geopolymer
 523 mixtures were analysed, in which pozzolan and the precursor were the same
 524 aluminosilicate waste (spent FCC catalyst).

525 The changes in the lime-pozzolan system made by adding the geopolymeric
 526 binder were highly positive in compressive strength development terms for mortars:

- 527 • It is highlighted the strength improvement at short times thus, the mortars
 528 with a 10-40% replacement of lime-pozzolan binder with geopolymer,
 529 prepared with the NaOH/waterglass solution, yielded strength values
 530 within the 9-25 MPa range at 7 curing days *versus* 3.59 MPa for the lime-
 531 pozzolan mortar.
- 532 • For the long curing time (90 days), the 10% geopolymer mortar was 50%
 533 higher than the lime-pozzolan one, and the 40% geopolymer mortar was
 534 almost double.

535 The contribution of RHA as a silica source in the alternative alkali activator was
 536 remarkably positive compared to the commercial chemical reagent (waterglass),
 537 especially at early curing ages (1-3 days) for the smallest geopolymer addition (10%).
 538 Apparently, the reason for the different nature of the binding gel formed when RHA was
 539 present was responsible for the achieved higher strength.

540 The addition of a geopolymer to a lime-pozzolan system brings about significant
 541 changes in the nature of hydration products:

1
2
3
4
5
6
7
8
9
10
11
12
13
14
15
16
17
18
19
20
21
22
23
24
25
26
27
28
29
30
31
32
33
34
35
36
37
38
39
40
41
42
43
44
45
46
47
48
49
50
51
52
53
54
55
56
57
58
59
60
61
62
63
64
65

1
2
3
4
5
6
7
8
9
10
11
12
13
14
15
16
17
18
19
20
21
22
23
24
25
26
27
28
29
30
31
32
33
34
35
36
37
38
39
40
41
42
43
44
45
46
47
48
49
50
51
52
53
54
55
56
57
58
59
60
61
62
63
64
65

- 542 • The hydration of lime-pozzolan systems produces typical products:
543 CSH/CASH gel, calcium carboaluminate hydrates and S, as well as
544 unreacted portlandite at early (3 days) and mid-term (28 days) curing ages.
- 545 • The addition of 10% geopolymer slightly modified the nature of hydration
546 products. However, the reaction rate rose and portlandite consumption was
547 significantly higher.
- 548 • The addition of 40% geopolymer led to a more marked modification in the
549 nature of hydration products: a NASH/C(N)ASH gel was formed, and no
550 presence of S and portlandite was detected.

551 In summary, adding geopolymer to a lime-pozzolan system is a good proposal for
552 improving the early- and long-term strength performance of mortars. Using RHA as an
553 alternative silica source for replacing waterglass has a very high potential to avoid or to
554 reduce employing synthetic chemical reagents that have a significant carbon footprint.

Acknowledgements

This research was supported by Centro de Cooperación al Desarrollo (CCD) of the Universitat Politècnica de València, ADSIDEO-COOPERACION 2017 Program “Reutilización de residuos agrícolas e industriales para la fabricación de conglomerantes sostenibles en países en desarrollo (AD1708)”. The investigation is framed within the ECOSOST (RTI2018-097612-B-C21-AR) project supported by MINECO and FEDER funds. The authors are grateful to the Electron Microscopy Service of the Universitat Politècnica de València, Dacsa Group S.A., Cales Pascual S.L. and BP Oil España S.A.U.

Bibliography

- [1] P. Maravelaki-Kalaitzaki, A. Bakolas, A. Moropoulou, Physico-chemical study of Cretan ancient mortars, *Cement and Concrete Research*. 33 (2003) 651–661. doi:10.1016/S0008-8846(02)01030-X.
- [2] A.M. Neville, *Properties of concrete*, Fifth, Pearson Education Limited, England, 1982. doi:10.4135/9781412975704.n88.
- [3] D.A. Silva, H.R. Wenk, P.J.M. Monteiro, Comparative investigation of mortars from Roman Colosseum and cistern, *Thermochimica Acta*. 438 (2005) 35–40. doi:10.1016/j.tca.2005.03.003.
- [4] G. Cook, J.P. Ponsard, A proposal for the renewal of sectoral approaches building on the cement sustainability initiative, *Climate Policy*. 11 (2011) 1246–1256. doi:10.1080/14693062.2011.602552.
- [5] L.K. Turner, F.G. Collins, Carbon dioxide equivalent (CO₂-e) emissions: A comparison between geopolymers and OPC cement concrete, *Construction and Building Materials*. 43 (2013) 125–130. doi:10.1016/j.conbuildmat.2013.01.023.
- [6] R. Maddalena, J.J. Roberts, A. Hamilton, Can Portland cement be replaced by low-carbon alternative materials? A study on the thermal properties and carbon emissions of innovative cements, *Journal of Cleaner Production*. 186 (2018) 933–942. doi:10.1016/j.jclepro.2018.02.138.
- [7] S. Xu, J. Wang, Q. Ma, X. Zhao, T. Zhang, Study on the lightweight hydraulic mortars designed by the use of diatomite as partial replacement of natural hydraulic lime and masonry waste as aggregate, *Construction and Building Materials*. 73 (2014) 33–40. doi:10.1016/j.conbuildmat.2014.09.062.

- 1
2
3
4
5
6
7
8
9
10
11
12
13
14
15
16
17
18
19
20
21
22
23
24
25
26
27
28
29
30
31
32
33
34
35
36
37
38
39
40
41
42
43
44
45
46
47
48
49
50
51
52
53
54
55
56
57
58
59
60
61
62
63
64
65
- [8] N. Billong, U.C. Melo, E. Kamseu, J.M. Kinuthia, D. Njopwouo, Improving hydraulic properties of lime-rice husk ash (RHA) binders with metakaolin (MK), *Construction and Building Materials*. 25 (2011) 2157–2161. doi:10.1016/j.conbuildmat.2010.11.013.
- [9] E.R. Grist, K.A. Paine, A. Heath, J. Norman, H. Pinder, Compressive strength development of binary and ternary lime-pozzolan mortars, *Materials and Design*. 52 (2013) 514–523. doi:10.1016/j.matdes.2013.05.006.
- [10] R. Méndez, M. V. Borrachero, J. Payá, J. Monzó, Mechanical strength of lime-rice husk ash mortars: A preliminary study, *Key Engineering Materials*. 517 (2012) 495–499. doi:10.4028/www.scientific.net/KEM.517.495.
- [11] A. Palomo, P. Monteiro, P. Martauz, V. Bilek, A. Fernandez-Jimenez, Hybrid binders: A journey from the past to a sustainable future (opus caementicium futurum), *Cement and Concrete Research*. 124 (2019). doi:10.1016/j.cemconres.2019.105829.
- [12] M.D. Jackson, S.R. Chae, S.R. Mulcahy, C. Meral, R. Taylor, P. Li, A.H. Emwas, J. Moon, S. Yoon, G. Vola, H.R. Wenk, P.J.M. Monteiro, Unlocking the secrets of Al-tobermorite in Roman seawater concrete, *American Mineralogist*. 98 (2012) 1669–1687. doi:10.2138/am.2013.4484.
- [13] M.D. Jackson, J. Moon, E. Gotti, R. Taylor, S.R. Chae, M. Kunz, A.H. Emwas, C. Meral, P. Guttman, P. Levitz, H.R. Wenk, P.J.M. Monteiro, Material and elastic properties of Al-tobermorite in ancient roman seawater concrete, *Journal of the American Ceramic Society*. 96 (2013) 2598–2606. doi:10.1111/jace.12407.
- [14] J.L. Provis, Alkali-activated materials, *Cement and Concrete Research*. 114 (2018) 40–48. doi:10.1016/j.cemconres.2017.02.009.
- [15] S. Seifi, N. Sebaibi, D. Levacher, M. Boutouil, Mechanical performance of a dry mortar without cement, based on paper fly ash and blast furnace slag, *Journal of Building Engineering*. 22 (2019) 113–121. doi:10.1016/j.job.2018.11.004.
- [16] S. Donatello, A. Fernández-Jimenez, A. Palomo, Very high volume fly ash cements. Early age hydration study using Na₂SO₄ as an activator, *Journal of the American Ceramic Society*. 96 (2013) 900–906. doi:10.1111/jace.12178.
- [17] J.M. Mejía, R. Mejía de Gutiérrez, F. Puertas, Rice husk ash as a source of silica

1
2
3
4
5
6
7
8
9
10
11
12
13
14
15
16
17
18
19
20
21
22
23
24
25
26
27
28
29
30
31
32
33
34
35
36
37
38
39
40
41
42
43
44
45
46
47
48
49
50
51
52
53
54
55
56
57
58
59
60
61
62
63
64
65

in alkali-activated fly ash and granulated blast furnace slag systems, *Materiales de Construcción*. 63 (2013) 361–375. doi:10.3989/mc.2013.04712.

- [18] N. Bouzón, J. Payá, M. V. Borrachero, L. Soriano, M.M. Tashima, J. Monzó, Refluxed rice husk ash/NaOH suspension for preparing alkali activated binders, *Materials Letters*. 115 (2014) 72–74. doi:10.1016/j.matlet.2013.10.001.
- [19] A. Font, L. Soriano, L. Reig, M.M. Tashima, M. V. Borrachero, J. Monzó, J. Payá, Use of residual diatomaceous earth as a silica source in geopolymer production, *Materials Letters*. 223 (2018) 10–13. doi:10.1016/j.matlet.2018.04.010.
- [20] S.A. Bernal, E.D. Rodríguez, R. Mejía de Gutiérrez, J.L. Provis, Performance at high temperature of alkali-activated slag pastes produced with silica fume and rice husk ash based activators, *Materiales de Construcción*. 65 (2015) e049. doi:10.3989/mc.2015.03114.
- [21] M. Torres-Carrasco, F. Puertas, Waste glass in the geopolymer preparation. Mechanical and microstructural characterisation, *Journal of Cleaner Production*. 90 (2015) 397–408. doi:10.1016/j.jclepro.2014.11.074.
- [22] J.C.B. Moraes, A. Font, L. Soriano, J.L. Akasaki, M.M. Tashima, J. Monzó, M.V. Borrachero, J. Payá, New use of sugar cane straw ash in alkali-activated materials: A silica source for the preparation of the alkaline activator, *Construction and Building Materials*. 171 (2018). 611-621. doi:10.1016/j.conbuildmat.2018.03.230.
- [23] K. Dombrowski, A. Buchwald, M. Weil, The influence of calcium content on the structure and thermal performance of fly ash based geopolymers, *Journal of Materials Science*. 42 (2007) 3033–3043. doi:10.1007/s10853-006-0532-7.
- [24] L. Reig, L. Soriano, M.M. Tashima, M. V. Borrachero, J. Monzó, J. Payá, Influence of calcium additions on the compressive strength and microstructure of alkali-activated ceramic sanitary-ware, *Journal of the American Ceramic Society*. 101 (2018) 3094–3104. doi:10.1111/jace.15436.
- [25] G. Huang, Y. Ji, J. Li, Z. Hou, Z. Dong, Improving strength of calcinated coal gangue geopolymer mortars via increasing calcium content, *Construction and Building Materials*. 166 (2018) 760–768.

doi:10.1016/j.conbuildmat.2018.02.005.

- 1
2
3
4
5
6
7
8
9
10
11
12
13
14
15
16
17
18
19
20
21
22
23
24
25
26
27
28
29
30
31
32
33
34
35
36
37
38
39
40
41
42
43
44
45
46
47
48
49
50
51
52
53
54
55
56
57
58
59
60
61
62
63
64
65
- [26] F. Allali, E. Joussein, N.I. Kandri, S. Rossignol, The influence of calcium content on the performance of metakaolin-based geomaterials applied in mortars restoration, *Materials and Design*. 103 (2016) 1–9.
doi:10.1016/j.matdes.2016.04.028.
- [27] H. Maraghechi, S. Salwocki, F. Rajabipour, Utilisation of alkali activated glass powder in binary mixtures with Portland cement, slag, fly ash and hydrated lime, *Materials and Structures/Materiaux et Constructions*. 50 (2017) 1–14.
doi:10.1617/s11527-016-0922-5.
- [28] S. Alonso, A. Palomo, Alkaline activation of metakaolin and calcium hydroxide mixtures: Influence of temperature, activator concentration and solids ratio, *Materials Letters*. 47 (2001) 55–62. doi:10.1016/S0167-577X(00)00212-3.
- [29] S. Alonso, A. Palomo, Calorimetric study of alkaline activation of calcium hydroxide-metakaolin solid mixtures, *Cement and Concrete Research*. 31 (2001) 25–30. doi:10.1016/S0008-8846(00)00435-X.
- [30] S. Boonjaeng, P. Chindaprasirt, K. Pimraksa, Lime-calcined clay materials with alkaline activation: Phase development and reaction transition zone, *Applied Clay Science*. 95 (2014) 357–364. doi:10.1016/j.clay.2014.05.002.
- [31] M.M. Tashima, J.L. Akasaki, J.L.P. Melges, L. Soriano, J. Monzó, J. Payá, M. V Borrachero, Alkali activated materials based on fluid catalytic cracking catalyst residue (FCC): Influence of $\text{SiO}_2/\text{Na}_2\text{O}$ and $\text{H}_2\text{O}/\text{FCC}$ ratio on mechanical strength and microstructure, *Fuel*. 108 (2013) 833–839.
doi:10.1016/j.fuel.2013.02.052.
- [32] J.J. Trochez, R. Mejía de Gutiérrez, J. Rivera, S.A. Bernal, Synthesis of geopolymer from spent FCC: Effect of $\text{SiO}_2/\text{Al}_2\text{O}_3$ and $\text{Na}_2\text{O}/\text{SiO}_2$ molar ratios, *Materiales de Construcción*. 65 (2015) e046. doi:10.3989/mc.2015.00814.
- [33] T. Luukkonen, Z. Abdollahnejad, J. Yliniemi, P. Kinnunen, M. Illikainen, Comparison of alkali and silica sources in one-part alkali-activated blast furnace slag mortar, *Journal of Cleaner Production*. 187 (2018) 171–179.
doi:10.1016/j.jclepro.2018.03.202.
- [34] M.A. Villaquirán-Caicedo, R. Mejía de Gutiérrez, Synthesis of ceramic materials

1
2 from ecofriendly geopolymer precursors, *Materials Letters*. 230 (2018) 300–304.
3 doi:10.1016/j.matlet.2018.07.128.

- 4 [35] AENOR, UNE-EN 459-1: Cales para la construcción Parte 1: Definiciones,
5 especificaciones y criterios de conformidad, 2015.
6
7
8 [36] J. Payá, J. Monzó, M. V. Borrachero, A. Mellado, L.M. Ordoñez, Determination
9 of amorphous silica in rice husk ash by a rapid analytical method, *Cement and
10 Concrete Research*. 31 (2001) 227–231. doi:10.1016/S0008-8846(00)00466-X.
11
12
13 [37] J.G. Martí, M. V. Borrachero, J. Payá, J. Monzó, D. Alveiro, A. Salas.
14 Reutilización de ceniza de cascarilla de arroz y residuo de catalizador de craqueo
15 catalítico en conglomerantes cal-puzolana para concretos de bajo coste
16 económico y medioambiental, *Proceedings of the 6th Amazon & Pacific Green
17 Materials Congress and Sustainable Construction Materials Lat-RILEM
18 Conference, Cali, Colombia, 2016*, 623–636.
19
20
21 [38] I. García-Lodeiro, A. Fernández-Jiménez, A. Palomo, Variation in hybrid
22 cements over time. Alkaline activation of fly ash-portland cement blends,
23 *Cement and Concrete Research*. 52 (2013) 112–122.
24 doi:10.1016/j.cemconres.2013.03.022.
25
26 [39] A. Font, M.V. Borrachero, L. Soriano, J. Monzó, A. Mellado, J. Payá, New eco-
27 cellular concretes: Sustainable and energy-efficient materials, *Green Chemistry*.
28 20 (2018) 14684. doi:10.1039/c8gc02066c.
29
30 [40] M.A. Villaquirán-Caicedo, Studying different silica sources for preparation of
31 alternative waterglass used in preparation of binary geopolymer binders from
32 metakaolin/boiler slag, *Construction and Building Materials*. 227 (2019) 116621.
33 doi:10.1016/j.conbuildmat.2019.08.002.
34
35 [41] A. Mellado, C. Catalán, N. Bouzón, M. V. Borrachero, J.M. Monzó, J. Payá,
36 Carbon footprint of geopolymeric mortar: study of the contribution of the
37 alkaline activating solution and assessment of an alternative route, *RSC Adv*. 4
38 (2014) 23846–23852. doi:10.1039/C4RA03375B.
39
40 [42] J. Payá, J. Monzó, M. V. Borrachero, S. Velázquez, M. Bonilla, Determination of
41 the pozzolanic activity of fluid catalytic cracking residue. Thermogravimetric
42 analysis studies on FC3R-lime pastes, *Cement and Concrete Research*. 33 (2003)
43
44
45
46
47
48
49
50
51
52
53
54
55
56
57
58
59
60
61
62
63
64
65

1085–1091. doi:10.1016/S0008-8846(03)00014-0.

- 1
2
3
4
5
6
7
8
9
10
11
12
13
14
15
16
17
18
19
20
21
22
23
24
25
26
27
28
29
30
31
32
33
34
35
36
37
38
39
40
41
42
43
44
45
46
47
48
49
50
51
52
53
54
55
56
57
58
59
60
61
62
63
64
65
- [43] M.M. Tashima, L. Soriano, J.L. Akasaki, V.N. Castaldelli, J. Monzó, J. Payá, M. V. Borrachero, Spent FCC catalyst for preparing alkali-activated binders: An opportunity for a high-degree valorization, *Key Engineering Materials*. 600 (2014) 709–716. doi:10.4028/www.scientific.net/KEM.600.709.
- [44] M.L. Granizo, S. Alonso, M.T. Blanco-Varela, A. Palomo, Alkaline Activation of Metakaolin: Effect of Calcium Hydroxide in the Products of Reaction, *Journal of the American Ceramic Society*. 85 (2002) 225–231. doi:10.1111/j.1151-2916.2002.tb00070.x.
- [45] B.A. Ramesh, B. Kondraivendhan, Effect of Accelerated Carbonation on the Performance of Concrete Containing Natural Zeolite, *Journal of Materials in Civil Engineering*. 32 (2020) 04020037. doi:10.1061/(ASCE)MT.1943-5533.0003050.
- [46] A. Hartmann, M. Khakhutov, J.C. Buhl, Hydrothermal synthesis of CSH-phases (tobermorite) under influence of Ca-formate, *Materials Research Bulletin*. 51 (2014) 389–396. doi:10.1016/j.materresbull.2013.12.030.
- [47] I. García-Lodeiro, A. Fernández-Jiménez, M.T. Blanco, A. Palomo, FTIR study of the sol-gel synthesis of cementitious gels: C-S-H and N-A-S-H, *Journal of Sol-Gel Science and Technology*. 45 (2008) 63–72. doi:10.1007/s10971-007-1643-6.
- [48] W. Mozgawa, J. Deja, Spectroscopic studies of alkaline activated slag geopolymers, *Journal of Molecular Structure*. 924–926 (2009) 434–441. doi:10.1016/j.molstruc.2008.12.026.
- [49] W.K.W. Lee, J.S.J. Van Deventer, Use of Infrared Spectroscopy to Study Geopolymerization of Heterogeneous Amorphous Aluminosilicates, *Langmuir*. 19 (2003) 8726–8734. doi:10.1021/la026127e.
- [50] I. García-Lodeiro, A. Fernández-Jiménez, A. Palomo, D.E. MacPhee, Effect of calcium additions on N-A-S-H cementitious gels, *Journal of the American Ceramic Society*. 93 (2010) 1934–1940. doi:10.1111/j.1551-2916.2010.03668.x.
- [51] N. Maubec, D. Deneele, G. Ouvrard, Influence of the clay type on the strength evolution of lime treated material, *Applied Clay Science*. 137 (2017) 107–114. doi:10.1016/j.clay.2016.11.033.

- 1
2
3
4
5
6
7
8
9
10
11
12
13
14
15
16
17
18
19
20
21
22
23
24
25
26
27
28
29
30
31
32
33
34
35
36
37
38
39
40
41
42
43
44
45
46
47
48
49
50
51
52
53
54
55
56
57
58
59
60
61
62
63
64
65
- [52] A.F.Nóbrega de Azeredo, L.J. Struble, A.M.P. Carneiro, Microstructural characteristics of lime-pozzolan pastes made from kaolin production wastes, *Materials and Structures/Materiaux et Constructions*. 48 (2015) 2123–2132. doi:10.1617/s11527-014-0297-4.
- [53] O.Rodríguez, R.Vigil de la Villa, R.García, B. Nebreda, M. Frías, Lower temperature activation for kaolinite-based clay waste: Evaluation of hydrated phases during the pozzolanic reaction, *Journal of the American Ceramic Society*. 94 (2011) 1224–1229. doi:10.1111/j.1551-2916.2010.04134.x.
- [54] K. Juengsuwattananon, F. Winnefeld, P. Chindaprasirt, K. Pimraksa, Correlation between initial $\text{SiO}_2/\text{Al}_2\text{O}_3$, $\text{Na}_2\text{O}/\text{Al}_2\text{O}_3$, $\text{Na}_2\text{O}/\text{SiO}_2$ and $\text{H}_2\text{O}/\text{Na}_2\text{O}$ ratios on phase and microstructure of reaction products of metakaolin-rice husk ash geopolymer, *Construction and Building Materials*. 226 (2019) 406–417. doi:10.1016/j.conbuildmat.2019.07.146.
- [55] H.K. Tchakouté, C.H. Rüscher, S. Kong, E. Kamseu, C. Leonelli, Comparison of metakaolin-based geopolymer cements from commercial sodium waterglass and sodium waterglass from rice husk ash, *Journal of Sol-Gel Science and Technology*. 78 (2016) 492–506. doi:10.1007/s10971-016-3983-6.
- [56] T. da Silva Rocha, D.P. Dias, F.C.C. França, R.R. de Salles Guerra, L.R. da Costa de Oliveira Marques, Metakaolin-based geopolymer mortars with different alkaline activators (Na^+ and K^+), *Construction and Building Materials*. 178 (2018) 453–461. doi:10.1016/j.conbuildmat.2018.05.172.
- [57] S. Dueramae, W. Tangchirapat, P. Sukontasukkul, P. Chindaprasirt, C. Jaturapitakkul, Investigation of compressive strength and microstructures of activated cement free binder from fly ash-calcium carbide residue mixture, *Journal of Materials Research and Technology*. 8 (2019) 4757–4765. doi:10.1016/j.jmrt.2019.08.022.
- [58] R.C. Andrades, R.F. Neves, F.R.V. Diaz, A.H.M. Júnior, Influence of alkalinity on the synthesis of zeolite A and hydroxysodalite from metakaolin, *Journal of Nano Research*. 61 (2020) 51–60. doi:10.4028/www.scientific.net/JNanoR.61.51.



INSTITUTO DE CIENCIA Y
TECNOLOGÍA DEL HORMIGÓN

Universitat Politècnica de València



UNIVERSITAT
POLITÈCNICA
DE VALÈNCIA

Maria Victoria Borrachero Rosado

Catedrático de Universidad

Edificio Caminos II (Edificio 4G)

Universitat Politècnica de València

Camino de Vera s/n 46071 Valencia (Spain)

<http://www.icitech.upv.es>

vborrachero@cst.upv.es

Tel: +34 96 3877564

Fax: +34 96 3877569

December 1, 2020

Professor Michael C Forde, PhD, FEng, FRSE, Hon.ACI
Editor-in-Chief
Construction & Building Materials

Re: REVISED Manuscript submission

Revision notes of the manuscript: **“Lime/pozzolan/geopolymer systems: performance in pastes and mortars”**

Paper number: CONBUILDMAT-D-20-09089 (First submission)

Authors: Ariel R. Villca, Lourdes Soriano, Alba Font, Mauro M. Tashima, José Monzó, María Victoria Borrachero, Jordi Payá.

Dear professor,

The authors would like to express their appreciation to the editor and the reviewers for their precious time in the revision of the paper. We have carefully addressed all the comments proposed by the two reviewers, and the refinements made in the revised paper are summarized in our response below to improve the quality of the manuscript for its publication in *Construction & Building Materials*.

First of all, we wish to apologize for the confusion in the numbering of the bibliography throughout the text. Apparently, in the latest version of the manuscript there was an unintended change from the database we are working with.

Reviewer #1 comments are in red

Reviewer #3 comments are in green

Author comments are in black.

Note: Line numbers and references in this letter correspond to those in the new manuscript.

Reviewer #1:

Comments to the authors:

It is an interesting paper with many results; however, the presentation of the results and the discussion should be improved because the interaction between lime/pozzolan/geopolymer for example in mechanical strength is not clear, there is absence of data compressive strength for geopolymer. The reaction and the formation of a mixture of gels (N-A-S-H and N, C-A-S-H) is not well supported. The authors could support their results with a greater comparison with literature.

1) Introduction - in part where the lime / pozzolan systems are indicated, article to be referenced below

The effect of type and concentration of activators on flowability and compressive strength of natural. Pages 337-347.

Thanks for your suggestion, it is a really attractive article but this did not work on lime / pozzolan systems that were partially replaced by a geopolymer, but on a study of the effect of different parameters in the alkaline solution on the slag-based geopolymer to which a pozzolana was added. natural.

This article must be used to analyze the results of mechanical resistance:

Studying different silica sources for preparation of alternative waterglass used in preparation of binary geopolymer binders from metakaolin/boiler slag. *Construction and Building Materials* 227 (2019) 116621.

This paper was included in the discussion to explain the good results of mortars with RHA as silica source:

“The good behaviour of RHA as silica source may be the result of a more enhanced connectivity in microstructure of the samples activated with this material as said Villaquirán- Caicedo in the paper published in 2019 [40].” (L: #288-290).

2) Materials and Method- Please, correct Table 1, the sum of the percentages does not give 100% and the Al₂O₃ content is missing.

There was some mistake in the last version of the submitted manuscript with the Table 1 format. In the new manuscript it has been modified as follows:

(L: #150)

Table 1. Chemical composition of the used materials: fluid catalytic cracking catalyst residue (FCC) and rice husk ash (RHA)

| | SiO ₂ | Al ₂ O ₃ | Fe ₂ O ₃ | CaO | MgO | SO ₃ | K ₂ O | Na ₂ O | P ₂ O ₅ | Others | *LOI |
|------------|------------------|--------------------------------|--------------------------------|------|------|-----------------|------------------|-------------------|-------------------------------|--------|------|
| FCC | 47.76 | 49.26 | 0.60 | 0.11 | 0.17 | 0.02 | 0.02 | 0.31 | 0.03 | 1.20 | 0.54 |
| RHA | 85.58 | 0.25 | 0.21 | 1.83 | 0.50 | 0.26 | 3.39 | - | 0.67 | 0.32 | 6.99 |

*LOI: loss on ignition

3) Materials and Method- line 13- the author indicates the sand/binder ratio is 3, if there is, the fluidity of samples is high. According to Table 2 is binder:sand ratio = 3, Please check and correct.

The correct form is SAND/BINDER RATIO = 3 (L: #159). With the data from Table 2 (L: #183):

Binder = 525.0 g >>>>> sand/binder = 3; Sand = 3 * 525 = 1575 g

4) Materials and Method- line 13- the author indicates "The lime/pozzolan ratio was chosen based on the research group's previous research [33]" but the reference [33] is T. Luukkonen, Z. Abdollahnejad, J. Yliniemi, P. Kinnunen, M. Illikainen, Comparison of alkali and silica sources in one-part alkali-activated

blast furnace slag mortar, *Journal of Cleaner Production*. 187 (2018) 171-179. doi:10.1016/j.jclepro.2018.03.202 from University of Oulu in Finland. Please check and correct.

All references in the new manuscript have been reviewed and actualized in order to correct its relationship with the text references.

The reference in this case is [37] (L: #160) related with:

[37] J.G. Martí, M. V. Borrachero, J. Payá, J. Monzó, D. Alveiro, A. Salas. Reutilización de ceniza de cascarilla de arroz y residuo de catalizador de craqueo catalítico en conglomerantes cal-puzolana para concretos de bajo coste económico y medioambiental, Proceedings of the 6th Amazon & Pacific Green Materials Congress and Sustainable Construction Materials Lat-RILEM Conference, Cali, Colombia, 2016, 623–636

5) Results and Discussion section- compressive strength... "The geopolymeric mortar without lime (pure geopolymer, GEOP) was analysed for the same curing ages. The compressive strength of this sample was generally very high, especially at early curing ages". What were the compressive strength reached by the geopolymer? I don't see the results for geopolymer only.

This paragraph has been completed with the mechanical results of the GEOP mortar as follow:

"The geopolymeric mortar without lime (pure geopolymer, GEOP) was analysed for the same curing ages. The compressive strength of this sample was very high, especially at early curing ages, between 1 and 7 curing days. After the first curing day the GEOP mortar yielded 13.38 MPa and the compressive strength increases until 53.90 MPa at 7 curing days. No CCx system had a compressive strength greater than 25 MPa." (L: #239 – 244)

6) Results and Discussion section- compressive strength... "Conversely in the research by Boonjaeng et al, the lime/MK mixture was considered the binder and was activated with NaOH [28]." The reference doesn't correspond to Boonjaeng, please check and confirm the references. The [28] is:

[28] S. Alonso, A. Palomo, Alkaline activation of metakaolin and calcium hydroxide mixtures: Influence of temperature, activator concentration and solids ratio, *Materials Letters*. 47 (2001) 55-62. doi:10.1016/S0167-577X(00)00212-3.

In the re-submitted manuscript this mistake has been corrected as follows:

"Conversely in the research by Boonjaeng et al, the lime/MK mixture was considered the binder and was activated with NaOH [30]." (L: #237 - 238).

Then in the bibliography section:

[30] S. Boonjaeng, P. Chindapasirt, K. Pimraksa, Lime-calcined clay materials with alkaline activation: Phase development and reaction transition zone, *Applied Clay Science*. 95 (2014) 357–364. doi:10.1016/j.clay.2014.05.002.

7) Results and Discussion section- compressive strength... the author saying "The nature of the gel in these mortars was the NASH type [34]" and reviewing this reference corresponds to a study where Na⁺ was not used. K⁺ was used as the alkali ion. So, the speculative explanation of formed gels does not correspond. please check and confirm the references. Rewrite this paragraph and make use of bibliographic references, also rely on the results of FITR.

[34] M.A. Villaquirán-Caicedo, R.M. de Gutiérrez, Synthesis of ceramic materials from ecofriendly geopolymer precursors, *Materials Letters*. 230 (2018) 300-304.

In the re-submitted manuscript this mistake has been corrected as follows:

"The nature of the gel in these mortars was the NASH type [39]." (L: #244)

Then in the bibliography section:

[39] A. Font, M.V. Borrachero, L. Soriano, J. Monzó, A. Mellado, J. Payá, New eco-cellular concretes: Sustainable and energy-efficient materials, *Green Chemistry*. 20 (2018) 14684. doi:10.1039/c8gc02066c.

8) Results and Discussion section- Please improve resolution for curved DTGs, they look blurry.

The all figures in the re-submitted manuscript have been improved and now are attached in tiff format and 300dpi.

9) Results and Discussion section- FTIR-line 58 "When the activator concentration was low, the principal reaction product was CSH; when the concentration was high, the main product was the C(N)ASH gel and CSH formed as a secondary reaction product".

According with previous explanations, I think the author want to say C(N)ASH gel and NASH. Please revising sentence.

This sentence (L: #335 – 338) is related with the thermogravimetric analysis but not with the FTIR. The authors checked this affirmation and is correct. When the concentration of the activator was high the main product formed was C(N)ASH. The CSH is also formed but in a lesser degree (as a secondary product). Please take advice the referenced papers for this affirmation [28,29,44].

10) Results and Discussion section- FTIR- In Figure 5b, numbers corresponding to $<993\text{ cm}^{-1}$ wavenumber are missing.

"The bands with lesser intensity, around 867 cm^{-1} , were identified as Si-O stretching and OH bending (Si-OH). The peak was attributed to bending bands (Si-O-Si and O-Si-O) with those at around 470 cm^{-1} [49]." Please identified in fig 5b.

These peaks are now identified in the Figure 5b. (L: #394)

11) Results and Discussion section- FTIR- "For the CC40 paste, the signal attributed to the gel was found at 968 cm^{-1} (after 90 curing days)." Please explaining which gel, NASH, N(C)ASH?

To clarify this the sentence has been modified as follow:

"For the CC40 paste, the signal attributed to the gel (NASH) was found at 968 cm^{-1} (after 90 curing days)." (L: 389 – 390)

12) Results and Discussion section- Please improve resolution for curved XRD, they look blurry.

As are above mentioned, the all figures in the re-submitted manuscript have been improved and now are attached in tiff format and 300dpi.

13) The unit for X axis in XRD figures is angle 2θ (angle) or 2θ ($^{\circ}$)

As is indicated in the figures the angle is the "Bragg's Angle (2θ)" this is the commonly referenced to the 2θ (angle).

Theta is the name of this Greek letter. To improve the understanding in the re-submitted manuscript the unit for X-axis in XRD figures are drawn as: "Bragg's Angle (2θ)".

14) Results and Discussion section- XRD -Why the XRD patterns for CC40 look different of CA40, if, is silica source from RHA is amorphous? in CC40 there is a peak for Q but in CA40 there is not. then one would expect the reaction products formed to be similar between the two binders. Please explaining.

In the CA40 XRD pattern there is the presence of Q peak, the same that for the CC40 paste, but with lower intensity. In some cases, depending on the preparation of the sample for XRD test (preferential orientation of particles) and depending on the intensity of the peaks from other crystalline phases and the baseline deviation (attributed to the amorphous content), it is usual to have apparently different composition. Quartz is not a reaction product, this SiO_2 crystalline phase is present in the FCC (yo can take advice on the following reference: Erich D. Rodríguez, Susan A. Bernal, John L. Provis, John D. Gehman, José M. Monzó, Jordi Payá, M. Victoria Borrachero, Geopolymers based on spent catalyst residue from a fluid catalytic cracking (FCC) process, *Fuel*, Volume 109, 2013, Pages 493-502, <https://doi.org/10.1016/j.fuel.2013.02.053>.)-

Reviewer #3:

1) The pozzolan used is not in the name of the article, nor at least in the name of the geopolymer. I think it is worth replacing the "pozzolan" by FCC.

Thanks for your consideration, but at least the authors decided to conserve the title: **"Lime/pozzolan/geopolymer systems: performance in pastes and mortars."**

The aim of the present paper is the study of development of binary mixtures where the lime/pozzolan binder was partially replaced with a geopolymeric mortar.

The FCC was employed as both the mineral admixture in the lime/pozzolan system and the precursor in the geopolymer formulation.

2) Abstract: The abstract must be written in a single paragraph containing: introduction, methodology, results and conclusions.

The abstract has been modified and in the re-submitted manuscript it is a single paragraph containing introduction, methodology, results and conclusions.

3) Keywords: the pozzolan chosen was FCC, why not put FCC as the keyword instead of "pozzolan"?

The "fluid catalytic cracking catalyst residue" has been added as a new keyword.

4) Item 3.1 Compressive strength development: I think it is worth highlighting in this item that as the geopolymer replacement is increased, little variation in resistance gain is observed after 10 days. It is worth remembering that geopolymers are famous for presenting a marked resistance gain in the first days, and this was proved by the CC30 samples and, mainly by the CC40, which had little variation after 10 days of cure.

This reflection about the gain of strength by the geopolymer addition into the lime/pozzolan system has been added in the following paragraph:

"It is highlighted the compressive strength gain at early ages with the incorporation of the geopolymer into the lime/pozzolan systems. With the 10% substitution (sample CC10), compressive strength was 45% greater than the strength for CON after 1 curing day and was 152% greater after 7 curing days." (L: #212 – 215).

5) Page 19, Line 28: You say "In our case ...". All text must be written in third person.

"In our case..." has been replaced by "In the present research..." (L: #385)

6) At least three articles have been published by some of the authors of this article on geopolymer based on fluid catalytic cracking catalyst residue and no comparison has been made with the results of this new geopolymer.

As you mentioned the previous works were about the geopolymer mortars based on FCC, but not about the incorporation into lime/pozzolan systems, thus the behavior of the geopolymer was not the aim in the present research. In the present research the influence of the combination of both systems in the resulted materials properties was discussed.

The previous works that you refer might be used to help the understanding and compare the chemical stoichiometry, the resulted reaction products and microstructural behavior of the new combined systems, but not to compare the mechanical behavior thus the nature of the mixes was completely different:

a) This paper aims to study the geopolymers based in FCC activated by silica from the RHA:

[18] N. Bouzón, J. Payá, M. V. Borrachero, L. Soriano, M.M. Tashima, J. Monzó, Refluxed rice husk ash/NaOH suspension for preparing alkali activated binders, *Materials Letters*. 115 (2014) 72–74. doi:10.1016/j.matlet.2013.10.001.

This investigation was employed in the present work:

“For the geopolymeric binder, the formulation of the alkaline activator solution was selected according to a previous work [18]” (L:#164 – 165).

- b) This paper aims to study the geopolymers based in FCC activated by silica from the residual diatomaceous earth:

[19] A. Font, L. Soriano, L. Reig, M.M. Tashima, M. V. Borrachero, J. Monzó, J. Payá, Use of residual diatomaceous earth as a silica source in geopolymer production, *Materials Letters*. 223 (2018) 10–13. doi:10.1016/j.matlet.2018.04.010.

- c) The last one, studied the influence of the activators into the conventional geopolymer based on FCC:

[31] M.M. Tashima, J.L. Akasaki, J.L.P. Melges, L. Soriano, J. Monzó, J. Payá, M. V Borrachero, Alkali activated materials based on fluid catalytic cracking catalyst residue (FCC): Influence of SiO₂/Na₂O and H₂O/FCC ratio on mechanical strength and microstructure, 108 (2013) 833–839.

These three previous works provide a scientific basis in the introduction about the use of FCC as a precursor in the geopolymers preparation.

Based on both, the aim of the present investigation and the obtained results, there are previous related investigations from other authors which allow a logical discussion and reflection about the behavior of the new lime / pozzolan / geopolymer systems presented.

7) Conclusions: write results in topics more succinctly.

The sentences in the conclusions section have been reorganized as the order that those appear in the results and discussion section. Furthermore, the conclusions have been rewritten and synthetized.

8) What criteria are being used to number citations? It is not in order that it appears in the text or in alphabetical order. Please review and choose a criterion. Citations [32] and [33] appear after [34] in the text. The quotations [35], [36] and [37] appear after [38] in the text. Following after [38] is [44]. So it is repeated, without a logical criterion.

References not cited in the text: [39], [43], [55] and [56]. Remove from the list of references or insert in the text.

Sorry, there was a mistake in the citations. The all references in re-submitted manuscript have been revised and actualized in order to correct its correlation with the text references.

Highlights

- Fluid catalytic cracking residue (FCC) was used as pozzolan and a precursor
- Rice husk ash (RHA) was used as an alternative source of silica
- Geopolymeric binders in classic pozzolan/lime mortars gave high strength gain
- Strength gain was obtained for short curing times

Declaration of interests

The authors declare that they have no known competing financial interests or personal relationships that could have appeared to influence the work reported in this paper.

The authors declare the following financial interests/personal relationships which may be considered as potential competing interests:

Credit Author Statement

| Term | Author | | | | | | |
|---------------------------------------|---------------|-----------|-----------------|------------------|------------|------------------------|------------|
| | Ariel Villca | Alba Font | Lourdes Soriano | Mauro M. Tashima | José Monzó | M. Victoria Borrachero | Jordi Payá |
| <i>Conceptualization</i> | | | X | | X | X | |
| <i>Methodology</i> | | X | | X | | X | X |
| <i>Formal analysis</i> | X | X | | X | X | | |
| <i>Investigation</i> | X | X | X | | X | X | X |
| <i>Resources</i> | | | X | | | X | X |
| <i>Writing - Original Draft</i> | | X | X | | | | |
| <i>Writing - Review & Editing</i> | X | X | X | X | X | X | X |
| <i>Visualization</i> | | X | | X | | | |
| <i>Supervision</i> | | | X | | X | X | |
| <i>Project administration</i> | | | | | X | X | |
| <i>Funding acquisition</i> | | | X | | X | X | |

Lime/pozzolan/geopolymer systems: performance in pastes and mortars.

Lime/pozzolan/geopolymer systems: performance in pastes and mortars.

Ariel R. Villca ⁽¹⁾, Lourdes Soriano ⁽¹⁾, Alba Font ⁽¹⁾, Mauro M. Tashima ⁽²⁾, José Monzó ⁽¹⁾, María Victoria Borrachero ⁽¹⁾, Jordi Payá ⁽¹⁾.

⁽¹⁾ ICITECH – GIQUIMA Group – Grupo de Investigación en Química de los Materiales de Construcción, Instituto de Ciencia y Tecnología del Hormigón, Universitat Politècnica de València, Valencia, Spain.

⁽²⁾ Universidade Estadual Paulista (UNESP), Faculdade de Engenharia de Ilha Solteira. MAC – Grupo de Pesquisa em Materiais Alternativos de Construção, Ilha Solteira-SP, Brazil.

Abstract

Use of lime as construction material is limited mainly by low initial strength. These properties can be improved by adding pozzolanic materials, but the evolution of the reaction usually needs older ages than 7 days. Alkali-activated materials, or geopolymers, are good-performance materials that can be produced with residual waste. The combination of traditional and new materials can lead to new uses of lime mortars. This paper studies a lime/pozzolan and geopolymer mixture. The chosen pozzolan is fluid catalytic cracking catalyst residue (FCC), a material employed as a precursor in alkali-activated material. FCC is activated by two activators: a mixture of NaOH and waterglass; a mixture of NaOH and rice husk ash (RHA). The new materials were studied in microstructure and mechanical behaviour terms. The results demonstrated that lime/pozzolan/geopolymer obtained superior compressive strengths after 1 curing day to that obtained for the corresponding lime/pozzolan mortar after 90 days. An improvement in compressive strength of around 145% was achieved for the mortar with 40% geopolymer compared to the mortar with only lime/pozzolan at 28 curing days.

Keywords: lime, pozzolan, geopolymer, waste material, fluid catalytic cracking catalyst residue

1
2
3
4
5
6
7
8
9
10
11
12
13
14
15
16
17
18
19
20
21
22
23
24
25
26
27
28
29
30
31
32
33
34
35
36
37
38
39
40
41
42
43
44
45
46
47
48
49
50
51
52
53
54
55
56
57
58
59
60
61
62
63
64
65

29 1 Introduction

30 Lime mortar is an ancient construction material that has been used in different
31 places and periods of history [1,2]. The Romans are certainly responsible for the main
32 technological contribution to lime mortars: addition of volcanic ash or calcined clay
33 significantly improved mechanical properties, and allowed it to set and harden under
34 water. The durability of lime mortars is demonstrated by today's good conditions from
35 the architectural heritage of Roman times [3].

36 After the discovery of Portland cement, the use of lime mortar drastically reduced
37 due to the new binder's excellent mechanical and durability properties: fast setting,
38 excellent strength development, etc. Nevertheless, current Portland cement (PC) mortars
39 do not meet some sustainability criteria designated by the international community
40 (sustainability development goals) [4]. PC production generates large amounts of CO₂
41 emissions to the atmosphere, and is responsible for about 5-8% of CO₂ emissions
42 worldwide [5]. Thus a good option is to use alternative binders (lime/pozzolan,
43 geopolymer systems, magnesium oxide cements, etc.) that are often associated with a
44 lower environmental impact [6].

45 Studies about lime/pozzolan binders report good mechanical strength and
46 durability aspects, depending on the type of used pozzolan [1,7–10]. However, in most
47 cases, the mechanical strength for early curing times (< 28 days) is reduced due to the
48 slow setting and hardening process of lime/pozzolan systems.

49 Palomo et al. studied the similarity between the ancient lime/pozzolan mortars of
50 historic Roman marine concrete and hybrid-Portland alkaline cement [11]. More
51 specifically, these researchers found similar products of reaction by comparing ancient
52 concrete in marine structures and hybrid alkaline materials (a combination of Portland
53 cement and alkali-activated fly ash). The particularity of seawater concretes in Roman
54 times was studied in depth in the last few years by paying attention to the formation of
55 the so-called "Al-tobermorite" [12,13]. The stability of Al-tobermorite can be a starting
56 point in an attempt to synthesise similar products.

57 Alkali-activated materials (AAM) are relatively new construction materials, and
58 geopolymer is often used as an additional terminology. Research into these systems is
59 growing and they are expected to be used in many applications in the construction
60 domain. These materials are basically a mixture of an aluminosilicate source and an

1
2
3
4
5
6
7
8
9
10
11
12
13
14
15
16
17
18
19
20
21
22
23
24
25
26
27
28
29
30
31
32
33
34
35
36
37
38
39
40
41
42
43
44
45
46
47
48
49
50
51
52
53
54
55
56
57
58
59
60
61
62
63
64
65
66
67
68
69
70
71
72
73
74
75
76
77
78
79
80
81
82
83
84
85
86
87
88
89
90
91

alkaline-activating solution [14]. The most typically used precursors are metakaolin (MK), fly ash (FA), ground granulated blast furnace (BFS), etc. Alkaline solutions are normally a mixture of sodium hydroxide and sodium silicate (or potassium as a cation), although other activators can be used: sodium carbonate, sodium sulphate, etc.[15,16].

The new geopolymer technology goal is to use residual materials to prepare alkaline solutions. The carbon footprint related to alkali hydroxides is smaller than that for alkali silicates. Many research groups are investigating the use of alternative silica sources to obtain a commercial silicate or waterglass alternative. These silica sources are mainly rice husk ash (RHA), diatomaceous earth residue, glass waste, sugar cane straw ash and silica fume, among others [17–22].

In some studies on geopolymeric systems, the addition of calcium compounds enhances the activation reaction to result in improved compressive strength [23,24]. Moreover, the use of materials that include calcium in their composition can improve the reactivity of waste, but an excess of calcium has negative effects on compressive strength [25].

The combination of these two binder types (lime/pozzolan and geopolymer) would reduce environmental issues caused by CO₂ emissions, increase waste valorisation and improve the mechanical properties at curing ages lasting less than 28 days.

Allali et al. studied the influence of calcium content on geopolymeric matrices for their use in restoration mortars [26]. They substituted metakaolin (MK) for calcium hydroxide in mortars with potassium and sodium salts as an alkaline solution. When they employed calcium hydroxide in both sodium or potassium solution, Ca(OH)₂ totally or partially dissolved. They observed fast setting and compressive strength was lower than for the mortar with only MK (42 MPa for the mortar without hydrated lime and 10 MPa for the mortars with 41% replacement of MK with hydrated lime at 7 curing days).

Recently, glass powder in different systems has been used. In mixtures with PC, it reacted as pozzolanic material. In geopolymeric systems, it was blended with slag, fly ash and lime [27]. With the glass powder and lime mixtures, which were activated by a 4M NaOH solution, a compressive strength of 31MPa was achieved in systems cured at 60°C for 28 days. The formation of a similar calcium silicate hydrate to tobermorite was suggested for the SEM/EDS study.

92 Several authors have studied the alkaline activation of MK with calcium
93 hydroxide [28,29]. They followed different analytical techniques to characterise the
94 products formed in this mixture, and concluded that reaction products differed depending
95 on the OH⁻ concentration in the aqueous medium. When the activator concentration was
96 high (> 10M of NaOH), the formed alkaline aluminosilicate gel was the principal product,
97 while hydrated calcium silicate was the secondary product. However, when the activator
98 concentration was low (< 5M of NaOH), dissolved aluminates were insufficient to
99 produce aluminosilicate gel and pozzolanic products predominated.

100 Boonjaeng et al. studied the system of lime and calcined clay materials with
101 different alkaline solutions of sodium hydroxide (NaOH). When comparing several
102 molarities (0.1M -10M), they concluded that the reaction of the mixture was dominated
103 by the NaOH concentration [30]. At low concentrations (<1M), the pozzolanic reaction
104 was dominant, while the zeolite-formation reaction predominated at medium NaOH
105 molarities (1M<NaOH<5M). Finally, at a high NaOH molarity (>5M), the principal
106 reaction was the geopolymerization process.

107 Fluid catalytic cracking catalyst residue (FCC) has been employed as a precursor
108 in geopolymeric mixtures in some reported studies. Tashima et al. made samples with
109 different SiO₂/Na₂O molar ratios [31]. These authors obtained mortars with a compressive
110 strength of 68 MPa after 3 curing days at 65°C. Trochez et al. obtained similar
111 compressive strength in pastes after curing at ambient temperature for 7 days [32].

112 The use of RHA has been studied by different research groups as an alternative
113 activator (source of silica). Mejía et al. employed two types of RHA and sodium silicate
114 (as a control mix) to activate mixtures with FA and BFS as precursors[17]. The samples
115 with sodium silicate displayed better mechanical strength than the mortars with RHA, but
116 the results of these mixtures gave a compressive strength close to 42 MPa. Bouzón et al.
117 employed RHA in systems with FCC as a precursor [18]. These authors obtained mortars
118 with very similar compressive strengths to the mortar with sodium silicate (40 MPa).
119 Another research work has reported poor results when RHA was compared to commercial
120 reagents. Luukkonen et al. compared the use of RHA and microsilica with that of sodium
121 silicate [33]. The compressive strength of mortars with an alternative activator was lower
122 than the commercial one, but proved sufficient for certain uses, and performed well with
123 freeze-thawing cycles. Villaquirán-Cacedo and Mejía de Gutiérrez [34] studied MK-
124 based geopolymers using mixtures of RHA or silica fume with KOH as activators. They

125 achieved a 47% reduction in the warming potential emissions for this system compared
126 to the corresponding commercial potassium silicate-activated system.

127 The present research studies the development of binary mixtures where the
128 lime/pozzolan binder was partially replaced with a geopolymeric mortar.

129 Lime mortars were made with a residual pozzolan, namely FCC. The
130 geopolymeric material was a mixture of FCC activated in two different ways: i) a solution
131 of sodium silicate (waterglass) and sodium hydroxide; ii) a suspension prepared as a
132 mixture of sodium hydroxide and RHA.

133 2 Materials and Methods

134 A commercial hydrated lime supplied by Cales Pascual (Paterna, Spain) was used.
135 This material is designed as CL90-S according to Spanish standard UNE-EN 459-1 [35].
136 The FCC residue was supplied by BP Oil España, S.A.U (Grao de Castellón, Spain). RHA
137 was supplied by Dacsa S.A (Tabernes Blanques, Spain).

138 FCC was employed as both the mineral admixture in the lime/pozzolan system
139 and a precursor in the geopolymer formulation.

140 The geopolymer was activated by two activators:

- 141 • A conventional alkaline solution prepared with a mix of waterglass (Na_2SiO_3 ,
142 commercial sodium silicate) (Merck, 28% SiO_2 ; 8% Na_2O and 64% H_2O) and
143 sodium hydroxide (Panreac-SA, 98% purity).
- 144 • An environmental-friendly alkaline solution where RHA was employed as an
145 alternative source of “sodium silicate”. RHA was mixed with water and sodium
146 hydroxide in a thermal bottle [22].

147 The chemical composition of FCC and RHA was analysed by X-Ray fluorescence
148 (XRF) equipment (Magic Pro Spectrometer-Philips). The results are summarised in Table
149 1.

150 **Table 1. Chemical composition of the used materials: fluid catalytic cracking catalyst**
151 **residue (FCC) and rice husk ash (RHA)**

| | SiO₂ | Al₂O₃ | Fe₂O₃ | CaO | MgO | SO₃ | K₂O | Na₂O | P₂O₅ | Others | *LOI |
|------------|------------------------|------------------------------------|------------------------------------|------------|------------|-----------------------|-----------------------|------------------------|-----------------------------------|---------------|-------------|
| FCC | 47.76 | 49.26 | 0.60 | 0.11 | 0.17 | 0.02 | 0.02 | 0.31 | 0.03 | 1.20 | 0.54 |
| RHA | 85.58 | 0.25 | 0.21 | 1.83 | 0.50 | 0.26 | 3.39 | ↓ | 0.67 | 0.32 | 6.99 |

152 *LOI: loss on ignition

153 The mean particle diameter of the supplied FCC was 21 μm . RHA was milled in
154 an industrial mill and its mean particle diameter was 20 μm . All the granulometric
155 measurements were taken in a Malvern Mastersizer 2000 in aqueous medium.

156 The amorphous content of RHA was 31.5%, calculated by an extractive method
157 using HCl and KOH [36].

158 Lime/pozzolan mortars and pastes were prepared at the following ratios:
159 lime/FCC = 1/1; water/binder = 0.8; sand/binder = 3. The lime/pozzolan ratio was chosen
160 based on the research group's previous research [37]. The employed sand was siliceous
161 in nature with a fineness modulus of 4.3. Mortars were moulded in cubic 40*40*40 mm³
162 casts and stored at 25°C and RH 73% for 24 h. Specimens were wrapped in film until
163 tested. Pastes were moulded in sealed polyethylene phials and stored at 25°C.

164 For the geopolymeric binder, the formulation of the alkaline activator solution was
165 selected according to a previous work [18]. The solution had a SiO₂/Na₂O molar ratio of
166 1.17, a sodium molality of 7.5 and a water/binder ratio of 0.6.

167 The replacements of lime/pozzolan binder mass with geopolymeric binder were
168 0% (control sample), 10%, 20%, 30% and 40%.

169 Table 2 summarises the quantity (expressed as grams) of the materials employed
170 in mortars. The control mortar was the mixture with only lime and pozzolan (CON). The
171 geopolymeric mortar (GEOP) was the mixture of FCC with the activator of NaOH and
172 Na₂SiO₃. The lime/pozzolan/GEOP mixtures were named CC_x or CA_x, where: i) CC is
173 the geopolymer activated by the conventional solution (waterglass and sodium hydroxide)
174 and CA is the geopolymer when RHA was employed as a silica source in alkaline
175 activator (RHA + water + sodium hydroxide); ii) x is the lime/pozzolan replacement
176 percentage with FCC geopolymer. For example, mortar CA10 contained 10%
177 geopolymer (FCC and an alkaline activator composed of a mixture of RHA, NaOH and
178 water).

179 The abbreviation FCC^P represents the quantity of FCC in the lime/pozzolan
180 binder, while the abbreviation FCC^G denotes the quantity of FCC in the geopolymeric
181 binder. H₂O^P was the water content in the lime/pozzolan system. The water used to
182 prepare the geopolymeric binder is indicated in the activator as H₂O^G.

183 **Table 2. Composition of lime/pozzolan mortar, lime/pozzolan/GEOP mortars and GEOP**
 184 **mortar (weight in grams).**

| | Lime/pozzolan binder | | GEOP binder | | | | | | Sand | |
|-------------|----------------------|------------------|-------------------------------|------------------|-------------------------------|------|----------------------------------|-----|------|---------------|
| | Lime | FCC ^P | H ₂ O ^P | FCC ^G | Activator | | | | | |
| | | | | | H ₂ O ^G | NaOH | Na ₂ SiO ₃ | RHA | | |
| CON | 262.5 | 262.5 | 420.0 | - | - | - | - | - | - | 1575.0 |
| CC10 | 236.3 | 236.3 | 378.0 | 52.5 | 12.6 | 6.4 | 29.5 | - | - | 1575.0 |
| CA10 | 236.3 | 236.3 | 378.0 | 52.5 | 31.5 | 9.4 | - | - | 9.2 | 1575.0 |
| CC20 | 210.0 | 210.0 | 336.0 | 105.0 | 25.2 | 12.8 | 59.1 | - | - | 1575.0 |
| CA20 | 210.0 | 210.0 | 336.0 | 105.0 | 63.0 | 18.9 | - | - | 18.4 | 1575.0 |
| CC30 | 183.8 | 183.8 | 294.0 | 157.5 | 37.8 | .2 | 88.6 | - | - | 1575.0 |
| CA30 | 183.8 | 183.8 | 294.0 | 157.5 | 94. | 28.4 | - | - | 27.6 | 1575.0 |
| CC40 | 157.5 | 157.5 | 252.0 | 210.0 | 50.4 | 25.6 | 118.3 | - | - | 1575.0 |
| CA40 | 157.5 | 157.5 | 252.0 | 210.0 | 126.0 | 37.8 | - | - | 36.7 | 1575.0 |
| GEOP | - | - | - | 525.0 | 126.0 | 64.0 | 295.3 | - | - | 1575.0 |

185

186 Pastes lime/pozzolan, lime/pozzolan/GEOP and GEOP had the same proportions
 187 of materials as the corresponding mortars, but without sand. An additional paste
 188 containing 80% GEOP and 20% hydrated lime was fabricated and called GEOP-CH.

189 Compressive strength was measured in an INSTRON 3282 machine for the ages
 190 of 1, 2, 3, 7, 28 and 90 days, and was the average of four individual tests.

191 The microstructural analysis of pastes was carried out by a thermogravimetric
 192 analysis (TG/DTG), powder X-Ray diffraction (XRD), Fourier transform infrared
 193 spectroscopy (FTIR) and field emission scanning electron microscopy (FESEM).

194 The TG analysis was done using a TGA 850 Mettler-Toledo thermobalance. The
 195 TG experiments were performed from 50°C to 600°C at a heating rate of 10°C.min⁻¹.
 196 Aluminium-sealed crucibles (70 µL volume) were used with a pinholed lid and a nitrogen
 197 atmosphere (flow gas rate of 75 mL.min⁻¹). The XRD analyses were carried out in a
 198 Bruker AXS D8 Advance device from 10° to 70° 2θ (2s accumulation time in a 0.02 angle
 199 step). The FTIR analyses were run in a Bruker Tensor 27 and analysed within the 400-
 200 4000 cm⁻¹ range. The FESEM micrographs were taken in a Zeiss ULTRA 55. Pastes were
 201 carbon-coated and images were taken at 2kV. For the EDS analysis (X-ray energy
 202 dispersive spectroscopy), data were taken at 15kV.

1
2
3
4
5
6
7
8
9
10
11
12
13
14
15
16
17
18
19
20
21
22
23
24
25
26
27
28
29
30
31
32
33
34
35
36
37
38
39
40
41
42
43
44
45
46
47
48
49
50
51
52
53
54
55
56
57
58
59
60
61
62
63
64
65

203 3 Results and Discussion

204 3.1 Compressive strength development

205 In the first stage, the study of incorporating the geopolymer fabricated with
206 commercial reagents (sodium silicate as a silica source) was analysed. The substitution
207 percentages went from 10% to 40%, and the selected curing ages were 1, 2, 3, 7, 28 and
208 90 days. The results are represented in Figure 1. For all the curing ages, the mortars with
209 geopolymer obtained higher compressive strengths than that for the mortar with only FCC
210 and lime (the control mortar: CON). After 1 curing day, mortar CC40 (14.9 MPa) had the
211 same compressive strength as CON (14.3 MPa) after 90 curing days.

212 **It is highlighted the compressive strength gain at early ages with the incorporation**
213 **of the geopolymer into the lime/pozzolan systems. With the 10% substitution (sample**
214 **CC10), compressive strength was 45% greater than the strength for CON after 1 curing**
215 **day and was 152% greater after 7 curing days.**

216 Figure 1 illustrates how the CON mortars had a low compressive strength (< 2
217 MPa) until 7 days. Compressive strength evolution was 190% from 7 days to 28 days,
218 with 37% evolution from 28 days to 90 curing days. Mixture CC40 yielded fast evolution
219 between 1 and 7 days (65%), when its evolution was asymptotic until 90 days with
220 compressive strength at around 25 MPa.

221 The evolution of mortar CC10 was remarkable. The sample began with only 2.08
222 MPa at 1 curing day, but reached 21.09 MPa at 90 curing days (913% evolution). This
223 compressive strength was only slightly lower than that found for the mortar with the
224 highest geopolymer content (CC40). The effect of a small amount of geopolymer on the
225 lime/pozzolan system was marked. The incorporation of geopolymer enhanced the
226 formation of the new reaction products, which improved the strength of the mortars. The
227 new aluminosilicate gel type C(N)ASH was probably formed in the
228 lime/pozzolan/geopolymer systems. García-Lodeiro et al.[38] reported the formation of
229 this product type in hybrid alkaline cements using FA and Portland cement. Sodium ions
230 replaced calcium ions as charge balancers.

231

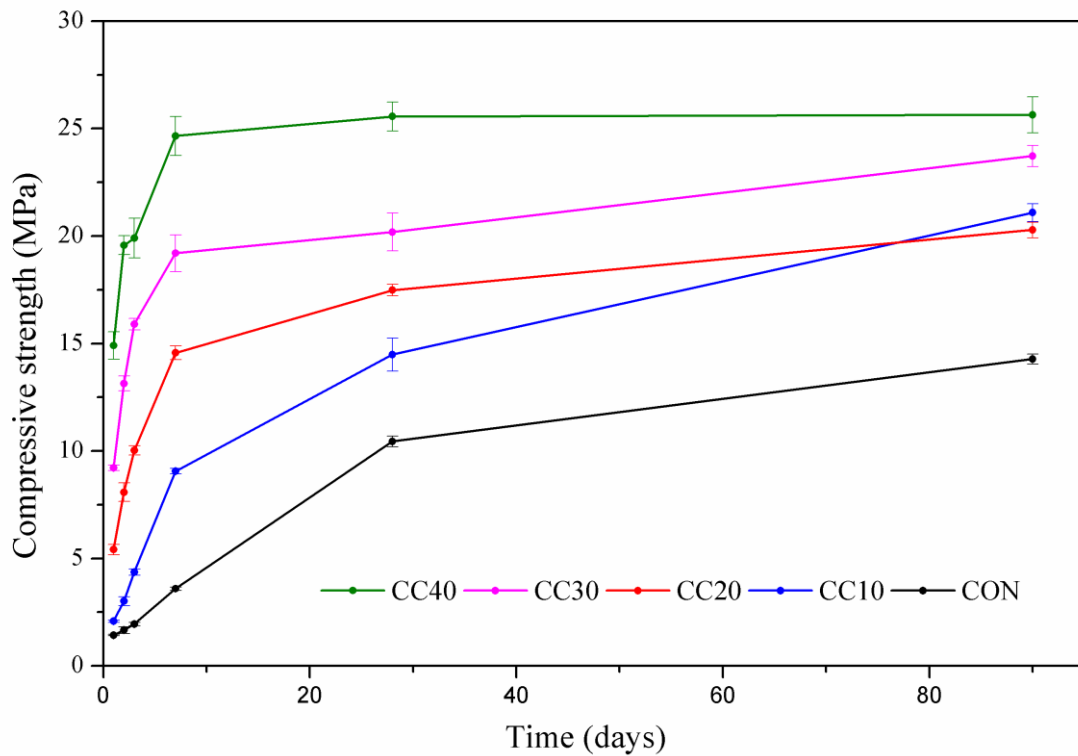


Fig 1. Evolution of the compressive strength of mortars CON and CC at 1, 2, 3, 7, 28 and 90 curing days.

232

233 For this above-discussed first stage, the obtained results contrasted those obtained
 234 by other researchers. Boonjaeng et al, used MK and lime systems, and indicated that
 235 geopolymeric gel was not as strong as CASH and CSH gel [30]. In the present work, the
 236 alkaline activator dose was used only for FCC as a precursor, and the other part of mortar
 237 (lime-pozzolan) was mixed only with water. Conversely in the research by Boonjaeng et
 238 al, the lime/MK mixture was considered the binder and was activated with NaOH [30].

239 The geopolymeric mortar without lime (pure geopolymer, GEOP) was analysed
 240 for the same curing ages. The compressive strength of this sample was generally very
 241 high, especially at early curing ages, between 1 and 7 curing days. After the first curing
 242 day the GEOP mortars yielded 13.38 MPa and the compressive strength increases until
 243 53.90 MPa at 7 curing days. No CCx system had a compressive strength greater than 25
 244 MPa. The nature of the gel in these mortars was the NASH type [39].

1
2
3
4
5
6
7
8
9
10
11
12
13
14
15
16
17
18
19
20
21
22
23
24
25
26
27
28
29
30
31
32
33
34
35
36
37
38
39
40
41
42
43
44
45
46
47
48
49
50
51
52
53
54
55
56
57
58
59
60
61
62
63
64
65

245 A comparison of the strength values at early (1-7 days) and long-term (28-90 days)
 246 ages can be made to analyse strength development in the different mortars CC.
 247 Theoretical strength (R_{th}) can be calculated by taking into account the contribution of the
 248 lime/pozzolan and geopolymer fractions as follows (Equation 1):

$$R_{th}=R_{lp}*X_{lp}+R_g*X_g \quad (1)$$

249
 250 Where R_{lp} and R_g are the strength of the mortar lime-pozzolan (CON) and the
 251 mortar pure geopolymer (GEOP), respectively; X_{lp} and X_g are the mass fractions of both
 252 mortars in the CC mixtures (0.9-0.6 for X_{lp} ; 0.1-0.4 for X_g).

253 Table 3 compares the theoretical values (R_{th}) to the experimental values (R_{ex}), and
 254 the difference in strength (D) is summarised for the mortars cured within the curing time
 255 range of 1-90 days. The D values for CC20, CC30 and CC40 were positive at early curing
 256 ages (1-3 days), which suggests that the role of calcium from lime is crucial for
 257 developing a strong cementing gel. In this case, gels CASH or C(N)ASH formed. For
 258 longer curing times, the opposite trend was seen, and the D values were negative after 28
 259 and 90 curing days. This behaviour suggests that the contribution of the NASH gel to
 260 strength became less relevant when the binary system was fabricated. It was noteworthy
 261 that for 1-3 curing days, the presence of calcium in the mixture enhanced the gel's
 262 strength properties, which confirmed the positive effect by mixing both types of
 263 cementing systems.

264 **Table 3.** Difference (D, in MPa) in mortar strengths, calculated as experimental strength
 265 (R_{ex}) minus theoretical strength (R_{th}).

| System | Curing days | | | | | |
|--------|-------------|-------|-------|------|-------|-------|
| | 1 | 2 | 3 | 7 | 28 | 90 |
| CC10 | -0.55 | -1.10 | -0.83 | 0.44 | -0.34 | 2.54 |
| CC20 | 1.59 | 1.52 | 1.59 | 0.91 | -1.71 | -2.55 |
| CC30 | 4.19 | 4.12 | 4.21 | 0.52 | -3.39 | -3.40 |
| CC40 | 8.69 | 8.11 | 4.97 | 0.94 | -2.39 | -5.76 |

266

267 In the second stage, the use of an alternative alkaline activator was explored.
 268 Resorting to RHA as a silica source was investigated as a sodium silicate substitute. The
 269 RHA and NaOH mixture in a thermal bottle was used as an activator at the same
 270 proportions as the commercial reagents. A strength variation percentage (VR) was
 271 calculated for the alternative mixtures (CA) using Equation 2:

$$VR = 100 * (R_{CAx} - R_{CCx} / R_{CCx}) \quad (2)$$

272
 273 Where R_{CAx} is the compressive strength for a given percentage of geopolymers (x)
 274 in a mortar with RHA (CA); R_{CCx} is the compressive strength for the same percentage (x)
 275 in a mortar with sodium silicate (CC).

276 Figure 2 represents the VR evolution for all the replacement percentages and
 277 curing ages. The samples with values over the red line yielded a compressive strength
 278 that was more than 2-fold higher than the values yielded by mortars CC.

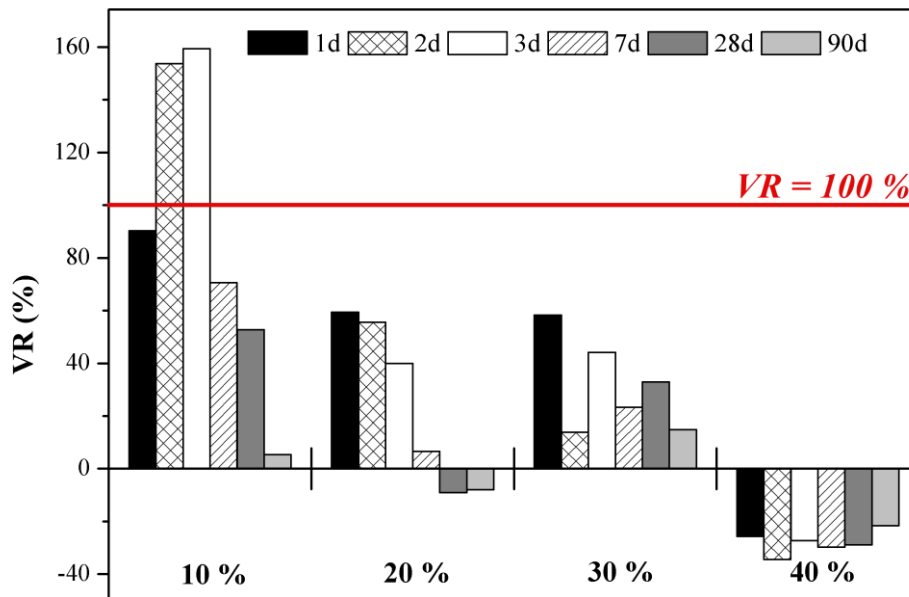


Figure 2. Strength variation (VR) percentages for the mortars with alternative silicate (CA samples).

279

280 Higher VR values were obtained for the 10% substitution percentage. For 2 and 3
281 curing days, these values were higher than 100% (153.7% and 159.3%, respectively) and
282 the minimum value was obtained at 90 curing days (5.34%). The systems with 20% and
283 30% geopolymers were less effective. With 20% (CA20 samples), mortars had low
284 negative VR values (-9.1% and -7.92%, respectively), even at 28 and 90 days. The
285 samples with the 40% substitution yielded negative VR values for all the curing ages.
286 These negative values can be attributed to the poor workability of the RHA-containing
287 mortars, whereas the mixtures with the commercial reagent were easily compacted.

288 **The good behaviour of RHA as silica source may be the result of a more enhanced**
289 **connectivity in microstructure of the samples activated with this material as said**
290 **Villaquirán- Caicedo in the paper published in 2019 [40].** The results were very
291 interesting from a practical viewpoint because mixtures can be obtained with good
292 compressive strength without using commercial sodium silicate, which is a synthetic
293 chemical reagent with a large carbon footprint, as previously reported [41]. The
294 replacement of commercial sodium silicate with RHA led to very good mortar
295 performance in terms of early-age compressive strength, which makes the small
296 geopolymer dose in the lime/pozzolan system more appealing.

297 3.2 Thermogravimetric studies

298 The lime-pozzolan (CON), lime-pozzolan/geopolymer (CC and CA samples) and
299 geopolymer (GEOP) pastes had the same proportions as the mortars, but without sand.
300 To simplify the study, it represented only the pastes with the 10% and 40% substitution
301 percentages, CON and GEOP. The selected curing ages were 3, 28 and 90 days. Figure 3
302 depicts the DTG curves.

303 Three principal zones of mass loss were observed in the CON paste, but a
304 continuous mass loss fell within the 100-600°C range. Zone 1 (100-180°C) was attributed
305 to the dehydration of CSH; zone 2 (180-300°C) was related to the dehydration of CASH
306 and CAH; zone 3 was assigned to the dehydroxylation of $\text{Ca}(\text{OH})_2$ [42]. The GEOP paste
307 had only one peak centred at about 150°C, attributed to the dehydration of the NASH gel
308 [43]. In the pastes with lime-pozzolan/geopolymer, peaks differed in accordance with the
309 substitution percentage. Pastes CC10 and CA10 with the 10% substitution looked a lot
310 like the CON paste, while pastes CC40 and CA40 with the 40% substitution had a similar
311 profile to the geopolymeric paste (GEOP).

312 The main peak in pastes CON, CC10 and CA10 at 3 and 7 curing days was centred
 313 in zone 2, and was attributed to the dehydration of CASH and CAH. At 90 days, a well-
 314 defined peak was seen for CSH dehydration on the DTG curves. The presence of hydrated
 315 lime was observed until 28 days for the control pastes, and in paste CC10 at 3 curing days.
 316 Hence, the reaction of hydrated lime to FCC was much faster when the geopolymer was
 317 present.

318 The principal peak in GEOP, CC40 and CA40 at all the curing ages was centred
 319 at about 150°C. This peak was attributed to the NASH gel for GEOP and a mixture of
 320 NASH and C(N)ASH gels for CC40 and CA40. The peak in paste GEOP was much wider
 321 than that in pastes CC40 and CA40. The NASH gel probably had a higher temperature
 322 decomposition range than the C(N)ASH gel.

323 The mass losses within the different temperature ranges were analysed to
 324 understand the evolution of the geopolymeric and pozzolanic reactions. The chosen mass
 325 loss zones were: 50°C to 180 °C (ML₁); 80°C to 300°C (ML₂); total mass loss went from
 326 35°C to 600°C (ML_T). Table 4 summarises the results.

327 **Table 4.** Mass loss (TG analysis) of pastes for 3, 28 and 90 curing days.

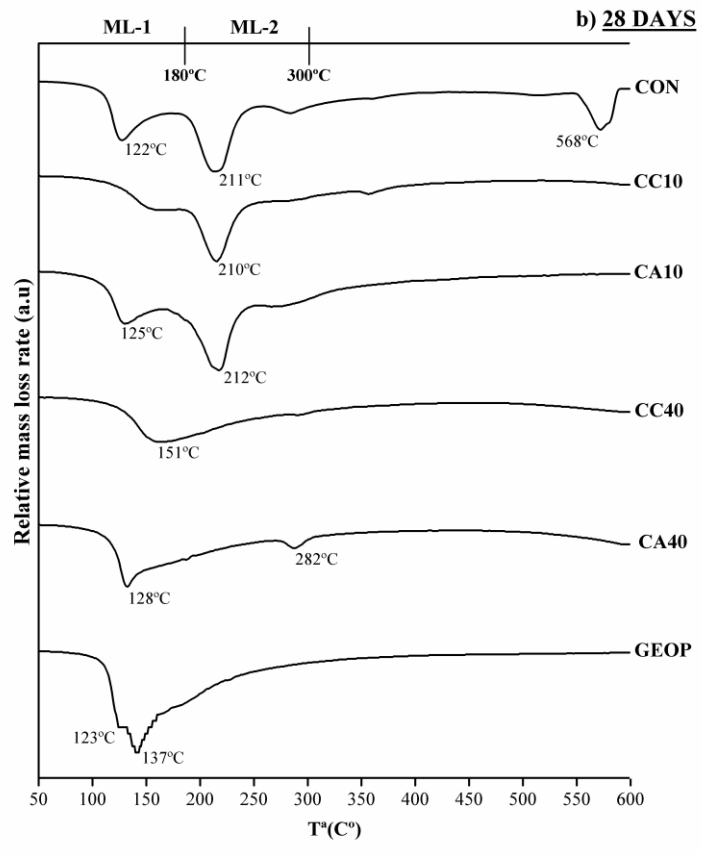
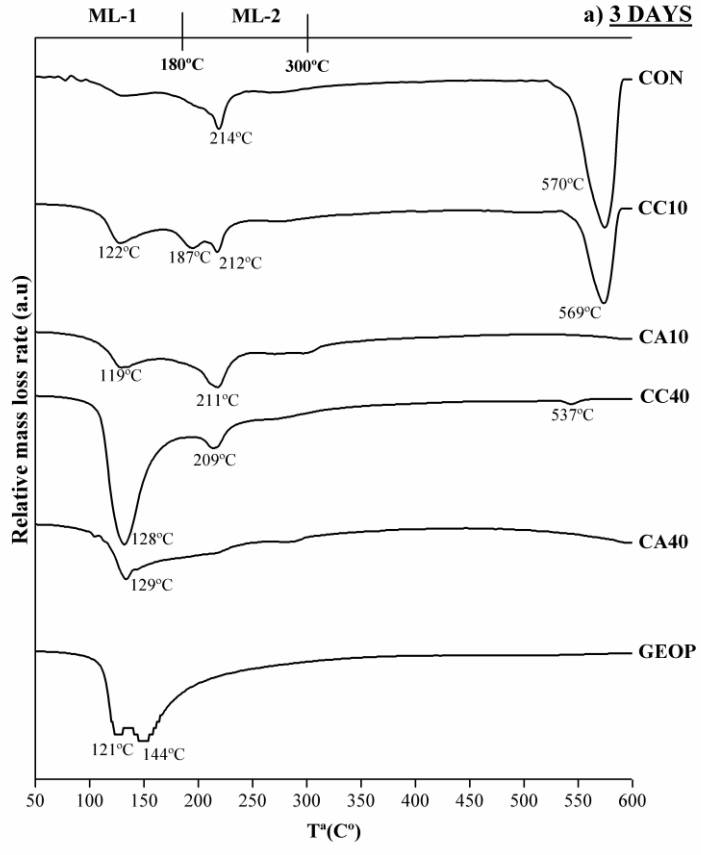
| | ML₁ (50-180°C) | ML₂ (180-300°C) | ML_T (35-600°C) |
|-----------------|--|---|--|
| CON 3d | 2.14 | 4.21 | 15.88 |
| CON 28d | 4.44 | 8.61 | 20.61 |
| CON 90d | 5.69 | 8.36 | 18.67 |
| CC10 3d | 3.49 | 4.87 | 15.43 |
| CC10 28d | 4.70 | 7.07 | 16.75 |
| CC10 90d | 5.43 | 8.09 | 18.05 |
| CA10 3d | 3.68 | 5.97 | 12.00 |
| CA10 28d | 4.28 | 10.17 | 18.59 |
| CA10 90d | 4.88 | 6.63 | 15.12 |
| CC40 3d | 6.12 | 3.79 | 14.67 |
| CC40 28d | 6.57 | 4.86 | 16.04 |
| CC40 90d | 6.92 | 4.13 | 15.27 |
| CA40 3d | 5.24 | 3.83 | 13.04 |
| CA40 28d | 5.32 | 3.78 | 13.51 |
| CA40 90d | 6.48 | 4.10 | 14.66 |
| GEOP 3d | 7.96 | 3.94 | 14.07 |
| GEOP 28d | 9.23 | 4.25 | 15.49 |
| GEOP 90d | 9.38 | 3.69 | 15.19 |

328 For the pastes in which the geopolymer reaction was the principal reaction and the
 329 gel C(N)ASH or NASH were the main products, the mass loss within the ML₁ range was
 330 greater than within the ML₂ range. The mass loss within interval ML₂ was, in this case,

1 331 attributed to the same product as the decomposition peak was wide. The geopolymer
2 332 reaction was the predominant reaction in pastes GEOP, CC40 and CA40 as the activator
3 333 concentration was higher than that in the samples with only the 10% substitution. This
4 334 conclusion falls in line with previously reported papers [28, 29, 44], which studied
5 335 lime/MK mixtures at different sodium hydroxide concentrations. When the activator
6 336 concentration was low, the principal reaction product was CSH; when the concentration
7 337 was high, the main product was the C(N)ASH gel and CSH formed as a secondary
8 338 reaction product.

9
10
11
12
13
14
15 339 In the paper published in 2013 by García-Lodeiro et al.[38] the authors explained
16 340 the conversion of NASH gel into C(N)ASH gel. The presence of a solution enriched with
17 341 Al(OH)_4^- and Si(OH)_4 species, in addition to the presence of sodium ions, induced this
18 342 type of NASH gel. Depending on the calcium concentration in the medium, total
19 343 conversion into CASH gel can take place.
20
21
22
23
24
25
26
27
28
29
30
31
32
33
34
35
36
37
38
39
40
41
42
43
44
45
46
47
48
49
50
51
52
53
54
55
56
57
58
59
60
61
62
63
64
65

1
2
3
4
5
6
7
8
9
10
11
12
13
14
15
16
17
18
19
20
21
22
23
24
25
26
27
28
29
30
31
32
33
34
35
36
37
38
39
40
41
42
43
44
45
46
47
48
49
50
51
52
53
54
55
56
57
58
59
60
61
62
63
64
65



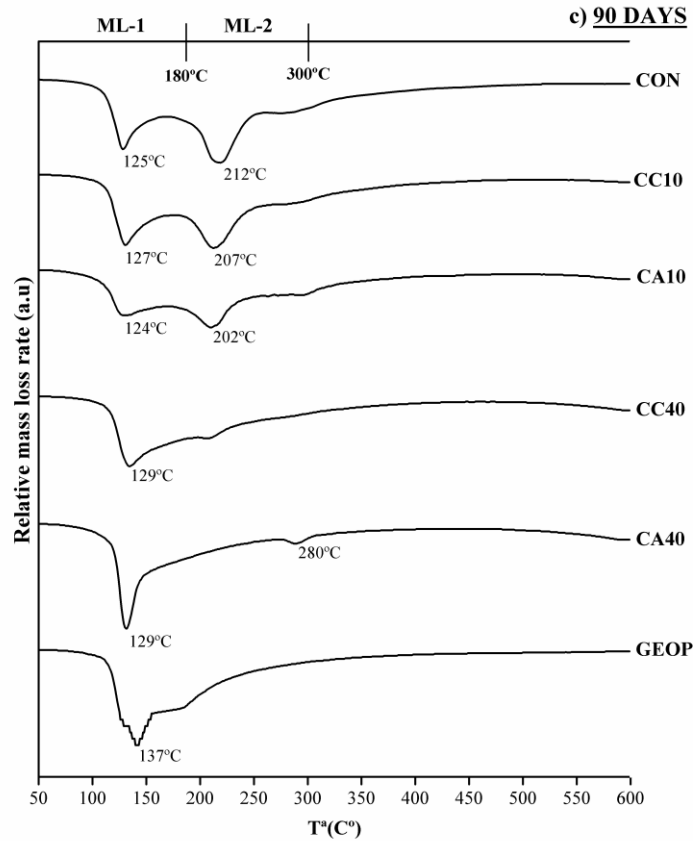


Figure 3. DTG curves for the pastes cured at: a) 3; b) 28; and c) 90 curing days.

To analyse the role of calcium in a geopolymeric paste, a paste (GEOP-CH) was fabricated by mixing 80% GEOP paste (FCC with NaOH and Na_2SiO_3 as an alkaline activator) and 20% hydrated lime. The first problem was that this paste (GEOP-CH) needed water, which was added because it was impossible to prepare paste at the 0.6 water/FCC ratio (lack of workability), and the new water/FCC ratio was increased to 1.1. The paste was analysed after 7 curing days. Figure 4 represents the DTG curves for pastes GEOP and GEOP-CH. GEOP-CH did not present a peak for the dehydroxylation of hydrated lime within the 500-600°C range. The calcium from the hydrated lime was incorporated into the aluminosilicate gel. Its decomposition peak fell within the same decomposition temperature range observed for the paste without hydrated lime.

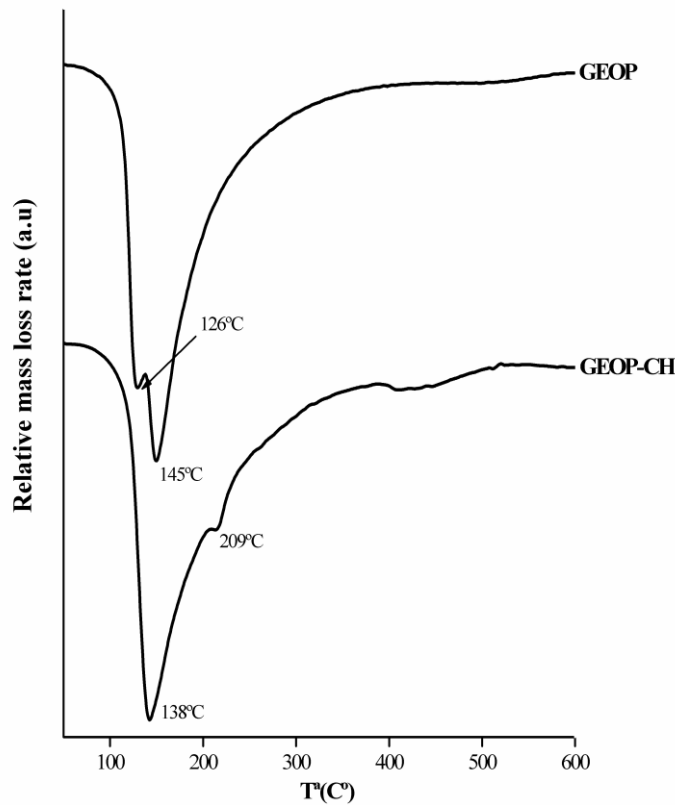


Figure 4. DTG curves for pastes GEOP and GEOP-CH after 7 curing days.

3.3 FTIR studies

Figure 5 illustrates the evolution of the reaction process for pastes CON, CC10, CA10, CC40, CA40 and GEOP at 3, 28 and 90 curing days by the FTIR technique.

The evolution of lime/pozzolan paste is represented in Figure 5.a, and the principal peaks were: i) presence of carbonates and carboaluminates (bands at 1,700, 1,435 and 875 cm^{-1}). The asymmetric stretching vibrations of the C-O group were represented at a wave number of around 1,435 cm^{-1} and the band at 875 cm^{-1} corresponded to the bending mode of the carbonate ion [40, 45]; ii) the bands of CSH caused by the bending of SiO_4 tetrahedral units fell within an approximate range of 400-500 cm^{-1} and the asymmetric Si-O stretching vibration of the CSH within the 1,100-960 cm^{-1} interval [42,46]; iii) the presence of the signals attributed to vibrations Si-O-Si, Si-O-Al and Al-O at 528 and 709 cm^{-1} as a result of the presence of CASH and CAH [42,47,48]. The presence of carbonates could be due to a number of factors: presence of calcite in the hydrated lime; formation of carboaluminate by a reaction of carbonate and the alumina of FCC; carbonation of reaction products. The band of the asymmetric Si-O stretching vibration

1
2
3
4
5
6
7
8
9
10
11
12
13
14
15
16
17
18
19
20
21
22
23
24
25
26
27
28
29
30
31
32
33
34
35
36
37
38
39
40
41
42
43
44
45
46
47
48
49
50
51
52
53
54
55
56
57
58
59
60
61
62
63
64
65

370 of CSH for the samples cured for 3 days was located at a higher wave number than for
371 the pastes cured for 28 and 90 days.

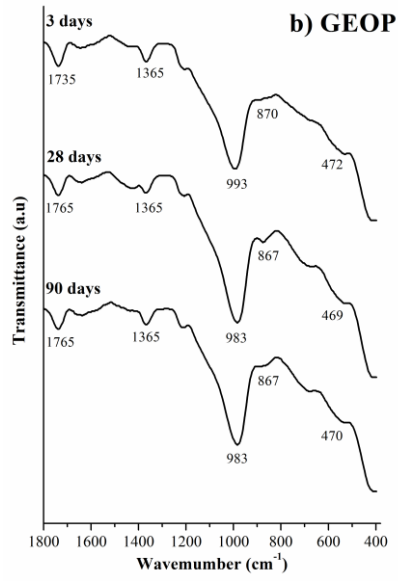
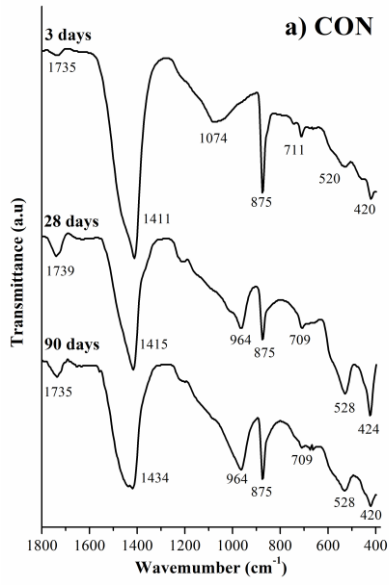
372 The geopolymeric paste is represented in Figure 5.b. The observed principal peak
373 was due to the presence of the NASH gel, with a band at 983-993 cm^{-1} for the
374 geopolymeric binder. A high-intensity broad band of between 1,200-900 cm^{-1} was
375 identified, which corresponded to the asymmetrical stretching of Si-O-T (T = Si or Al
376 bonds [40]). In particular, the SiQ^2 unit showed infrared absorption at around 950 cm^{-1} .
377 The bands at 1,735 and 1,365 cm^{-1} were attributed to the presence of carbonate [47,48].
378 The bands with lesser intensity, around 867 cm^{-1} , were identified as Si-O stretching and
379 OH bending (Si-OH). The peak was attributed to bending bands (Si-O-Si and O-Si-O)
380 with those at around 470 cm^{-1} [49].

381 The pastes containing 10% geopolymer showed similar peaks to the lime-
382 pozzolan paste. These peaks were located at around 1,460-1,420, 1,014-950, 875 and 435-
383 420 cm^{-1} . Allali et al.[26] established that when the MK geopolymer included calcium in
384 the system, the Si-O-Si band was displaced from 985 cm^{-1} to an Si-O-Ca band at 930 cm^{-1} .
385 In the present research, this displacement was especially observed for the CA sample
386 at 90 curing days. The corresponding band was found at 950 cm^{-1} , and significantly
387 differed from that for the CC sample (968 cm^{-1}). This meant that the presence of a
388 different source of silica in the geopolymer changed the final geopolymeric gel structure.

389 For the CC40 paste, the signal attributed to the gel (NASH) was found at 968 cm^{-1}
390 (after 90 curing days). For the CA40 paste, the corresponding signal was displaced at a
391 lower wave number (950 cm^{-1}). Once again, the different source of silica modified the
392 gel's nature.

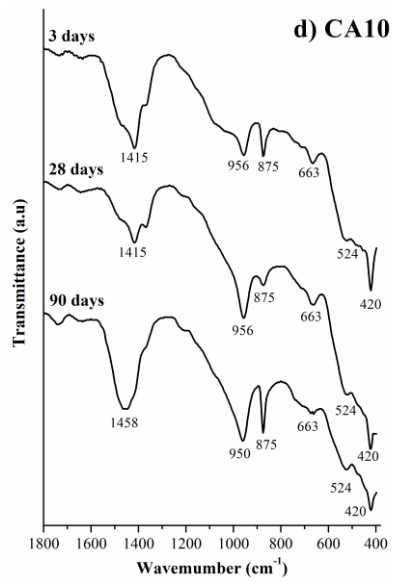
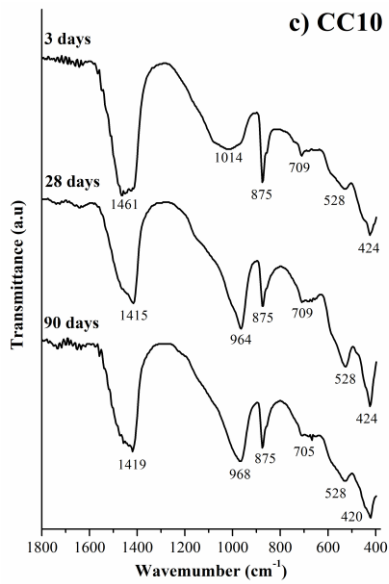
393 García Lodeiro et al. established that adding Ca to the NASH gel would change
394 the orientation of the structure, but this change was not easily observed by FTIR [50].

1
2
3
4
5
6
7
8
9
10
11
12
13
14
15
16
17
18
19
20
21
22
23
24
25
26
27
28
29
30
31
32
33
34
35
36
37
38
39
40
41
42
43
44
45
46
47
48
49
50
51
52
53
54
55
56
57
58
59
60
61
62
63
64
65



figure

modified



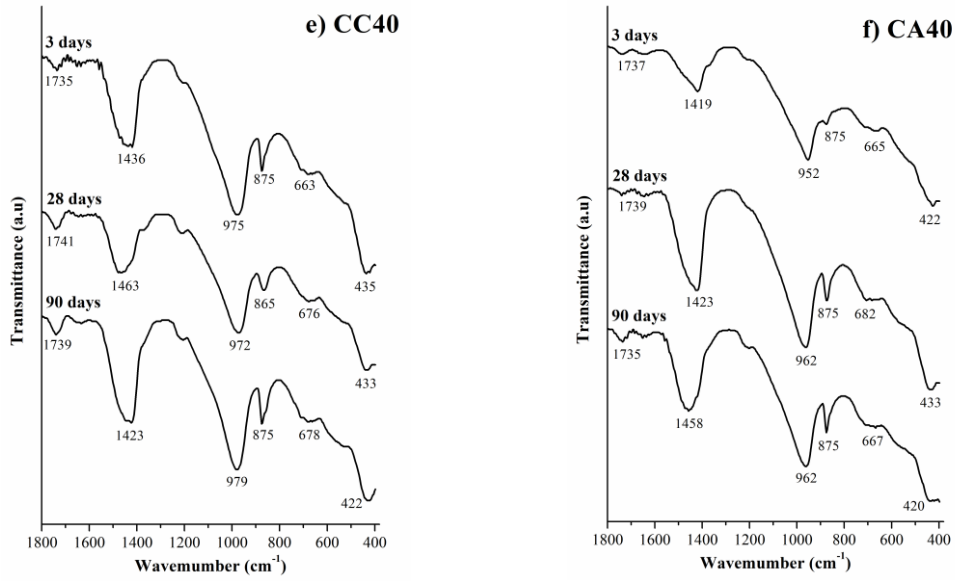


Figure 5. FTIR curves for the pastes cured at 3, 28 and 90 days

395

396 Paste GEOP-CH was also studied by FTIR. Figure 6 represents pastes GEOP-CH
 397 and GEOP at 7 curing days. A displacement of the band (995 cm^{-1} vs. 948 cm^{-1}) related
 398 to the NASH gel took place in the paste with lime (GEOP-CH). This spectrum confirmed
 399 the incorporation of Ca into the aluminosilicate gel's structure.

400

401

1
2
3
4
5
6
7
8
9
10
11
12
13
14
15
16
17
18
19
20
21
22
23
24
25
26
27
28
29
30
31
32
33
34
35
36
37
38
39
40
41
42
43
44
45
46
47
48
49
50
51
52
53
54
55
56
57
58
59
60
61
62
63
64
65

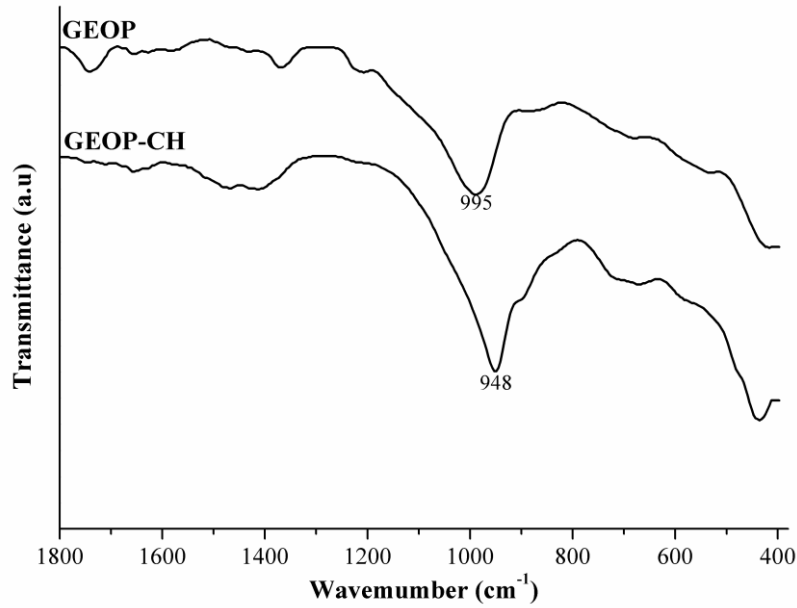


Figure 6. FTIR curves for GEOP and pastes GEOP-CH after 7 curing days.

402

403 3.4 XRD studies

404 The X-ray diffraction patterns are depicted in Figures 7-10. Pastes CON, CC10,
 405 CC40, CA10 and CA40 were studied by comparing 3, 28 and 90 curing days, and pastes
 406 GEOP and GEOP-CH were also compared. In general, a baseline deviation within the
 407 $2\Theta=20^\circ - 40^\circ$ range in all the studied pastes suggested the presence of an amorphous
 408 phase. With the progress made in curing time, the baseline deviation was more evident
 409 given the progress made in the geopolymerization reaction. Table 5 summarises the
 410 employed key, name of phases, chemical formula and PDF Card for the mineral phases
 411 found in the pastes.

412

413

414

415

416

417

418

419 **Table 5.** PDF Card of the phases and chemical formula of phases present in pastes.

| Key | Phase | Chemical formula | PDF Card |
|-----|----------------|--|----------|
| P | Portlandite | Ca(OH) ₂ | #040733 |
| S | Strätlingite | Ca ₂ Al ₂ SiO ₇ .8H ₂ O | #290285 |
| Q | Quartz | SiO ₂ | #331161 |
| A | Albite | NaAlSi ₃ O ₈ | #191184 |
| M | Mullite | Al ₆ Si ₂ O ₁₃ | #150776 |
| C | Calcite | CaCO ₃ | #050586 |
| L | Carboaluminate | Ca ₄ Al ₂ O ₆ CO ₃ .11H ₂ O | #410210 |
| B | Carboaluminate | Ca ₈ Al ₄ O ₁₄ CO ₂ .24H ₂ O | #360129 |
| Z | Zeolite A | Na ₂ Al ₂ Si _{3.3} O _{10.6} .7H ₂ O | #120228 |
| T | Trona | Na ₃ H(CO ₃) ₂ .2H ₂ O | #291447 |
| W | Wollastonite | CaSiO ₃ | #100489 |
| V | Vaterite | CaCO ₃ | #240030 |
| X | Zeolite X type | Na ₂ Al ₂ Si _{2.4} O _{8.8} .6.7H ₂ O | #120246 |
| Za | Zeolite ZK5 | 2.85Na ₂ O.1.89Al ₂ O ₃ .7.92SiO ₂ .12.2H ₂ O | #370360 |
| Cr | Cristobalite | SiO ₂ | #391425 |
| F | Faujasite | Na ₂ Al ₂ Si ₄ O ₁₂ .8H ₂ O | #391380 |

420

421 Figure 7 shows the XRD patterns of paste CON (lime-pozzolan) after 3, 28 and
 422 90 curing days. The peaks of the non-reacted portlandite (P) were observed after 3 curing
 423 days. Characteristic peaks of albite (A) and traces of faujasite were also found. It was
 424 noteworthy that calcite was not present in the CON paste at an early age and carbonate
 425 was combined with aluminium as carboaluminates (characteristic L and B peaks). Other
 426 authors have made these observations in lime-pozzolan samples [51,52]. After 28 curing
 427 days, less intense portlandite peaks were detected as the FCC reaction progressed, and no
 428 faujasite peaks appeared in the XRD pattern. Traces of quartz (Q), A and mullite (M)
 429 were also observed. Characteristic strätlingite (S) peaks were noted in the CON paste at
 430 this age, which confirmed the peak observed on the DTG curves within the 210-280°C
 431 temperature range. This compound is typical in lime-pozzolan materials with a high
 432 aluminium content [52,53], as for FCC (Al₂O₃ = 49.26 %; see Table 1). After 90 curing
 433 days, the diffractogram of paste CON was similar to that for 28 curing days. To a large
 434 extent, the P peaks had mitigated and the main S peak appeared more intensely, which

435 suggests high pozzolanic reactivity with curing time. A broad peak was seen within the
 436 28.5°-29.5° 2 θ range, which suggests the presence of the CSH/CASH gel, especially after
 437 90 curing days.

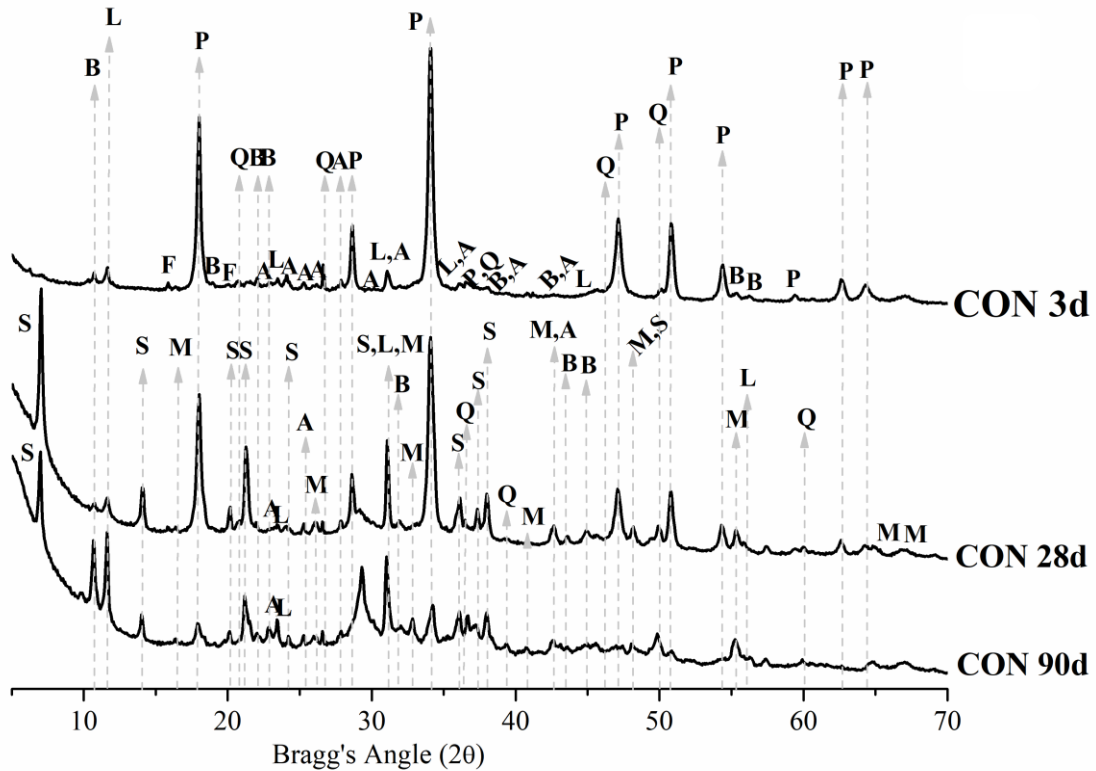


Figure 7. XRD patterns of the CON paste after 3, 28 and 90 days

438
 439 Figures 8-9 show the XRD patterns of the lime-pozzolan/geopolymer activated
 440 with the alkali solution prepared by using commercial sodium silicate and RHA,
 441 respectively. The pastes with 10% geopolymer (CC10 or CA10) and with 40%
 442 geopolymer (CC40 or CA40) were tested and analysed after 3, 28 and 90 curing days.

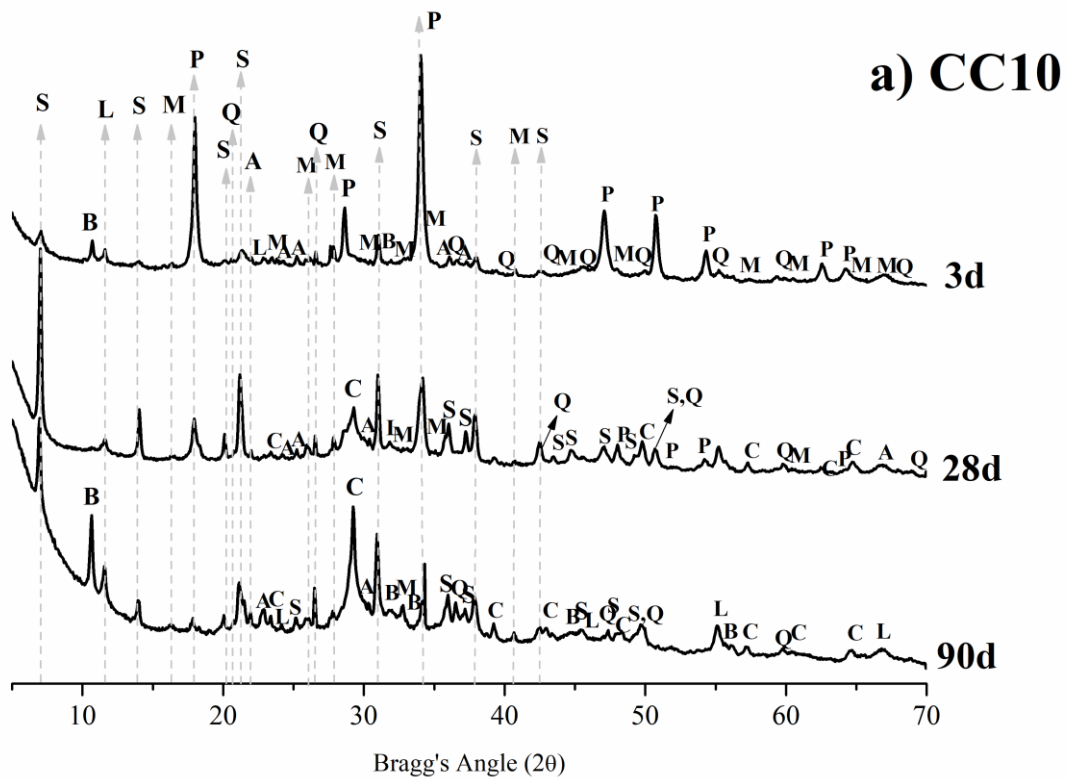
443 In paste CC10 (Figure 8a), the main characteristics peaks were P and S at 28 at 90
 444 curing day. Strätlingite (S) was attributed to the pozzolanic reaction. As with the CON
 445 paste, the intensity of the peaks corresponding to P and S diminished and increased,
 446 respectively, with curing time. Minority peaks (Q and A) were present at the three
 447 analysed curing times. Carboaluminate peaks (L and B) were found, whose intensity
 448 increased with time. Calcite (C) peaks were also found after 28 and 90 curing days. In
 449 this case, the broad peak related to CSH/CASH, together with the main C peak whose

1
2
3
4
5
6
7
8
9
10
11
12
13
14
15
16
17
18
19
20
21
22
23
24
25
26
27
28
29
30
31
32
33
34
35
36
37
38
39
40
41
42
43
44
45
46
47
48
49
50
51
52
53
54
55
56
57
58
59
60
61
62
63
64
65

450 intensity was significant after 28 days, which was earlier than for CON and suggests a
451 faster reaction rate for this gel type to form.

452 When the 40% geopolymer was employed (CC40), the portlandite peaks were low
453 in intensity (especially for 90 curing days) and the peak of the CSH/CASH gel was strong
454 in this XRD pattern. A new crystalline phase Z (Zeolite A) was also detected, mainly at
455 90 curing days. The formation of Zeolite A and Zeolite X has been reported in other
456 papers in which geopolymers were prepared with the activation of MK/RHA [54]. As the
457 CC10 paste pattern shows, traces of Q and A and B/L carboaluminate peaks were present
458 throughout the three analysed ages for paste CC40. No S was detected in this paste, which
459 suggests that its formation by the pozzolanic reaction was not favourable, and gels NASH
460 or C(N)ASH should be preferably produced, as corroborated by the large broad peak
461 shown (28.5°-29.5° 2 θ ,) after 3 curing days.

462



463

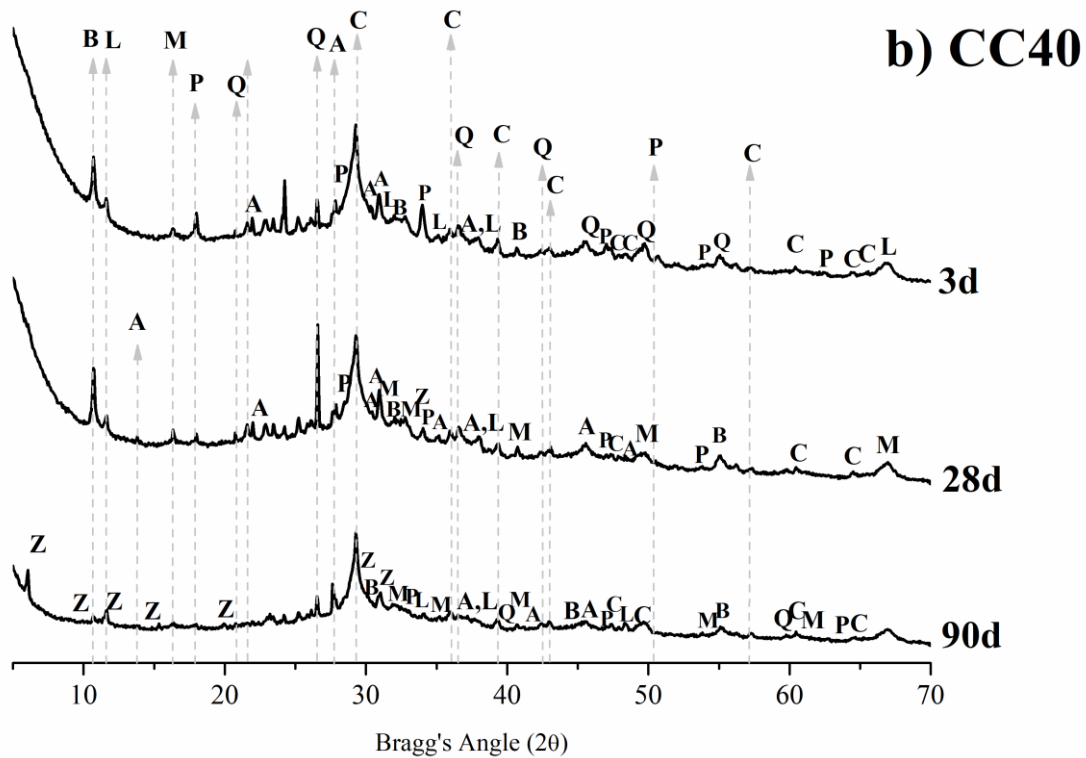
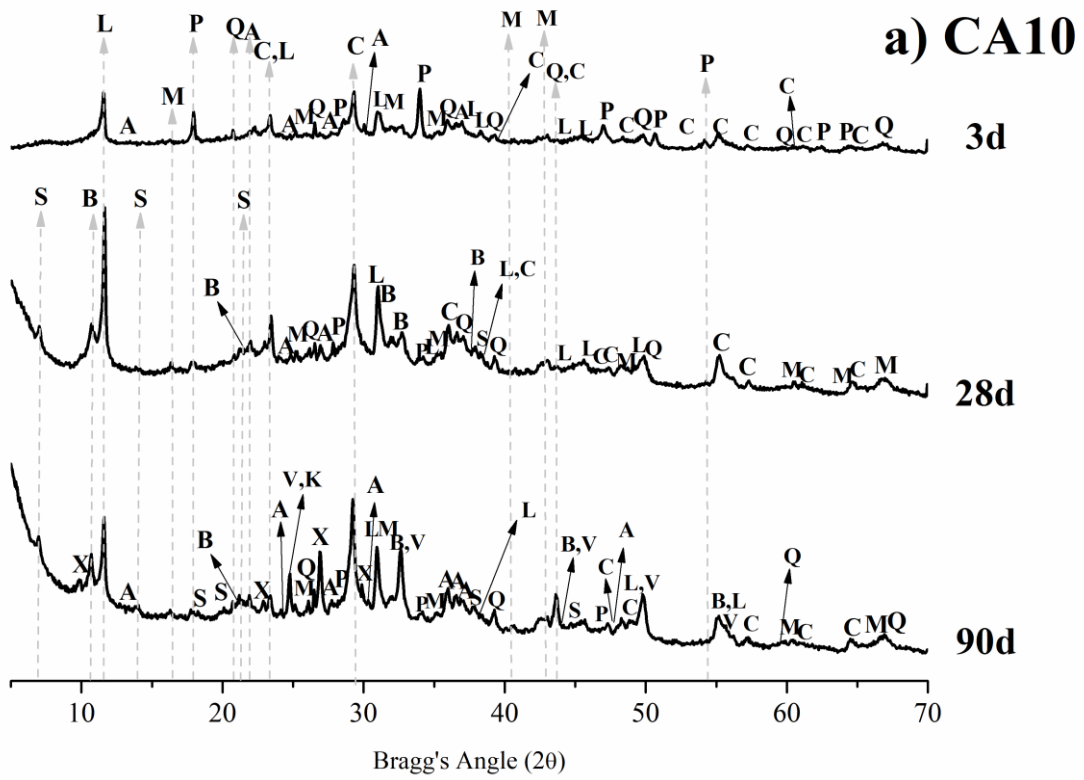
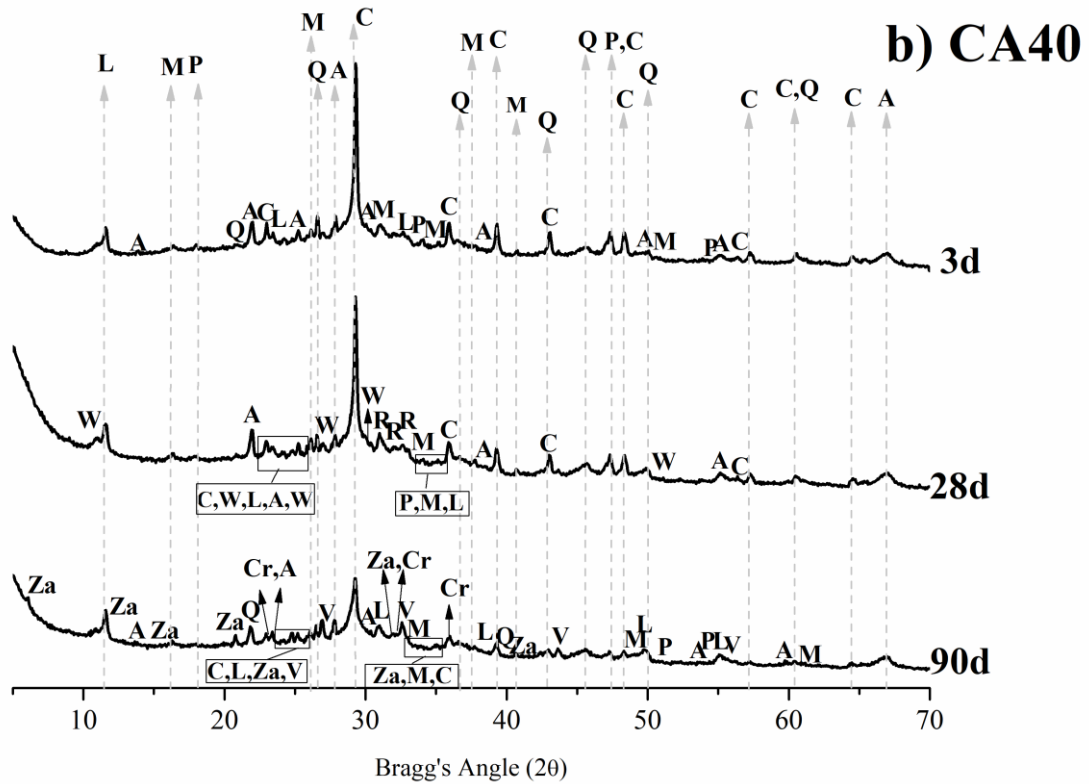


Figure 8. XRD patterns of the lime-pozzolan/geopolymer pastes activated with the alkali solution prepared using commercial sodium silicate (CC) after 3, 28 and 90 days: a) paste CC10; b) paste CC40.

When RHA was employed as the silica source in the alkali activator for the lime-pozzolan/geopolymer systems, changes were evidenced in the XRD patterns. Figures 9a and 9b show the patterns for paste CA10 and paste CA40, respectively. We can see that the signals corresponding to P for the 10% geopolymer paste were not intense after 28 curing days, unlike CC10, which suggests that the presence of RHA favoured the pozzolanic reaction rate. The signals for S were also slightly intense after 28 and 90 days, which indicates that S formation was not favoured. Probably due to the presence of amorphous SiO_2 in RHA, the pozzolanic reaction was activated and more CSH was formed. The main signal for this gel was considerably intense in the XRD pattern in CA10. The broad peak related to the presence of gel was intense after 3 curing days. Some traces of zeolite X (X) were identified after 90 curing days. For paste CA40, the intensity of the P signals in the XRD pattern were very low at the early curing age and a baseline deviation appeared within the 28-32° 2θ range in relation to the formed gels (NASH, C(N)ASH, CSH). Some zeolitic structures (Z) appeared after 90 curing days.



483

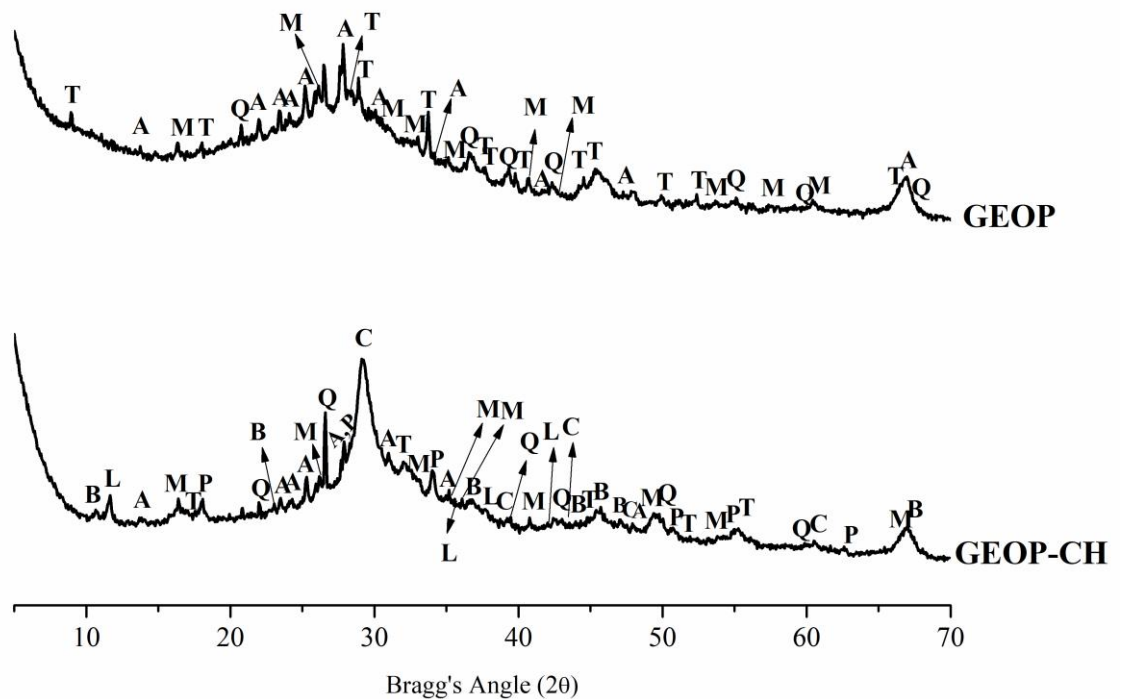


484

485 **Figure 9.** XRD patterns of the lime-pozzolan/geopolymer pastes activated with the
 486 alkali solution prepared by using RHA (CA pastes) after 3, 28 and 90 days: a) paste
 487 CA10; b) paste CA40.

488

489 The XRD patterns (Figure 10) of GEOP and GEOP-CH at 28 days displayed
 490 major changes. A baseline deviation was observed in GEOP and GEOP-CH, with a
 491 relative high intensity of peaks Q, M and A due to the crystalline phases from FCC. The
 492 F peaks disappeared in these two pastes, which indicated that the zeolitic fraction of FCC
 493 was highly reactive. Excess sodium ions favoured the formation of trona (T) in paste
 494 GEOP. In this case, the nature of the gel, mainly NASH, was shown as a baseline
 495 deviation within the 20-32° range. Due to calcium addition, carboaluminate peaks (L and
 496 B) were identified in the GEOP-CH pattern. In this case, the baseline deviation was strong
 497 and the broadness within the 25-32° range indicates CASH/C(N)ASH formation. This
 498 means that if a large amount of calcium is present, CASH/C(N)ASH gels form. They are
 499 easily observed in the XRD patterns for CC10, CC40, CA10 and CA40. It was more
 500 difficult to identify the presence of NASH because this gel showed less intensity and a
 501 more broadly shaped diffraction signal.

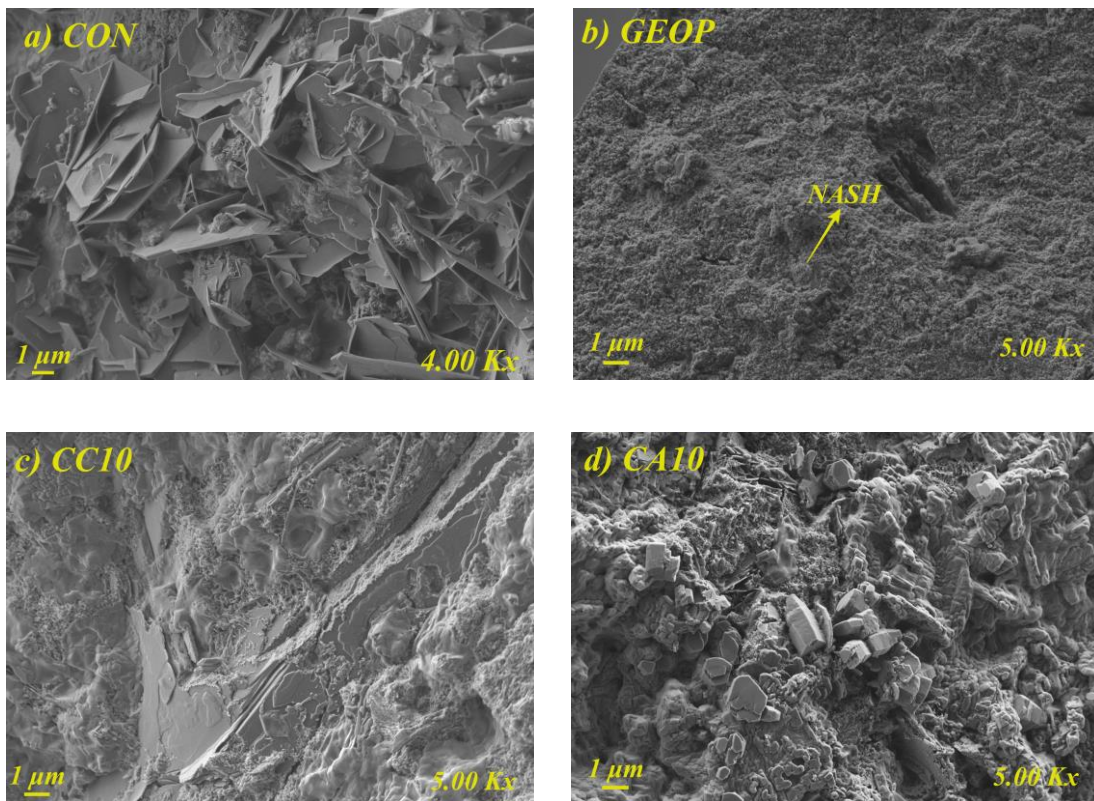


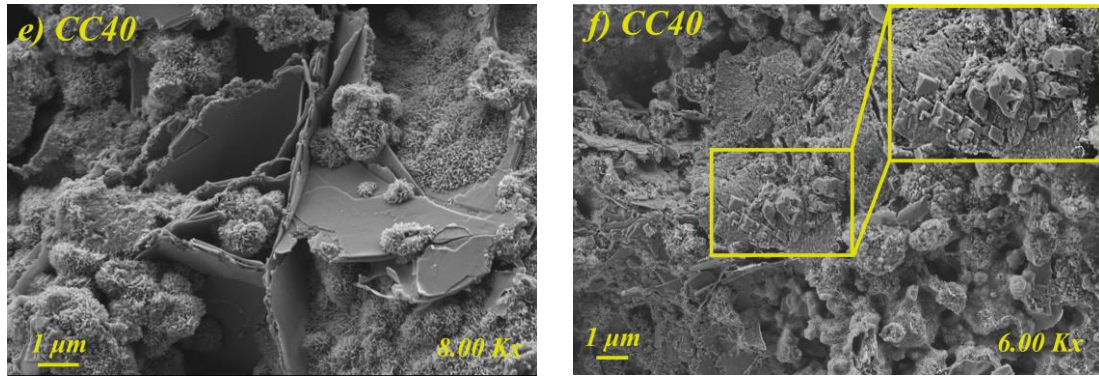
502
 503 **Figure 10.** XRD patterns for pastes GEOP and GEOP-CH after 28 curing days.

506 3.5 FESEM studies

507 The FESEM images for all the pastes cured for 28 days are depicted in Figure 11.
508 In the lime-pozzolan paste (CON), the typical reaction product from the pozzolanic
509 process was observed (Figure 11.a) (strätlingite) [53] Figure 11.b represents the GEOP
510 paste, where the paste's microstructure was denser and the principal formed product was
511 the NASH gel [55, 56].

512 In pastes CC10 and CA10 (Figures 11.c and 11.d), products were observed with a
513 different appearance to those for pastes CON and GEOP. In these pastes, pozzolanic and
514 geopolymeric products probably coexisted. Finally, in pastes CC40 and CA40 (Figures
515 11.e and 11.f), the principal reaction product was C(N)ASH gel, although some NASH
516 gel was probably present. Duramae et al reported C(N)ASH formation as a result of partial
517 NASH substitution in the system [57]. In the CA40 paste, the formation of little cubic-
518 shape particles took place, which may be attributed to the presence of zeolite A [58].





519 **Figure 11.** FESEM micrographs for pastes after 28 curing days: a) CON; b)
 520 GEOP; c) CC10; d) CA10; e) CC40; f) CA40.

521 **4 CONCLUSIONS**

522 The mechanical behaviour and microstructure of lime-pozzolan/geopolymer
 523 mixtures were analysed, in which pozzolan and the precursor were the same
 524 aluminosilicate waste (spent FCC catalyst).

525 The changes in the lime-pozzolan system made by adding the geopolymeric
 526 binder were highly positive in compressive strength development terms for mortars:

- 527 • It is highlighted the strength improvement at short times thus, the mortars
 528 with a 10-40% replacement of lime-pozzolan binder with geopolymer,
 529 prepared with the NaOH/waterglass solution, yielded strength values
 530 within the 9-25 MPa range at 7 curing days *versus* 3.59 MPa for the lime-
 531 pozzolan mortar.
- 532 • For the long curing time (90 days), the 10% geopolymer mortar was 50%
 533 higher than the lime-pozzolan one, and the 40% geopolymer mortar was
 534 almost double.

535 The contribution of RHA as a silica source in the alternative alkali activator was
 536 remarkably positive compared to the commercial chemical reagent (waterglass),
 537 especially at early curing ages (1-3 days) for the smallest geopolymer addition (10%).
 538 Apparently, the reason for the different nature of the binding gel formed when RHA was
 539 present was responsible for the achieved higher strength.

540 The addition of a geopolymer to a lime-pozzolan system brings about significant
 541 changes in the nature of hydration products:

1
2
3
4
5
6
7
8
9
10
11
12
13
14
15
16
17
18
19
20
21
22
23
24
25
26
27
28
29
30
31
32
33
34
35
36
37
38
39
40
41
42
43
44
45
46
47
48
49
50
51
52
53
54
55
56
57
58
59
60
61
62
63
64
65

- 1
2
3
4
5
6
7
8
9
10
11
12
13
14
15
16
- 542 • The hydration of lime-pozzolan systems produces typical products:
543 CSH/CASH gel, calcium carboaluminate hydrates and S, as well as
544 unreacted portlandite at early (3 days) and mid-term (28 days) curing ages.
 - 545 • The addition of 10% geopolymer slightly modified the nature of hydration
546 products. However, the reaction rate rose and portlandite consumption was
547 significantly higher.
 - 548 • The addition of 40% geopolymer led to a more marked modification in the
549 nature of hydration products: a NASH/C(N)ASH gel was formed, and no
550 presence of S and portlandite was detected.

17
18
19
20
21
22
23
24
25
26
27
28
29
30
31
32
33
34
35
36
37
38
39
40
41
42
43
44
45
46
47
48
49
50
51
52
53
54
55
56
57
58
59
60
61
62
63
64
65

551 In summary, adding geopolymer to a lime-pozzolan system is a good proposal for
552 improving the early- and long-term strength performance of mortars. Using RHA as an
553 alternative silica source for replacing waterglass has a very high potential to avoid or to
554 reduce employing synthetic chemical reagents that have a significant carbon footprint.

Acknowledgements

This research was supported by Centro de Cooperación al Desarrollo (CCD) of the Universitat Politècnica de València, ADSIDEO-COOPERACION 2017 Program “Reutilización de residuos agrícolas e industriales para la fabricación de conglomerantes sostenibles en países en desarrollo (AD1708)”. The investigation is framed within the ECOSOST (RTI2018-097612-B-C21-AR) project supported by MINECO and FEDER funds. The authors are grateful to the Electron Microscopy Service of the Universitat Politècnica de València, Dacsa Group S.A., Cales Pascual S.L. and BP Oil España S.A.U.

Bibliography (References revised)

- [1] P. Maravelaki-Kalaitzaki, A. Bakolas, A. Moropoulou, Physico-chemical study of Cretan ancient mortars, *Cement and Concrete Research*. 33 (2003) 651–661. doi:10.1016/S0008-8846(02)01030-X.
- [2] A.M. Neville, *Properties of concrete*, Fifth, Pearson Education Limited, England, 1982. doi:10.4135/9781412975704.n88.
- [3] D.A. Silva, H.R. Wenk, P.J.M. Monteiro, Comparative investigation of mortars from Roman Colosseum and cistern, *Thermochimica Acta*. 438 (2005) 35–40. doi:10.1016/j.tca.2005.03.003.
- [4] G. Cook, J.P. Ponsard, A proposal for the renewal of sectoral approaches building on the cement sustainability initiative, *Climate Policy*. 11 (2011) 1246–1256. doi:10.1080/14693062.2011.602552.
- [5] L.K. Turner, F.G. Collins, Carbon dioxide equivalent (CO₂-e) emissions: A comparison between geopolymers and OPC cement concrete, *Construction and Building Materials*. 43 (2013) 125–130. doi:10.1016/j.conbuildmat.2013.01.023.
- [6] R. Maddalena, J.J. Roberts, A. Hamilton, Can Portland cement be replaced by low-carbon alternative materials? A study on the thermal properties and carbon emissions of innovative cements, *Journal of Cleaner Production*. 186 (2018) 933–942. doi:10.1016/j.jclepro.2018.02.138.
- [7] S. Xu, J. Wang, Q. Ma, X. Zhao, T. Zhang, Study on the lightweight hydraulic mortars designed by the use of diatomite as partial replacement of natural hydraulic lime and masonry waste as aggregate, *Construction and Building Materials*. 73 (2014) 33–40. doi:10.1016/j.conbuildmat.2014.09.062.

- 1
2
3
4
5
6
7
8
9
10
11
12
13
14
15
16
17
18
19
20
21
22
23
24
25
26
27
28
29
30
31
32
33
34
35
36
37
38
39
40
41
42
43
44
45
46
47
48
49
50
51
52
53
54
55
56
57
58
59
60
61
62
63
64
65
- [8] N. Billong, U.C. Melo, E. Kamseu, J.M. Kinuthia, D. Njopwouo, Improving hydraulic properties of lime-rice husk ash (RHA) binders with metakaolin (MK), *Construction and Building Materials*. 25 (2011) 2157–2161. doi:10.1016/j.conbuildmat.2010.11.013.
- [9] E.R. Grist, K.A. Paine, A. Heath, J. Norman, H. Pinder, Compressive strength development of binary and ternary lime-pozzolan mortars, *Materials and Design*. 52 (2013) 514–523. doi:10.1016/j.matdes.2013.05.006.
- [10] R. Méndez, M. V. Borrachero, J. Payá, J. Monzó, Mechanical strength of lime-rice husk ash mortars: A preliminary study, *Key Engineering Materials*. 517 (2012) 495–499. doi:10.4028/www.scientific.net/KEM.517.495.
- [11] A. Palomo, P. Monteiro, P. Martauz, V. Bilek, A. Fernandez-Jimenez, Hybrid binders: A journey from the past to a sustainable future (opus caementicium futurum), *Cement and Concrete Research*. 124 (2019). doi:10.1016/j.cemconres.2019.105829.
- [12] M.D. Jackson, S.R. Chae, S.R. Mulcahy, C. Meral, R. Taylor, P. Li, A.H. Emwas, J. Moon, S. Yoon, G. Vola, H.R. Wenk, P.J.M. Monteiro, Unlocking the secrets of Al-tobermorite in Roman seawater concrete, *American Mineralogist*. 98 (2012) 1669–1687. doi:10.2138/am.2013.4484.
- [13] M.D. Jackson, J. Moon, E. Gotti, R. Taylor, S.R. Chae, M. Kunz, A.H. Emwas, C. Meral, P. Guttman, P. Levitz, H.R. Wenk, P.J.M. Monteiro, Material and elastic properties of Al-tobermorite in ancient roman seawater concrete, *Journal of the American Ceramic Society*. 96 (2013) 2598–2606. doi:10.1111/jace.12407.
- [14] J.L. Provis, Alkali-activated materials, *Cement and Concrete Research*. 114 (2018) 40–48. doi:10.1016/j.cemconres.2017.02.009.
- [15] S. Seifi, N. Sebaibi, D. Levacher, M. Boutouil, Mechanical performance of a dry mortar without cement, based on paper fly ash and blast furnace slag, *Journal of Building Engineering*. 22 (2019) 113–121. doi:10.1016/j.job.2018.11.004.
- [16] S. Donatello, A. Fernández-Jimenez, A. Palomo, Very high volume fly ash cements. Early age hydration study using Na₂SO₄ as an activator, *Journal of the American Ceramic Society*. 96 (2013) 900–906. doi:10.1111/jace.12178.
- [17] J.M. Mejía, R. Mejía de Gutiérrez, F. Puertas, Rice husk ash as a source of silica

1
2
3
4
5
6
7
8
9
10
11
12
13
14
15
16
17
18
19
20
21
22
23
24
25
26
27
28
29
30
31
32
33
34
35
36
37
38
39
40
41
42
43
44
45
46
47
48
49
50
51
52
53
54
55
56
57
58
59
60
61
62
63
64
65

in alkali-activated fly ash and granulated blast furnace slag systems, *Materiales de Construcción*. 63 (2013) 361–375. doi:10.3989/mc.2013.04712.

- [18] N. Bouzón, J. Payá, M. V. Borrachero, L. Soriano, M.M. Tashima, J. Monzó, Refluxed rice husk ash/NaOH suspension for preparing alkali activated binders, *Materials Letters*. 115 (2014) 72–74. doi:10.1016/j.matlet.2013.10.001.
- [19] A. Font, L. Soriano, L. Reig, M.M. Tashima, M. V. Borrachero, J. Monzó, J. Payá, Use of residual diatomaceous earth as a silica source in geopolymer production, *Materials Letters*. 223 (2018) 10–13. doi:10.1016/j.matlet.2018.04.010.
- [20] S.A. Bernal, E.D. Rodríguez, R. Mejía de Gutiérrez, J.L. Provis, Performance at high temperature of alkali-activated slag pastes produced with silica fume and rice husk ash based activators, *Materiales de Construcción*. 65 (2015) e049. doi:10.3989/mc.2015.03114.
- [21] M. Torres-Carrasco, F. Puertas, Waste glass in the geopolymer preparation. Mechanical and microstructural characterisation, *Journal of Cleaner Production*. 90 (2015) 397–408. doi:10.1016/j.jclepro.2014.11.074.
- [22] J.C.B. Moraes, A. Font, L. Soriano, J.L. Akasaki, M.M. Tashima, J. Monzó, M.V. Borrachero, J. Payá, New use of sugar cane straw ash in alkali-activated materials: A silica source for the preparation of the alkaline activator, *Construction and Building Materials*. 171 (2018). 611-621. doi:10.1016/j.conbuildmat.2018.03.230.
- [23] K. Dombrowski, A. Buchwald, M. Weil, The influence of calcium content on the structure and thermal performance of fly ash based geopolymers, *Journal of Materials Science*. 42 (2007) 3033–3043. doi:10.1007/s10853-006-0532-7.
- [24] L. Reig, L. Soriano, M.M. Tashima, M. V. Borrachero, J. Monzó, J. Payá, Influence of calcium additions on the compressive strength and microstructure of alkali-activated ceramic sanitary-ware, *Journal of the American Ceramic Society*. 101 (2018) 3094–3104. doi:10.1111/jace.15436.
- [25] G. Huang, Y. Ji, J. Li, Z. Hou, Z. Dong, Improving strength of calcinated coal gangue geopolymer mortars via increasing calcium content, *Construction and Building Materials*. 166 (2018) 760–768.

doi:10.1016/j.conbuildmat.2018.02.005.

- 1
2
3
4
5
6
7
8
9
10
11
12
13
14
15
16
17
18
19
20
21
22
23
24
25
26
27
28
29
30
31
32
33
34
35
36
37
38
39
40
41
42
43
44
45
46
47
48
49
50
51
52
53
54
55
56
57
58
59
60
61
62
63
64
65
- [26] F. Allali, E. Joussein, N.I. Kandri, S. Rossignol, The influence of calcium content on the performance of metakaolin-based geomaterials applied in mortars restoration, *Materials and Design*. 103 (2016) 1–9.
doi:10.1016/j.matdes.2016.04.028.
- [27] H. Maraghechi, S. Salwocki, F. Rajabipour, Utilisation of alkali activated glass powder in binary mixtures with Portland cement, slag, fly ash and hydrated lime, *Materials and Structures/Materiaux et Constructions*. 50 (2017) 1–14.
doi:10.1617/s11527-016-0922-5.
- [28] S. Alonso, A. Palomo, Alkaline activation of metakaolin and calcium hydroxide mixtures: Influence of temperature, activator concentration and solids ratio, *Materials Letters*. 47 (2001) 55–62. doi:10.1016/S0167-577X(00)00212-3.
- [29] S. Alonso, A. Palomo, Calorimetric study of alkaline activation of calcium hydroxide-metakaolin solid mixtures, *Cement and Concrete Research*. 31 (2001) 25–30. doi:10.1016/S0008-8846(00)00435-X.
- [30] S. Boonjaeng, P. Chindapasirt, K. Pimraksa, Lime-calcined clay materials with alkaline activation: Phase development and reaction transition zone, *Applied Clay Science*. 95 (2014) 357–364. doi:10.1016/j.clay.2014.05.002.
- [31] M.M. Tashima, J.L. Akasaki, J.L.P. Melges, L. Soriano, J. Monzó, J. Payá, M. V Borrachero, Alkali activated materials based on fluid catalytic cracking catalyst residue (FCC): Influence of $\text{SiO}_2/\text{Na}_2\text{O}$ and $\text{H}_2\text{O}/\text{FCC}$ ratio on mechanical strength and microstructure, *Fuel*. 108 (2013) 833–839.
doi:10.1016/j.fuel.2013.02.052.
- [32] J.J. Trochez, R. Mejía de Gutiérrez, J. Rivera, S.A. Bernal, Synthesis of geopolymer from spent FCC: Effect of $\text{SiO}_2/\text{Al}_2\text{O}_3$ and $\text{Na}_2\text{O}/\text{SiO}_2$ molar ratios, *Materiales de Construcción*. 65 (2015) e046. doi:10.3989/mc.2015.00814.
- [33] T. Luukkonen, Z. Abdollahnejad, J. Yliniemi, P. Kinnunen, M. Illikainen, Comparison of alkali and silica sources in one-part alkali-activated blast furnace slag mortar, *Journal of Cleaner Production*. 187 (2018) 171–179.
doi:10.1016/j.jclepro.2018.03.202.
- [34] M.A. Villaquirán-Caicedo, R. Mejía de Gutiérrez, Synthesis of ceramic materials

1
2 from ecofriendly geopolymer precursors, *Materials Letters*. 230 (2018) 300–304.
3 doi:10.1016/j.matlet.2018.07.128.

- 4 [35] AENOR, UNE-EN 459-1: Cales para la construcción Parte 1: Definiciones,
5 especificaciones y criterios de conformidad, 2015.
- 6
7
8 [36] J. Payá, J. Monzó, M. V. Borrachero, A. Mellado, L.M. Ordoñez, Determination
9 of amorphous silica in rice husk ash by a rapid analytical method, *Cement and
10 Concrete Research*. 31 (2001) 227–231. doi:10.1016/S0008-8846(00)00466-X.
- 11
12
13 [37] J.G. Martí, M. V. Borrachero, J. Payá, J. Monzó, D. Alveiro, A. Salas.
14 Reutilización de ceniza de cascarilla de arroz y residuo de catalizador de craqueo
15 catalítico en conglomerantes cal-puzolana para concretos de bajo coste
16 económico y medioambiental, *Proceedings of the 6th Amazon & Pacific Green
17 Materials Congress and Sustainable Construction Materials Lat-RILEM
18 Conference, Cali, Colombia, 2016*, 623–636.
- 19
20
21 [38] I. García-Lodeiro, A. Fernández-Jiménez, A. Palomo, Variation in hybrid
22 cements over time. Alkaline activation of fly ash-portland cement blends,
23 *Cement and Concrete Research*. 52 (2013) 112–122.
24 doi:10.1016/j.cemconres.2013.03.022.
- 25
26 [39] A. Font, M.V. Borrachero, L. Soriano, J. Monzó, A. Mellado, J. Payá, New eco-
27 cellular concretes: Sustainable and energy-efficient materials, *Green Chemistry*.
28 20 (2018) 14684. doi:10.1039/c8gc02066c.
- 29
30
31 [40] M.A. Villaquirán-Caicedo, Studying different silica sources for preparation of
32 alternative waterglass used in preparation of binary geopolymer binders from
33 metakaolin/boiler slag, *Construction and Building Materials*. 227 (2019) 116621.
34 doi:10.1016/j.conbuildmat.2019.08.002.
- 35
36
37 [41] A. Mellado, C. Catalán, N. Bouzón, M. V. Borrachero, J.M. Monzó, J. Payá,
38 Carbon footprint of geopolymeric mortar: study of the contribution of the
39 alkaline activating solution and assessment of an alternative route, *RSC Adv*. 4
40 (2014) 23846–23852. doi:10.1039/C4RA03375B.
- 41
42
43 [42] J. Payá, J. Monzó, M. V. Borrachero, S. Velázquez, M. Bonilla, Determination of
44 the pozzolanic activity of fluid catalytic cracking residue. Thermogravimetric
45 analysis studies on FC3R-lime pastes, *Cement and Concrete Research*. 33 (2003)
- 46
47
48
49
50
51
52
53
54
55
56
57
58
59
60
61
62
63
64
65

1085–1091. doi:10.1016/S0008-8846(03)00014-0.

- 1
2
3
4
5
6
7
8
9
10
11
12
13
14
15
16
17
18
19
20
21
22
23
24
25
26
27
28
29
30
31
32
33
34
35
36
37
38
39
40
41
42
43
44
45
46
47
48
49
50
51
52
53
54
55
56
57
58
59
60
61
62
63
64
65
- [43] M.M. Tashima, L. Soriano, J.L. Akasaki, V.N. Castaldelli, J. Monzó, J. Payá, M. V. Borrachero, Spent FCC catalyst for preparing alkali-activated binders: An opportunity for a high-degree valorization, *Key Engineering Materials*. 600 (2014) 709–716. doi:10.4028/www.scientific.net/KEM.600.709.
- [44] M.L. Granizo, S. Alonso, M.T. Blanco-Varela, A. Palomo, Alkaline Activation of Metakaolin: Effect of Calcium Hydroxide in the Products of Reaction, *Journal of the American Ceramic Society*. 85 (2002) 225–231. doi:10.1111/j.1151-2916.2002.tb00070.x.
- [45] B.A. Ramesh, B. Kondraivendhan, Effect of Accelerated Carbonation on the Performance of Concrete Containing Natural Zeolite, *Journal of Materials in Civil Engineering*. 32 (2020) 04020037. doi:10.1061/(ASCE)MT.1943-5533.0003050.
- [46] A. Hartmann, M. Khakhutov, J.C. Buhl, Hydrothermal synthesis of CSH-phases (tobermorite) under influence of Ca-formate, *Materials Research Bulletin*. 51 (2014) 389–396. doi:10.1016/j.materresbull.2013.12.030.
- [47] I. García-Lodeiro, A. Fernández-Jiménez, M.T. Blanco, A. Palomo, FTIR study of the sol-gel synthesis of cementitious gels: C-S-H and N-A-S-H, *Journal of Sol-Gel Science and Technology*. 45 (2008) 63–72. doi:10.1007/s10971-007-1643-6.
- [48] W. Mozgawa, J. Deja, Spectroscopic studies of alkaline activated slag geopolymers, *Journal of Molecular Structure*. 924–926 (2009) 434–441. doi:10.1016/j.molstruc.2008.12.026.
- [49] W.K.W. Lee, J.S.J. Van Deventer, Use of Infrared Spectroscopy to Study Geopolymerization of Heterogeneous Amorphous Aluminosilicates, *Langmuir*. 19 (2003) 8726–8734. doi:10.1021/la026127e.
- [50] I. García-Lodeiro, A. Fernández-Jiménez, A. Palomo, D.E. MacPhee, Effect of calcium additions on N-A-S-H cementitious gels, *Journal of the American Ceramic Society*. 93 (2010) 1934–1940. doi:10.1111/j.1551-2916.2010.03668.x.
- [51] N. Maubec, D. Deneele, G. Ouvrard, Influence of the clay type on the strength evolution of lime treated material, *Applied Clay Science*. 137 (2017) 107–114. doi:10.1016/j.clay.2016.11.033.

- 1
2
3
4
5
6
7
8
9
10
11
12
13
14
15
16
17
18
19
20
21
22
23
24
25
26
27
28
29
30
31
32
33
34
35
36
37
38
39
40
41
42
43
44
45
46
47
48
49
50
51
52
53
54
55
56
57
58
59
60
61
62
63
64
65
- [52] A.F.Nóbrega de Azeredo, L.J. Struble, A.M.P. Carneiro, Microstructural characteristics of lime-pozzolan pastes made from kaolin production wastes, *Materials and Structures/Materiaux et Constructions*. 48 (2015) 2123–2132. doi:10.1617/s11527-014-0297-4.
- [53] O.Rodríguez, R.Vigil de la Villa, R.García, B. Nebreda, M. Frías, Lower temperature activation for kaolinite-based clay waste: Evaluation of hydrated phases during the pozzolanic reaction, *Journal of the American Ceramic Society*. 94 (2011) 1224–1229. doi:10.1111/j.1551-2916.2010.04134.x.
- [54] K. Juengsuwattananon, F. Winnefeld, P. Chindaprasirt, K. Pimraksa, Correlation between initial $\text{SiO}_2/\text{Al}_2\text{O}_3$, $\text{Na}_2\text{O}/\text{Al}_2\text{O}_3$, $\text{Na}_2\text{O}/\text{SiO}_2$ and $\text{H}_2\text{O}/\text{Na}_2\text{O}$ ratios on phase and microstructure of reaction products of metakaolin-rice husk ash geopolymer, *Construction and Building Materials*. 226 (2019) 406–417. doi:10.1016/j.conbuildmat.2019.07.146.
- [55] H.K. Tchakouté, C.H. Rüscher, S. Kong, E. Kamseu, C. Leonelli, Comparison of metakaolin-based geopolymer cements from commercial sodium waterglass and sodium waterglass from rice husk ash, *Journal of Sol-Gel Science and Technology*. 78 (2016) 492–506. doi:10.1007/s10971-016-3983-6.
- [56] T. da Silva Rocha, D.P. Dias, F.C.C. França, R.R. de Salles Guerra, L.R. da Costa de Oliveira Marques, Metakaolin-based geopolymer mortars with different alkaline activators (Na^+ and K^+), *Construction and Building Materials*. 178 (2018) 453–461. doi:10.1016/j.conbuildmat.2018.05.172.
- [57] S. Dueramae, W. Tangchirapat, P. Sukontasukkul, P. Chindaprasirt, C. Jaturapitakkul, Investigation of compressive strength and microstructures of activated cement free binder from fly ash-calcium carbide residue mixture, *Journal of Materials Research and Technology*. 8 (2019) 4757–4765. doi:10.1016/j.jmrt.2019.08.022.
- [58] R.C. Andrades, R.F. Neves, F.R.V. Diaz, A.H.M. Júnior, Influence of alkalinity on the synthesis of zeolite A and hydroxysodalite from metakaolin, *Journal of Nano Research*. 61 (2020) 51–60. doi:10.4028/www.scientific.net/JNanoR.61.51.